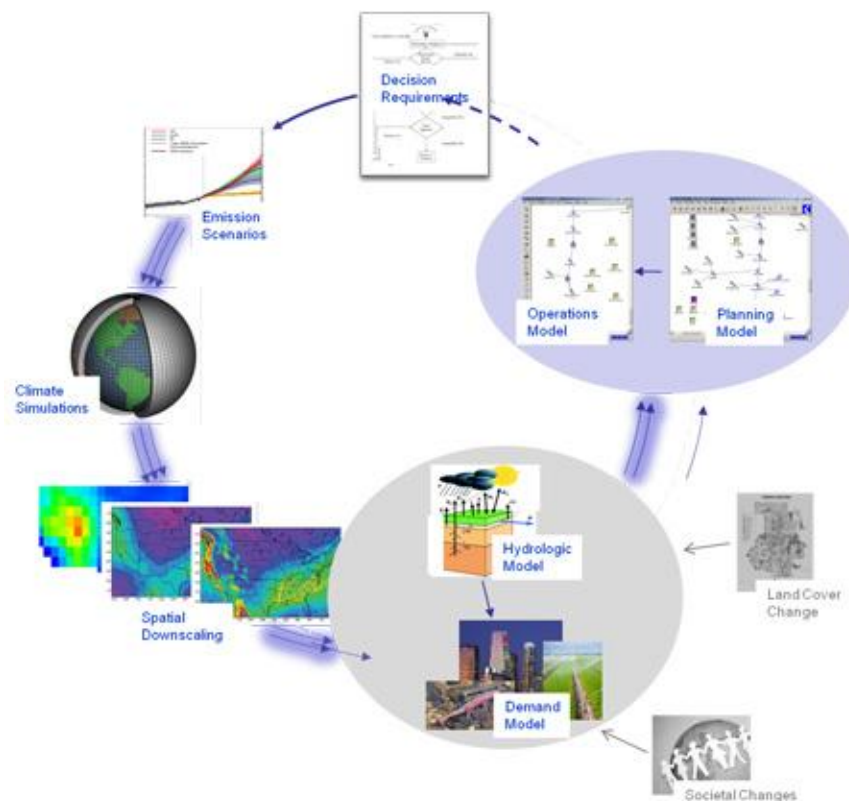


RECLAMATION

Managing Water in the West

Technical Memorandum No. 86-68210-2011-01

West-Wide Climate Risk Assessments: Bias-Corrected and Spatially Downscaled Surface Water Projections



Mission Statements

The U.S. Department of the Interior protects America's natural resources and heritage, honors our cultures and tribal communities, and supplies the energy to power our future.

The mission of the Bureau of Reclamation is to manage, develop, and protect water and related resources in an environmentally and economically sound manner in the interest of the American public.

Technical Memorandum No. 86-68210–2011-01

West-Wide Climate Risk Assessments: Bias-Corrected and Spatially Downscaled Surface Water Projections

Prepared by:

Water and Environmental Resources Division (86-68200)
Water Resources Planning and Operations Support Group (86-68210)
Subhrendu Gangopadhyay, Hydrologic Engineer
Tom Pruitt, Civil Engineer

Peer reviewed by:

Levi Brekke, Bureau of Reclamation
Andy Wood, National Weather Service
Ed Maurer, Santa Clara University
Tapash Das, Scripps Institute of Oceanography



U.S. Department of the Interior
Bureau of Reclamation
Technical Service Center
Denver, Colorado

March 2011

Executive Summary

Public Law 111-11, Subtitle F (SECURE Water Act), section (§) 9503 authorizes the U.S. Department of Interior’s Bureau of Reclamation (Reclamation) to assess climate change risks for water and environmental resources in “major Reclamation river basins.” Section 9503 also includes the authorities to evaluate potential climate change impacts on water resource management and development of strategies to either mitigate or adapt to *impacts*. The major Reclamation river basins listed within the SECURE Water Act are the Colorado and Columbia River Basins and the Klamath, Missouri, Rio Grande, Sacramento, San Joaquin, and Truckee River basins. Reclamation is accomplishing the SECURE Water Act authorities through activities within its WaterSMART Basin Study Program.

This technical assessment report provides: (1) an analysis of changes in hydroclimate variables—namely, precipitation, temperature, snow water equivalent, and streamflow across the major Reclamation river basins—and the technical foundation for the SECURE report and (2) documentation for this new hydrologic projections dataset that will be made publicly available over the Western United States. The analysis involves developing hydrologic projections associated with World Climate Research Programme Coupled Model Intercomparison Project3 (WCRP CMIP3) climate projections that have been bias-corrected and spatially downscaled and served at the following Web site: http://gdo-dcp.ucllnl.org/downscaled_cmip3_projections. In total, 112 hydrologic projections were developed, relying on watershed applications of the Variable Infiltration Capacity (VIC) macroscale hydrology model (described below). From these time-series climate and hydrologic projections (or hydroclimate projections), changes in hydroclimate variables were computed for three future decades: 2020s (water years 2020–2029), 2050s (water years 2050–2059) and 2070 (water years 2070–2079) from the reference 1990s’ decade (water years 1990–1999). The reference 1990s are from the ensemble of simulated historical hydroclimates, not from the observed 1990s.

Gridded (1/8 degree [°] by [x] 1/8°, latitude by longitude) VIC applications covering the major Reclamation basins and the Western United States were obtained from University of Washington personnel and from Dr. Andrew Wood, now at the National Oceanic and Atmospheric Administration (NOAA) National Weather Service (NWS) Colorado Basin River Forecast Center, formerly at University of Washington. These VIC applications are described at the University of Washington Westwide Streamflow Forecasting System, formerly featured at <http://www.hydro.washington.edu/forecast/westwide/> and documented

in Wood and Lettenmaier 2006, Wood et al. 2005, and also Maurer et al. 2002. Before performing climate change simulation runs, these VIC applications were used to simulate historical streamflow at a menu of locations across the Western United States. This included a total of 43 West-Wide Climate Risk Assessment (WWCRA) sites and 152 Hydroclimate Data Network (HCDN) sites spanning the major Reclamation river basins and the Western United States. A subset of these locations was used to compare VIC simulated historical flows with observed natural or unimpaired flows to characterize the VIC simulation biases (difference between observed and simulated streamflow magnitudes). For this assessment report, the VIC applications largely were applied “as-is,” (i.e., without any additional efforts to improve upon their existing level of calibration).

The VIC model requires gridded daily precipitation, maximum and minimum temperatures, and wind magnitude as input to simulate gridded daily state variables such as snow water equivalent and runoff (both surface and subsurface runoff). These gridded runoffs are then hydraulically routed to the menu of locations. To develop the hydrologic projections, the Bias Correction and Spatial Disaggregation (BCSD) archive of gridded ($1/8^\circ \times 1/8^\circ$, latitude by longitude) monthly total precipitation and average temperature for each of the 112 projections temporally was disaggregated to develop daily time-series of precipitation and maximum and minimum temperatures.

Use of the climate projections in this assessment involved several important choices, specifically:

- *Why did we use BCSD projections?*
 - The BCSD methodology is:
 - Well tested and documented, especially for applications in the United States.
 - Efficient enough to permit the downscaling of many 21st century climate projections, thereby supporting a comprehensive assessment of regional to local climate projection uncertainty.
 - Able to produce output that statistically reproduces a range of characteristics (including spatial and temporal patterns) of historical observations when driven by climate simulations for retrospective periods.
 - Capable of producing spatially continuous, fine scale fields of precipitation and temperature suitable for water resources and other watershed-scale impacts analysis.

- *Why did we keep all the 112 projections?*
 - Basis for culling projections is weak. Neither the Intergovernmental Panel on Climate Change (IPCC) 2000 nor IPCC 2007 reports offer suggestions on which scenario pathway may be more likely. Hence, no assumptions are made in this study about this matter, and no projection culling is performed on the basis of relative regard for the three IPCC Special Reports on Emissions Scenarios (SRES) emission scenarios A2, A1B, and B1.
- *Why did we do a time-evolving analysis rather than a step-change climate analysis?*
 - Time-evolving applications are useful for characterizing an envelope of hydroclimate possibility evolving from global climate model- (GCM) simulated past to GCM-simulated future. Choice of a time-evolving application implies that the ensemble of monthly BCSD climate projections is translated into an associated ensemble of hydrologic projections for the Western United States. This provides flexibility to support planning on many different timeframes.
- *What are some interpretation issues of which the user should be aware when using BCSD climate projections?*
 - Residual bias in historical climate conditions at nonmonthly time scales.
 - Different bias correction of 21st century temperature and precipitation.
 - Both bias correction and spatial disaggregation affect locally portrayed climate change in BCSD projections.

In the context of assessing future hydrologic impacts using these BCSD hydrologic projections, the findings from the assessment are:

- Precipitation is expected to increase from the 1990s' level during the 2020s and 2050s but to decline nominally during the 2070s (though the early to middle 21st century, increases could be artifacts of the BCSD climate projections development leading to slightly wetter projections).
- Temperature shows a persistent increasing trend from the 1990s' level.
- April 1st snow water equivalent (SWE) shows a persistent decreasing trend from the 1990s' level.

West-Wide Climate Risk Assessments:
BCSD Surface Water Projections

- Annual runoff shows some increase for the 2020s' decade from the 1990s' level but shows decline moving forward to the 2050s' and 2070s' decade from the 1990s' reference, suggesting that, although precipitation changes are projected to remain positive through the 2050s, temperature changes begin to offset these precipitation increases leading to net loss in the water balance through increased evapotranspiration losses.
- Winter season (December–March) runoff shows an increasing trend.
- Spring–summer season (April–July) runoff shows a decreasing trend.
- Lack of calibration of the hydrologic models is a real issue that needs to be addressed and should be addressed before these models are used in future assessments. Reclamation will (a) refine the VIC application and/or (b) introduce more appropriate hydrologic models. However, before implementing west-wide calibration efforts, it also is important to assess the fitness of the chosen model structure for some geographic situations, particularly basins where ground water interactions with surface water may be an important process and not well simulated in VIC.

Contents

	<i>Page</i>
Acronyms	xiii
Chapter 1 – Introduction	1
Chapter 2 – Background.....	5
Chapter 3 – Climate Projections	9
3.1 Survey of Available Global and Downscaled Climate Projections	9
3.2 Decisions on Whether to Cull Available Downscaled Climate Projections (BCSD Climate Projections)	11
3.3 Decisions on How To Use Retained BCSD Climate Projections	13
3.4 Methodological Issues Affecting Interpretation of the BCSD Climate and Hydrologic Projections	14
Chapter 4 – Developing Hydrologic Projections from Climate Projections	27
4.1 Hydrologic Model Selection Considerations	29
4.2 About the VIC Hydrology Model-Applications	31
4.2.1 Model Description	31
4.2.2 Applications Description.....	33
4.3 Use of VIC Model Applications To Develop BCSD Surface Water Hydrologic Projections.....	36
4.4 Assessment of VIC Model-Applications’ Historical Simulations	37
4.5 Flow Bias and Bias Correction	44
Chapter 5 – Hydroclimate Projections for Major Reclamation River Basins Under Climate Change	51
5.1 Evaluation Approach	51
5.1.1 Time Series Plots.....	52
5.1.2 Spatial Plots	53
5.1.3 Impacts on Runoff Annual and Seasonal Cycles	54
5.2 Colorado River Basin.....	55
5.2.1 Hydroclimate Projections	55
5.2.2 Impacts on Runoff Annual and Seasonal Cycles	60
5.3 Columbia River Basin.....	62
5.3.1 Hydroclimate Projections	62
5.3.2 Impacts on Runoff Annual and Seasonal Cycles	68
5.4 Klamath River Basin.....	70
5.4.1 Hydroclimate Projections	70
5.4.2 Impacts on Runoff Annual and Seasonal Cycles	75
5.5 Missouri River Basin	76
5.5.1 Hydroclimate Projections	76

Contents (continued)

	<i>Page</i>
5.5.2 Impacts on Runoff Annual and Seasonal Cycles	81
5.6 Rio Grande Basin	82
5.6.1 Hydroclimate Projections	82
5.6.2 Impacts on Runoff Annual and Seasonal Cycles	84
5.7 Sacramento and San Joaquin River Basins	89
5.7.1 Hydroclimate Projections	89
5.7.2 Impacts on Runoff Annual and Seasonal Cycles	92
5.8 Truckee and Carson River Basins	97
5.8.1 Hydroclimate Projections	97
5.8.2 Impacts on Runoff Annual and Seasonal Cycles	102
5.9 West-Wide Summary of Results	103
Chapter 6 – Uncertainties	111
6.1 Climate Projection Information	111
6.1.1 Global Climate Forcing.....	111
6.1.2 Global Climate Simulation	111
6.1.3 Climate Projection Bias Correction.....	112
6.1.4 Climate Projection Spatial Downscaling.....	112
6.2 Assessing Hydrologic Impacts.....	112
6.2.1 Generating Weather Sequences Consistent with Climate Projections	112
6.2.2 Natural Runoff Response	113
6.2.3 Hydrologic Modeling.....	113
6.2.4 Bias and Calibration	113
6.2.5 Spatial Resolution of the Applications.....	113
6.2.6 Time Resolution of the Applications	114
Chapter 7 – References	115

Tables

	<i>Page</i>
Table 1 Station description for the 43 WWCRA reporting locations.....	35
Table 2 Bias in historical flow simulations for selected WWCRA locations	38

Tables (continued)

	<i>Page</i>	
Table 3	Median of median change for precipitation, mean temperature, April 1 st SWE from the 1990s for the 43 WWCRA reporting watersheds in 2020s; for runoff, it is the median change.....	105
Table 4	Median of median change for precipitation, mean temperature, April 1 st SWE from the 1990s for the 43 WWCRA reporting watersheds in 2050s;for runoff, it is the median change.....	106
Table 5	Median of median change for precipitation, mean temperature, April 1 st SWE from the 1990s for the 43 WWCRA reporting watersheds in 2070s; for runoff, it is the median change.....	107

Figures

	<i>Page</i>	
Figure 1	Climate-related Assumptions in Longer-term Operations Planning.....	6
Figure 2	Framework for Relating Climate Projection Information to Longer-term Operations Planning.....	6
Figure 3	Climate Projection Bias Correction Example: Location	17
Figure 4	Climate Projection Bias Correction Example: Monthly Temperature	17
Figure 5	Climate Projection Bias Correction Example: Seasonal Temperature	18
Figure 6	Climate Projection Bias Correction Example: Monthly Precipitation	19
Figure 7	Climate Projection Bias Correction Example: Seasonal Precipitation.....	20
Figure 8	Climate Projections: Effects of Bias Correction and Spatial Downscaling, One Location	23
Figure 9	Climate Projections: Effects of Bias Correction, Contiguous United States Locations	24
Figure 10	Schematic of VIC Hydrologic Model and Energy Balance Snow Model.....	32
Figure 11	Schematic of VIC River Network Routing Model	33
Figure 12	VIC Applications at 1/8° Resolution with the Two Sets of Routing Locations—HCDN (Blue Triangles, Total 152) and WWCRA Locations (Red Triangles, Total 43) Used in the Study ...	34
Figure 13	Historical Simulated Runoff, Small-Bias Example: Monthly Time Series	39

Figures (continued)

	<i>Page</i>
Figure 14	Historical Simulated Runoff, Small-Bias Example: Monthly and Annual Means 40
Figure 15	Historical Simulated Runoff, Large-Bias Example: Monthly Time Series 41
Figure 16	Historical Simulated Runoff, Large-Bias Example: Monthly and Annual Means 42
Figure 17	Historical Simulated Runoff, West-wide Bias Summary: Annual Mean 43
Figure 18	Historical Simulated Runoff, Small-Bias Example: Monthly Time Series Before and After Bias Correction..... 46
Figure 19	Historical Simulated Runoff, Small-Bias Example: Monthly and Annual Means Before and After Bias Correction 47
Figure 20	Historical Simulated Runoff, Large-Bias Example: Monthly Time Series Before and After Bias Correction..... 48
Figure 21	Historical Simulated Runoff, Large-Bias Example: Monthly and Annual Means Before and After Bias Correction..... 49
Figure 22	Colorado Basin – Projections Ensembles for Six Hydroclimate Indicators..... 57
Figure 23	Colorado Basin – Spatial Distribution of Simulated Decadal Precipitation..... 58
Figure 24	Colorado Basin – Spatial Distribution of Simulated Decadal Temperature 59
Figure 25	Colorado Basin – Spatial Distribution of Simulated Decadal April 1 st SWE..... 60
Figure 26	Colorado Basin – Simulated Mean-Monthly Runoff for Various Subbasins 61
Figure 27	Colorado Basin –Simulated Mean-Seasonal Runoff for Various Subbasins 62
Figure 28	Columbia Basin – Projections Ensembles for Six Hydroclimate Indicators..... 64
Figure 29	Columbia Basin – Spatial Distribution of Simulated Decadal Precipitation..... 65
Figure 30	Columbia Basin – Spatial Distribution of Simulated Decadal Temperature..... 66
Figure 31	Columbia Basin –Spatial Distribution of Simulated Decadal April 1 st SWE..... 67
Figure 32	Columbia Basin – Simulated Mean-Monthly Runoff for Various Subbasins..... 68
Figure 33	Columbia Basin – Simulated Mean-Seasonal Runoff for Various Subbasins..... 69
Figure 34	Klamath Basin – Projections Ensembles for Six Hydroclimate Indicators..... 71
Figure 35	Klamath Basin – Spatial Distribution of Simulated Decadal Precipitation 72

Figures (continued)

		<i>Page</i>
Figure 36	Klamath Basin – Spatial Distribution of Simulated Decadal Temperature	73
Figure 37	Klamath Basin – Spatial Distribution of Simulated Decadal April 1 st SWE.....	74
Figure 38	Klamath Basin - Simulated Mean-Monthly Runoff for Various Subbasins.....	75
Figure 39	Klamath Basin – Simulated Mean-Seasonal Runoff for Various Subbasins.....	76
Figure 40	Missouri Basin – Projections Ensembles for Six Hydroclimate Indicators.....	77
Figure 41	Missouri Basin – Spatial Distribution of Simulated Decadal Precipitation	78
Figure 42	Missouri Basin – Spatial Distribution of Simulated Decadal Temperature	79
Figure 43	Missouri Basin –Spatial Distribution of Simulated Decadal April 1 st SWE.....	80
Figure 44	Missouri Basin – Simulated Mean-Monthly Runoff for Various Subbasins.....	81
Figure 45	Missouri Basin – Simulated Mean-Seasonal Runoff for Various Subbasins	82
Figure 46	Rio Grande Basin – Projections Ensembles for Six Hydroclimate Indicators.....	83
Figure 47	Rio Grande Basin – Spatial Distribution of Simulated Decadal Precipitation	85
Figure 48	Rio Grande Basin – Spatial Distribution of Simulated Decadal Temperature	86
Figure 49	Rio Grande Basin – Spatial Distribution of Simulated Decadal April 1 st SWE.....	87
Figure 50	Rio Grande Basin – Simulated Mean-Monthly Runoff for Various Subbasins.....	88
Figure 51	Rio Grande Basin – Simulated Mean-Seasonal Runoff for Various Subbasins.....	89
Figure 52	Sacramento and San Joaquin Basins – Hydroclimate Projections.....	90
Figure 53	Sacramento and San Joaquin Basins – Spatial Distribution of Simulated Decadal Precipitation	91
Figure 54	Sacramento and San Joaquin Basins – Spatial Distribution of Simulated Decadal Temperature	93
Figure 55	Sacramento and San Joaquin Basins – Spatial Distribution of Simulated Decadal April 1 st SWE	94
Figure 56	Sacramento and San Joaquin Basins – Simulated Mean-Monthly Runoff for Various Subbasins.....	95
Figure 57	Sacramento and San Joaquin Basins – Simulated Mean-Seasonal Runoff for Various Subbasins	96
Figure 58	Truckee Basin – Hydroclimate Projections.....	98

Figures (continued)

	<i>Page</i>
Figure 59	Truckee Basin – Spatial Distribution of Simulated Decadal Precipitation 99
Figure 60	Truckee Basin – Spatial Distribution of Simulated Decadal Temperature 100
Figure 61	Truckee Basin – Spatial Distribution of Simulated Decadal April 1 st SWE..... 101
Figure 62	Truckee and Carson Basins – Simulated Mean-Monthly Runoff for Various Subbasins..... 102
Figure 63	Truckee and Carson Basins – Simulated Mean-Seasonal Runoff for Various Subbasins 103
Figure 64	Ensemble Median Percentage Change in Annual Runoff for 2020s from the 1990s Across HCDN Sites..... 108
Figure 65	Ensemble Median Percentage Change in Annual Runoff for 2050s from the 1990s Across HCDN Sites..... 109
Figure 66	Ensemble Median Percentage Change in Annual Runoff for 2070s from the 1990s Across HCDN Sites..... 110

Acronyms

AMJJ	April–July
BC	Bias Corrected
BCF	bias-corrected simulated flow
BCSD	Bias Correction and Spatial Disaggregation or bias-corrected and spatially downscaled
CDF	Cumulative Distribution Function
CMIP	Coupled Model Intercomparison Project (CMIP1, CMIP2, and CMIP3 are CMIP phases 1, 2, and 3, respectively)
DCP	Downscaled Climate Projections
DEM	Digital Elevation Model
DJFM	December–March
ET	evapotranspiration
FY	fiscal year
GCM	General Circulation Model or Global Climate Model
GHG	greenhouse gas
GIS	Geographic Information System
HCDN	Hydro-Climatic Data Network
IPCC	Intergovernmental Panel on Climate Change
IQR	interquartile range
km	kilometer
LCCS	Landscape Conservation Cooperatives
MAF	million acre-feet
NOAA	National Oceanic and Atmospheric Administration
NWS	National Weather Service
PET	Potential Evapotranspiration
RCM	Regional Climate Model

West-Wide Climate Risk Assessments:
BCSD Surface Water Projections

Reclamation	Bureau of Reclamation
SECURE	Science and Engineering to Comprehensively Understand and Responsibly Enhance
SRES	IPCC's Special Report on Emissions Scenarios
SWAT	Soil and Water Assessment Tool
SWE	snow water equivalent
TAF	thousand acre-feet
USGCRP	U.S. Global Change Research Program
USGS	U.S. Geological Survey
VIC	Variable Infiltration Capacity hydrologic model
WaterSMART	WaterSMART (Sustain and Manage America's Resources for Tomorrow)
WCRP	World Climate Research Programme
WWCRA	West-Wide Climate Risk Assessments
°	degree
°C	degrees Celsius
°F	degrees Fahrenheit
%	percent
>	greater than
<	less than
≤	less than or equal to

CHAPTER 1

Introduction

Public Law 111-11, Subtitle F (SECURE¹ Water Act), section (§) 9503 authorizes the U.S. Department of Interior’s Bureau of Reclamation (Reclamation) to assess climate change risks for water and environmental resources in “major Reclamation river basins.” Section 9503 also includes the authorities to evaluate potential climate change impacts on water resource management, and development of strategies to either mitigate or adapt to impacts. The major Reclamation river basins listed within the SECURE Water Act are the Colorado and Columbia River Basins and the Klamath, Missouri, Rio Grande, Sacramento, San Joaquin, and Truckee River basins.

Reclamation is accomplishing the SECURE Water Act (SWA) authorities through activities within its WaterSMART Basin Study Program,² which also includes implementation of West-Wide Climate Risk Assessments and Landscape Conservation Cooperatives (LCCs) as well as its Science and Technology Program. The WaterSMART activities are complementary and represent a three-part approach to the assessment of climate change risks and impacts for water and environmental resources and development of strategies to mitigate or adapt to such impacts. Through the Basin Studies, Reclamation works with State and local partners in a cooperative manner to evaluate the ability to meet future water demands within a river basin and to identify adaptation and mitigation strategies of the potential impacts of climate change. Through its participation within the LCCs, Reclamation is partnering with Federal, State, and local governments as well as conservation groups and nongovernmental organizations. The West-Wide Climate Risk Assessments (WWCRA) are meant to complement these two activities, where the WWCRA will provide future projections of water supplies, water demands, and river system operations, characterized in a consistent manner within the eight major Reclamation river basins listed within the SECURE Water Act.

Beginning in fiscal year (FY) 2010, one of the WWCRA activities has been the development of surface water hydrologic projections over the Western United States. These projections are intended to provide risk assessment information for metrics described in the SECURE Water Act 9503(b)(2), including climate change risks to snowpack, changes in the timing of streamflow, and changes in

¹ SECURE is the acronym for Science and Engineering to Comprehensively Understand and Responsibly Enhance.

² <http://www.usbr.gov/WaterSMART/>.

the quantity of runoff. SECURE Water 9503(b)(2) also calls for assessment of climate change risks to ground water recharge and discharge, as well as any increase in the demand for water as a result of increasing temperatures and the rate of reservoir evaporation. Although WaterSMART Basin Study Program activities will eventually address these additional metrics under §9503(b)(2), the surface water hydrologic projections are intended to inform assessment of impacts related to snowpack and streamflow.

The focus of this report is to describe the development of these surface water hydrologic projections and to provide a summary evaluation of climate change implications for surface water hydrology in the eight major Reclamation river basins listed in the SECURE Water Act. The evaluation includes assessment of future climate conditions over the basin (i.e., precipitation and temperature) as well as surface water hydrologic response (i.e., snow water equivalent as a measure of water availability from snowpack and streamflow runoff).

The report is organized as follows:

- Chapter 2 of the report provides background on the role of climate information in water resources planning and management.
- Chapter 3 describes the future climate projections used for developing the surface water hydrologic projections, including how the climate projections were bias-corrected and spatially downscaled for use in this activity.
- Chapter 4 presents the methodology used for developing the hydrologic projections, including:
 - Rationale for selecting hydrologic model applications for use in this activity.
 - Description of the chosen hydrologic model-applications
 - A discussion of how these hydrologic model-applications were used in a climate projection context, including simulation setup and generation of weather inputs consistent with climate projections.
 - Characterization of runoff simulation biases and their implications for assessing hydrologic impacts.
- Chapter 5 presents the summary overview of hydrologic projections in the eight major Reclamation river basins listed above. The overview focuses on annual climate projections over the basins, decadal changes in

temperature and precipitation, decadal changes in April 1st snowpack, and decadal changes in mean-monthly and mean-seasonal runoff.

- Chapter 6 presents a summary discussion of the uncertainties associated with the hydrologic analysis. These uncertainties range from the climate through the hydrologic tool utilized to assess the natural hydrologic response to the climate projections.

CHAPTER 2

Background

Reclamation and other water resource management agencies regularly conduct assessments of water resources management and reservoir systems operations. Such assessments might focus on current system conditions or analysis of proposed changes in operations and/or infrastructure conditions intended to provide service through an identified future time period. For discussion purposes here, assessments that consider operations over a future time period greater than 10 to 20 years in duration are referred to as long-term assessments, and require making assumptions about possible future water supplies, demands and operational constraints that would affect system operations. As illustrated in figure 1(adapted from U.S. Geological Survey Circular 1331 [Brekke et al. 2009a]), assumptions about water supplies, demands, and constraints are characterized within a climate context. Traditionally, long-term assessments have assumed that this climate context can be defined by historical records, meaning that the envelope of historical climate variability is reasonable for planning purposes. At a minimum, such historical information includes observations from the period of instrumental records; however, for some regions, there are also indicators of paleoclimate variability from the pre-instrumental record (e.g., tree ring chronologies describing annual climate fluctuations in the Southwest United States). In any case, traditional assumptions have been made based on instrumental records or a blend of paleoclimate proxies and instrumental records.

Recent information suggests that future envelopes of climate variability may differ from historical, particularly in terms of temperature for all regions and precipitation for many regions (Intergovernmental Panel on Climate Change [IPCC] 2007; U.S. Global Change Research Program [USGCRP] 2009). As a result, future climate projections have become increasingly relevant as a source of information to be blended with historical information when defining planning assumptions about future water supplies, demands, and operational constraints. Such blending often involves combining variability information from the historical context (e.g., sequencing information, such as the interarrival of wet/dry spells or cool/warm spells) with climatology information suggested by climate projections (e.g., mean or distribution of climate conditions). The process of incorporating climate projection information into longer-term water resources assessments leads to several method choices, highlighted on figure 2, and related questions:

West-Wide Climate Risk Assessments:
BCSD Surface Water Projections

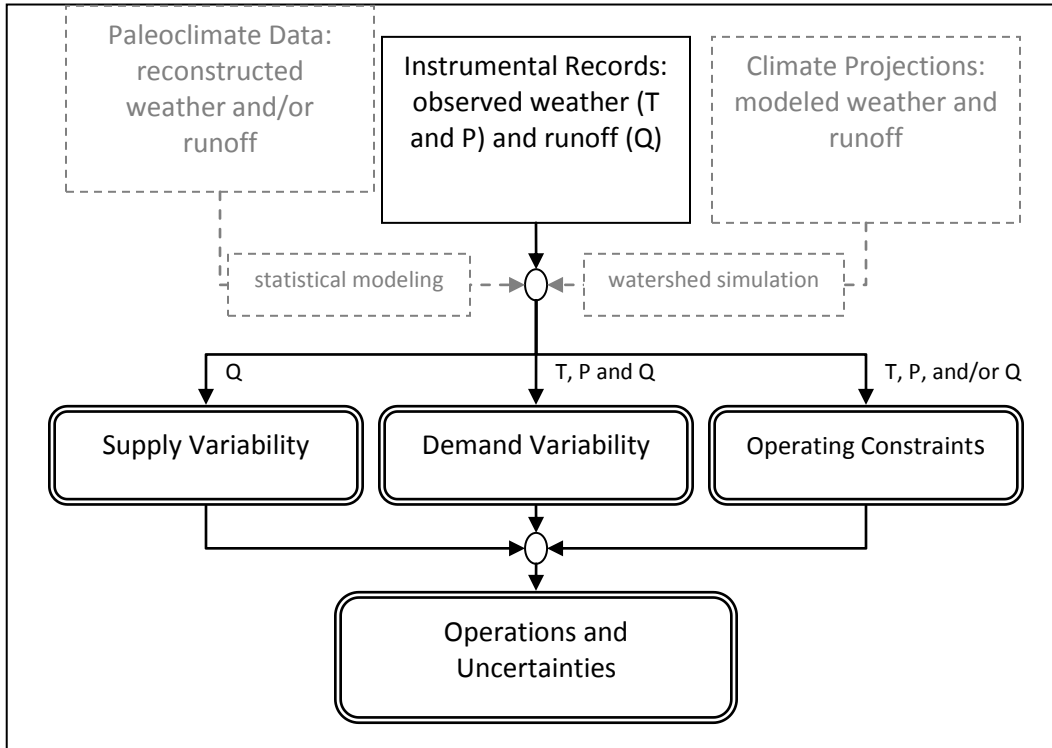


Figure 1. Climate-related Assumptions in Longer-term Operations Planning.

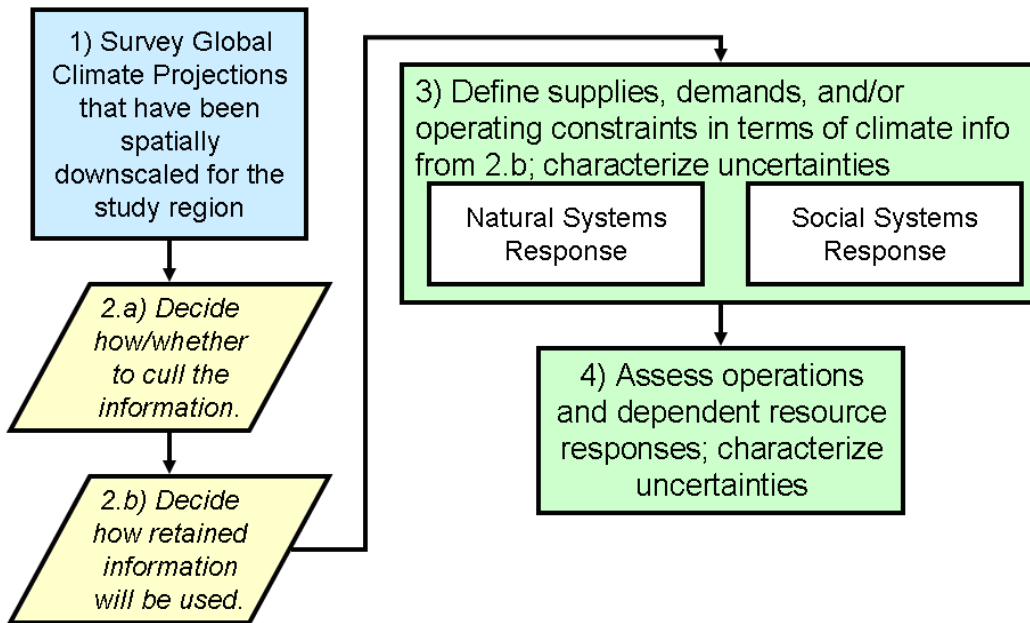


Figure 2. Framework for Relating Climate Projection Information to Longer-term Operations Planning.

(Figure 2, step 1) *Survey of available climate projections:* There is a wealth of climate projection made available through the World Climate Research Programme's (WCRP) Coupled Model Intercomparison Project phase 3 (Meehl et al. 2007). Recently developed projections from this effort are discussed in chapter 3. Projections from these activities continue to evolve as the climate science community develops improved methods for defining future scenarios of climate forcing as well as improved approaches for modeling climate in response to these forcings.

(Figure 2, step 2.a) *Decision on which climate projections are credible for assessment purposes:* After surveying available projections, a fundamental question emerges: should all available climate projections be regarded as suitable for assessment purposes, or is there a more credible subset that should be used to inform assessment assumptions? If a subset is chosen, a secondary question emerges: how does one determine relative credibility to support such projection "culling"?

(Figure 2, step 2.b) *Decision on how to use "credible" and retained projections for assessment purposes:* Questions under this heading relate to the blend of historical information and climate projection information: how much climate projection information should influence assessment assumptions (e.g., change in climatological means; change in climatological distributions; sequencing of climate projection conditions)? Answers to these questions lead to different method classes of incorporating climate projection information into water resources assessments:

- Step-change or "climate change" methods
 - Delta method (e.g., Hamlet and Lettenmaier 1999; Lettenmaier and Gan 1990; Lettenmaier et al. 1999; Miller et al. 2003)
 - Hybrid-Delta method (e.g., McGuire and Hamlet 2010)
 - Ensemble-informed versions of both (e.g., Vano et al. 2010; Reclamation 2010)
- Time-evolving projection methods that map climate projection sequences to hydrologic or operations sequences (e.g., Wood et al. 2004; Payne et al. 2004; Christensen et al. 2004; Van Rheezen et al. 2004; Christensen and Lettenmaier 2007; Maurer 2007).

(Figure 2, step 3) Given the choice on how to use the retained climate projection information and an implicit method class for relating these projections to planning assumptions (e.g., step-change versus time-evolving), choices then follow on

which types of natural and/or social systems studies need to be conducted to adequately characterize assumptions about future supplies, demands, and operational constraints under the chosen climate context.

This report focuses on only steps 1 through 3 in figure 2. For step 3, the focus is specifically on climate change implications for surface water hydrology conditions in the Western United States. Conceptually, it is reasonable to expect a changing climate to affect the relationship between basin precipitation, temperature, and runoff. For example, warming air temperatures over a snowmelt-dominated basin likely is to lead to proportionally more rainfall and less snowfall and likely to increased rainfall-driven runoff volumes during winter; such winter impacts would be amplified or offset if precipitation generally increases or decreases, respectively. Winter warming likely would reduce the areal extent and seasonal duration of snowpack and, subsequently, lead to reduced spring–summer snowmelt-runoff. Given changes in precipitation regime and runoff response, the fate of precipitation over the basin would be affected over time (i.e., runoff versus evapotranspiration).

Chapter 3 of this report provides information on this study’s decisions related to steps 1 and 2. Chapter 4 provides information on this study’s decisions related to step 3. To briefly preview: hydrologic projections presented in this report are developed based on available projections from the “Bias-Corrected and Spatially Downscaled WCRP CMIP3 Climate Projections” archive,³ basin applications of the Variable Infiltration Capacity (VIC) hydrologic model spanning the Western United States, and hydrologic impacts assessment methodologies previously demonstrated in peer-reviewed literature. Additional assessment activities as authorized within the SECURE Water Act, analyzing potential impacts, and the development of adaptation and mitigation strategies are being addressed through efforts within Reclamation’s WaterSMART Basin Study Program.

³ http://gdo-dcp.ucllnl.org/downscaled_cmip3_projections/dcpInterface.html.

CHAPTER 3

Climate Projections

3.1 Survey of Available Global and Downscaled Climate Projections

During the past decade, global climate projections have been made available through the efforts of the World Climate Research Programme (WCRP) Coupled Model Intercomparison Project (CMIP), which has advanced in three phases—CMIP1 (Meehl et al. 2000), CMIP2 (Covey et al. 2003), and CMIP3 (Meehl et al. 2007). The WCRP CMIP3 efforts were fundamental to completing the IPCC Fourth Assessment Report (IPCC 2007). The CMIP3 dataset was produced using climate models that include coupled atmosphere and ocean general circulation models, each applied to simulate global climate response to future greenhouse gas (GHG) emissions paths (IPCC 2000) from various end-of-20th century climate conditions (“runs”). The emissions paths vary from lower to higher emissions rates, depending on scenarios of global technological and economic developments during the 21st century. As mentioned in chapter 2, the climate science community continues to develop improved methods for defining future scenarios of climate forcing and approaches for modeling climate in response to these forcings. Such activities are expected to lead to the release of an updated set of global climate projections sometime during 2011—labeled CMIP5⁴ to numerically coincide with IPCC’s Fifth Assessment (expected in approximately [~] 2014)). For the purposes of this study, CMIP3 projections were used because they represented the best available collection of climate projection information at the onset of this effort (summer 2010). It is anticipated that, given continued authorizations and appropriations, the hydrologic projections presented within this report will be updated as new methods and information become available in conjunction with the SECURE Water Act.

One issue with the CMIP3 dataset and climate models projections, in general, is that the spatial scale of climate model output is too coarse for regional studies on water resources response (Fowler et al. 2007; Maurer et al. 2007). Spatial downscaling of global climate model (GCM) outputs typically is conducted to address this issue. By definition, spatial downscaling is the process of taking GCM output on simulated climate and translating that to a finer spatial scale that

⁴ See CMIP5 overview information at <http://cmip-pcmdi.llnl.gov/cmip5/index.html?submenuheader=0>.

is more meaningful for analyzing local and regional climate conditions. Many downscaling methods have been developed, all of which have strengths and weaknesses. Several reports offer discussion on the various methodologies, notably the IPCC Fourth Assessment (IPCC 2007 [Chapter 11, “Regional Climate Projections”]; Wigley 2004; and Brekke et al. 2009a [Appendix B]). The various methodologies generally can be classified into two classes:

- Dynamical
 - Where a fine scale regional climate model (RCM) with a better representation of local terrain simulates climate processes over the region of interest
- Statistical
 - Where large-scale climate features are statistically related to fine scale climate for the region

Dynamical downscaling has yet to produce an archive that comprehensively reflects the 100 plus CMIP3 climate projections available, particularly to characterize climate projection uncertainty throughout the 21st century. While there are new efforts to downscale multiple climate projections using multiple RCMs, such as the North American Regional Climate Change Assessment Program (<http://www.narccap.ucar.edu/>), the computational requirements of RCM implementation for more than a few projections and decades of simulation have limited the feasibility of using dynamical downscaling for the purpose above. Although various statistical methods might be considered for the given purpose, certain method characteristics are desirable:

- Well tested and documented, especially for applications in the United States
- Efficient enough to permit the downscaling of many 21st century climate projections, thereby supporting a comprehensive assessment of regional to local climate projection uncertainty
- Able to produce output that statistically reproduces a range of characteristics (including spatial and temporal patterns) of historical observations when driven by climate simulations for retrospective periods
- Capable of producing spatially continuous, fine scale fields of precipitation and temperature suitable for water resources and other watershed-scale impacts analysis

One technique that satisfies these criteria is the Bias Correction and Spatial Disaggregation (BCSD) approach of Wood et al. 2002. This technique was used to generate downscaled translations of 112 CMIP3 projections, which are available online at the “Bias-Corrected and Downscaled WCRP CMIP3 Climate Projections” archive⁵ (BCSD climate projections, referring to the methodology described above). The BCSD climate projections ensemble was produced collectively by 16 different CMIP3 models simulating 3 different emissions paths—carbon dioxide [CO₂] concentrations of B1 (low), A1B (middle), and A2 (high) from different end-of-20th century climate conditions. Compared to dynamical downscaling approaches, the BCSD method has been shown to provide downscaling capabilities comparable to other statistical and dynamical methods in the context of hydrologic impacts (Wood et al. 2004). However, there are limitations to statistical downscaling; dynamical downscaling has been shown to identify some local climate effects and land surface feedbacks that BCSD cannot readily characterize (Salathé et al. 2007). Another potential limitation of BCSD, like any statistical downscaling method, is the assumption of some statistical stationarity in the relationship between GCM scale precipitation and temperature and finer-scale precipitation and temperature.

3.2 Decisions on Whether to Cull Available Downscaled Climate Projections (BCSD Climate Projections)

For this study, consideration was given toward the view that some of the BCSD climate projections might be relatively more credible to support surface water hydrologic projection purposes for the WWCRA activity, based on some relative regard for the global climate projections that underlie the BCSD projections. A credibility evaluation leads to some projections culling rationale. Relative credibility of available projections might be based on views about the likelihood of the future emissions scenario underlying the given climate projection (IPCC 2000) or the views about the skill of the CMIP3 GCM used to simulate climate conditions within the given emissions scenario. Briefly stated, the basis for establishing such culling rationale was found to be unclear; and all BCSD climate projections were regarded as eligible in this activity. The remainder of this section discusses considerations that led to this determination.

On determining relative likelihood for emissions scenarios, there is limited guidance on which scenario pathway is more probable (IPCC 2007). As stated above, the BCSD climate projections dataset represents three potential

⁵ Available from http://gdo-dcp.ucllnl.org/downscaled_cmip3_projections/. Accessed July 2010.

scenarios of greenhouse gas emissions and associated climate forcing from the IPCC Special Report on Emissions Scenarios (SRES) (IPCC 2000): A1B, A2, and B1 (IPCC 2000). These SRES scenarios might be qualitatively described as follows:

- SRES A2: (~ “higher” emissions path) Technological change and economic growth more fragmented, slower, higher population growth.
- SRES A1B: (~ “middle” emissions path) Technological change in the energy system is balanced across all fossil and nonfossil energy sources, where balanced is defined as not relying too heavily on one particular energy source.
- SRES B1: (~ “lower” emissions path) Rapid change in economic structures toward service and information, with emphasis on clean, sustainable technology. Reduced material intensity and improved social equity.

Neither the IPCC 2000 nor the IPCC 2007 report offers suggestions on which scenario pathway may be more likely. Hence, no assumptions are made in this study about this matter, and no projection culling is performed on the basis of relative regard for these emission scenarios. For projection results during the first part of the 21st century, this discussion may be moot anyway, as the distribution of CMIP3 climate projections do not appear to become dependent on the IPCC SRES pathway until about the middle 21st century (IPCC 2007).

On determining relative credibility of climate models, there has been more research activity (e.g., Dettinger 2005; Tebaldi et al. 2005; Brekke et al. 2008; Reichler and Kim 2008; Gleckler et al. 2008; Mote and Salathé 2010). The general approach has been to evaluate the relative capabilities, or “skill,” of climate models when they are used to simulate past climate conditions under assumed historical climate forcings (e.g., solar activity, volcanic events, gradual observed buildup of atmospheric greenhouse gases and aerosols). Climate models that simulate climate conditions closer to observations then are regarded as having better skill. A philosophical bridge then can be made—that the better climate models, based on historical simulation skill, should offer more reliable climate simulations for the future. To date, there is still limited evidence to support such a philosophical bridge (Reichler and Kim 2008; Santer et al. 2009; Pierce et al. 2009). It also has been shown that when such skill assessments are based on many climate metrics (e.g., Tebaldi et al. 2005; Mote and Salathé 2010), the clarity of “better” versus “worse” climate models is less obvious than when the assessment is based on few metrics (Brekke et al. 2008; Reichler and Kim 2008; Gleckler et al. 2008). Even when the historical skill assessment results have been used to rank and cull climate models, thereby conditioning the assessments of

future climate uncertainty (Brekke et al. 2008) or detection and attribution of causes for trends in historical atmospheric water vapor over large spatial scales (Santer et al. 2009), the effect of model culling on assessments has been minor. These latter results suggest that other factors, beyond historical skill, are driving impact assessments from projected climate conditions within an ensemble, including emissions pathway and a GCM's "natural variability." The latter is important because sequences of simulated regional climate variability depend on initial global climate state (i.e., distributed ocean heat content or phase-state of ocean cycles like the Pacific Decadal Oscillation), and CMIP3 projections do not exhibit consistent initial global climate states. Reconciling initial climate system conditions for future climate projections is a research issue being addressed in CMIP5. As for interpreting CMIP3, the matter of inconsistent initial conditions has been shown to be significant on interpreting climate projection uncertainty at a spatial scale of the British Isles (e.g., interpreting decadal temperature uncertainty in Hawkins and Sutton 2009) and the major river basins of the Western United States (e.g., interpreting decadal precipitation uncertainty in Hawkins and Sutton 2010).

In summary, given inconclusive evidence to demonstrate the utility of culling projections based on relative GCM skill or evidence suggesting greater likelihood of one GHG emissions path over another, this activity includes all projections from the chosen data source.

3.3 Decisions on How To Use Retained BCSD Climate Projections

Either step-change or time-evolving applications might have been featured in this effort. A decision was subjectively made to focus on a time-evolving application, following the methods first introduced in Wood et al. (2002) and later applied in numerous other studies (e.g., Wood et al. 2004; Payne et al. 2004; Christensen et al. 2004; Christensen and Lettenmaier 2007; Van Rheezen et al. 2004; and Maurer 2007). Choice of a time-evolving application implies that the ensemble of monthly BCSD climate projections are translated into an associated ensemble of hydrologic projections for the Western United States. For comparison of step-change versus time-evolving applications, including discussion of strengths and weaknesses, the reader is invited to Brekke et al. 2009a and Hamlet et al. 2010.

In summary, time-evolving applications are useful for characterizing an envelope of hydroclimate possibility evolving from GCM-simulated past to GCM-simulated future. In this manner, it is possible to assess when hydroclimate conditions are expected to cross management thresholds of

interest, which is useful for adaptation planning exercises where the onset of impacts matters. However, for impact assessments that are more localized in space or time, a step-change approach might be a more conservative and appropriate use of GCM-simulated climate information. Time-evolving applications feature a richer sampling of GCM-simulated climate information than what might be featured in step-changes applications (e.g., sampling monthly climatic sequences in time-evolving compared to only sampling climatological conditions in a step-change application while relying on historical information to define sequence possibilities). At this time, there is no well established practice or guidance on when step-change or time-evolving applications should be used,⁶ and developing such guidance remains an area of active research. For SECURE Water Act assessment purposes, a range of hydrologic impacts metrics are being assessed ranging from regional to local scales. Noting that output information generated from a time-evolving hydrologic study could be flexibly evaluated through a step-change view or projection view, it was decided to follow the time-evolving methodology cited above.

3.4 Methodological Issues Affecting Interpretation of the BCSD Climate and Hydrologic Projections

Each BCSD climate projection is specified on a monthly time step from January 1950 to December 2099 and at roughly a 12-kilometer (km) (1/8-degree [°] latitude by longitude) spatial resolution over the contiguous United States.

Application of BCSD involves:

- Choosing a gridded monthly time step observations (termed “obs”) dataset, also called an observed climatology, to guide both bias correction of GCM output and subsequent spatial disaggregation, which, in this case, the observed data are from Maurer et al. 2002 (1/8° obs).
- Aggregating gridded observations to the coarse scale of bias correction (2° obs).
- Generating two intermediate datasets: (a) GCM monthly temperature and precipitation outputs interpolated to the bias correction grid (2° Raw) and (b) bias-corrected versions of these GCM outputs trained to 2° obs (2° BC). The use of a single bias correction grid is a convenience; but in practice, the native resolution grid of each climate model could be used for bias correction, provided a coarse-scale obs grid is created for each.

⁶ Climate Change and Water Working Group Workshop “Assessing a Portfolio of Approaches for Producing Climate Change Information to Support Adaptation Decisions,” Boulder, Colorado, November 2010.

- Forming a quantile-map relationship from an historical overlap period of observations and simulations (e.g., 1950–1999).
- Bias correction: using the quantile-map relationship to translates GCM outputs to matching quantiles from the coarse-scaled observed (2° obs) dataset for both past and future periods of the climate simulation. For temperature, a filtered trend is removed before the mapping and replaced afterward to avoid the problem of a climate model temperature distribution, which shifts significantly in the future. In contrast, precipitation shifts generally are found to be nonsignificant; and this step is not imposed.
- Generating the final BCSD where coarse-scale changes are spatially disaggregated to finer scale changes and merged with the 1/8° obs information (1/8° BCSD). Future climate anomalies (percent [%] change for precipitation and +/- change for temperature) are interpolated to the fine scale and applied to the observed fine scale historical temperature and precipitation means.

For more illustration of the BCSD methodology, see the “About” page at the archive Web site⁷ or consult Wood et al. (2002; 2004).

The BCSD methodology introduces some issues that affect interpretation of BCSD climate and hydrologic projections, four of which are described in this section.

1. **Residual Bias in Historical Climate Conditions:** The BCSD methodology’s *bias correction* step addresses climate model biases in simulating monthly climatology. This bias is identified during a period of common historical overlap between observations and climate simulation (i.e., the 1950–1999 period of Maurer et al. 2002, comparing the Maurer et al. 2002 data aggregated to 2° obs and to a given GCM’s historical climate simulation regridded to be 2° Raw). The resulting 2° bias-corrected (BC) data feature monthly temperature and precipitation distributions that match those of 2° obs, by design of the methodology. However, there are no constraints that the 2° Raw and 2° obs distributions of *seasonal* or *annual* temperature and precipitation conditions should match. Thus, residual biases remain at nonmonthly time scales.
2. **Different Bias Correction of 21st Century Temperature and Precipitation:** The BCSD methodology’s *bias correction* step typically has been applied (Wood et al. 2002, 2004) differently for monthly temperature versus monthly precipitation. The net effect is that 20th to

⁷ http://gdo-dcp.ucllnl.org/downscaled_cmip3_projections/dcpInterface.html#About.

21st century raw climate model projected *changes* in mean-annual *precipitation* from 2° Raw are not necessarily preserved and equally expressed by the 2° BC data. In contrast, changes in mean-annual *temperature* are largely the same in the 2° Raw and 2° BC data.

- 3. Both Bias Correction and Spatial Disaggregation Affect Locally Portrayed Climate Change in BCSD projections:** Changes in period-climate (e.g., 1970–1999 climate to 2040–2069 climate) are affected by both bias correction and spatial downscaling. It has been shown that when assessing local climate changes in the BCSD data, the assessed changes can be influenced by both steps of the BCSD methodology, and to a varying degree based on the location being considered.⁸ For precipitation projections, it is shown in this section that the bias correction method appears to have introduced a positive shift in the distribution of precipitation “climate changes” (from 2° Raw to 2° BC) for much of the BCSD’s geographic domain.⁹ This shift may stem from issue (2) above; however, more method diagnosis is required to make a determination. The result implies that, relative to the underlying CMIP3 precipitation ensemble, the BCSD future precipitation ensemble is slightly wetter (up to 5 percent) relative to current period precipitation.¹⁰

The remainder of this section provides graphical examples to illustrate the first three issues. On the first issue, figures 3–7 illustrate bias between 2° obs and 2° Raw monthly climate distributions and the effect of bias correction to produce 2° BC results. The figures focus on results in a 2° grid cell located in northern California (centered at 39N and 121W, figure 3). Application of the bias correction procedure involves first identifying bias during a period of common historical overlap between observed and simulated conditions (1950–1999). Simulated values are then forced to match observed values at corresponding quantiles (e.g., figure 4 for temperature and figure 6 for precipitation). When bias-corrected monthly values are aggregated to seasonal values during this period (e.g., three 3-month seasons shown on figure 5 for temperature and figure 7 or precipitation), the resultant seasonal observed and simulated distributions do not necessarily match. Thus, when interpreting the 1950–1999 historical period of BCSD data, it is expected to match monthly climatology at 2° resolution but not necessarily seasonal, annual, or other nonmonthly climatology.

⁸ http://gdo-dcp.ucllnl.org/downscaled_cmip3_projections/docs/Brekke%20Poster_9DEC09.pdf.

⁹ Also is discussed in the American Geophysical Union (AGU) 2010 fall meeting presentation, “What’s a billion cubic meters among friends: The impacts of quantile mapping bias correction on climate projections,” J. Barsugli, GC51A-0737.

¹⁰ Ed Maurer (personal communication). “Dave Pierce has pointed me toward some other behavior of quantile mapping, where GCM bias in variance can cause this. I believe this may overlap with Joe Barsugli’s analysis, where he used a skewed distribution. In any case, there is more work to be done on this.”

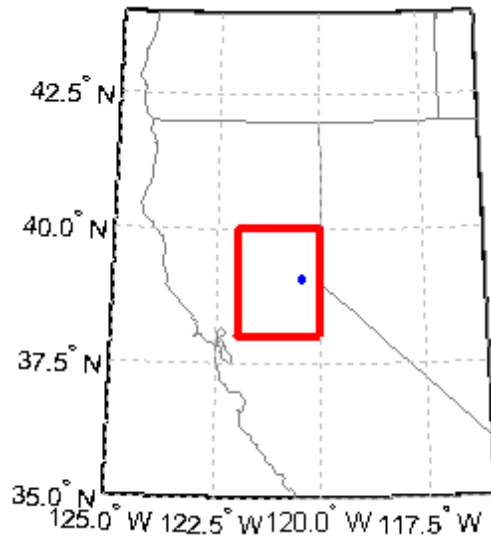


Figure 3. Climate Projection Bias Correction
Example: Location.

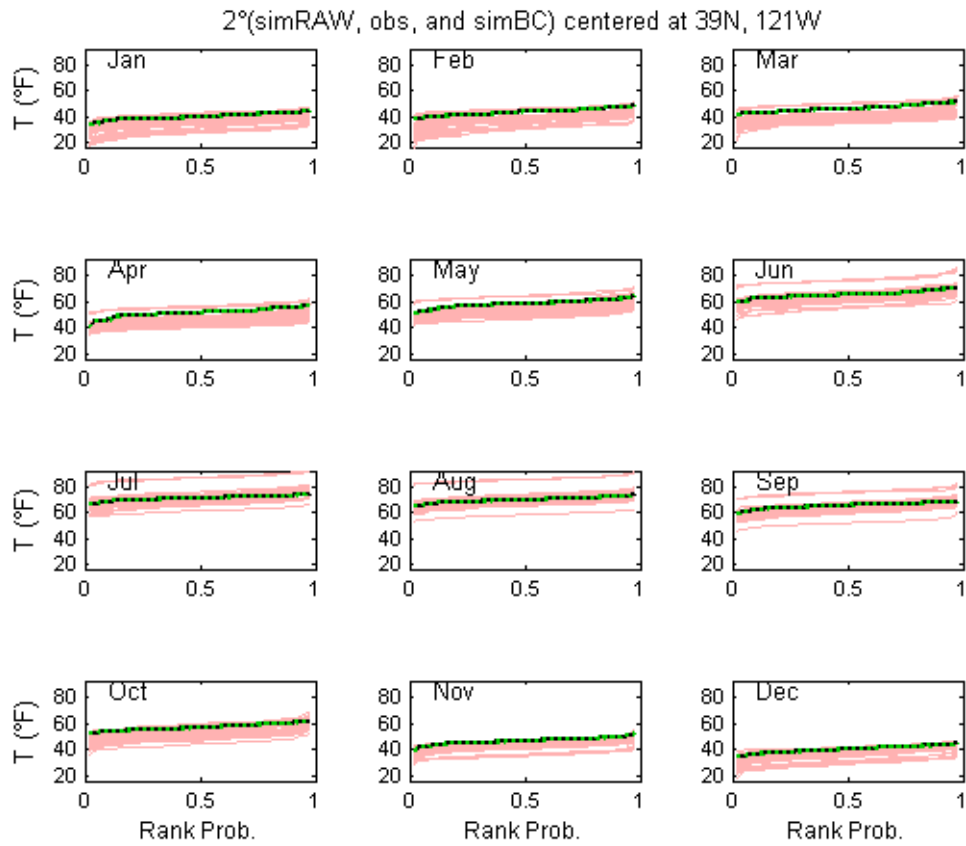


Figure 4. Climate Projection Bias Correction Example: Monthly Temperature.

Figure 4 shows month-specific panels, where each panel shows a single 1950–1999 distribution of 2° obs (heavy black line), 112 simulation-specific 1950–1999 distributions of 2° Raw (red lines), and 112 simulation-specific 1950–1999 distributions of 2° BC (dashed green lines, all superimposed on one another by design of the bias correction procedure).

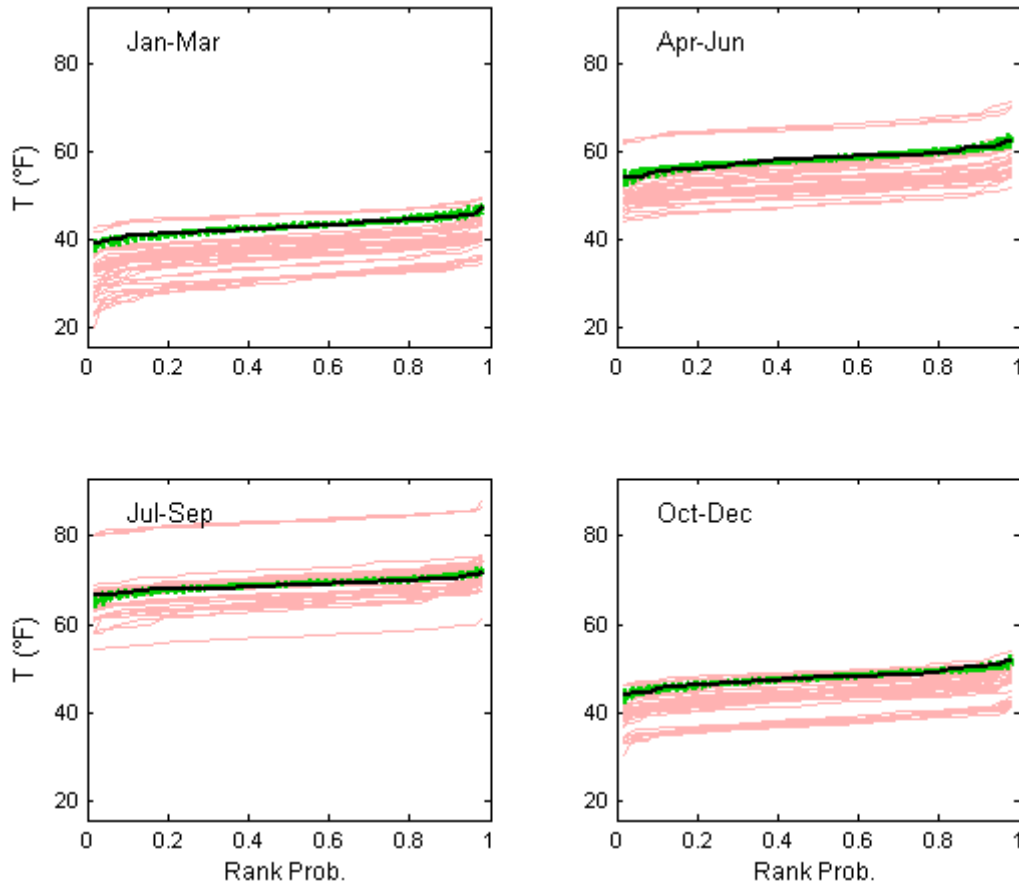


Figure 5. Climate Projection Bias Correction Example: Seasonal Temperature.

Figure 5 shows season-specific panels, where each panel shows a single 1950–1999 distribution of 2° obs (heavy black line), 112 simulation-specific 1950–1999 distributions of 2° Raw (red lines), and 112 simulation-specific 1950–1999 distributions of 2° BC (dashed green lines, free to vary by design of the bias correction procedure).

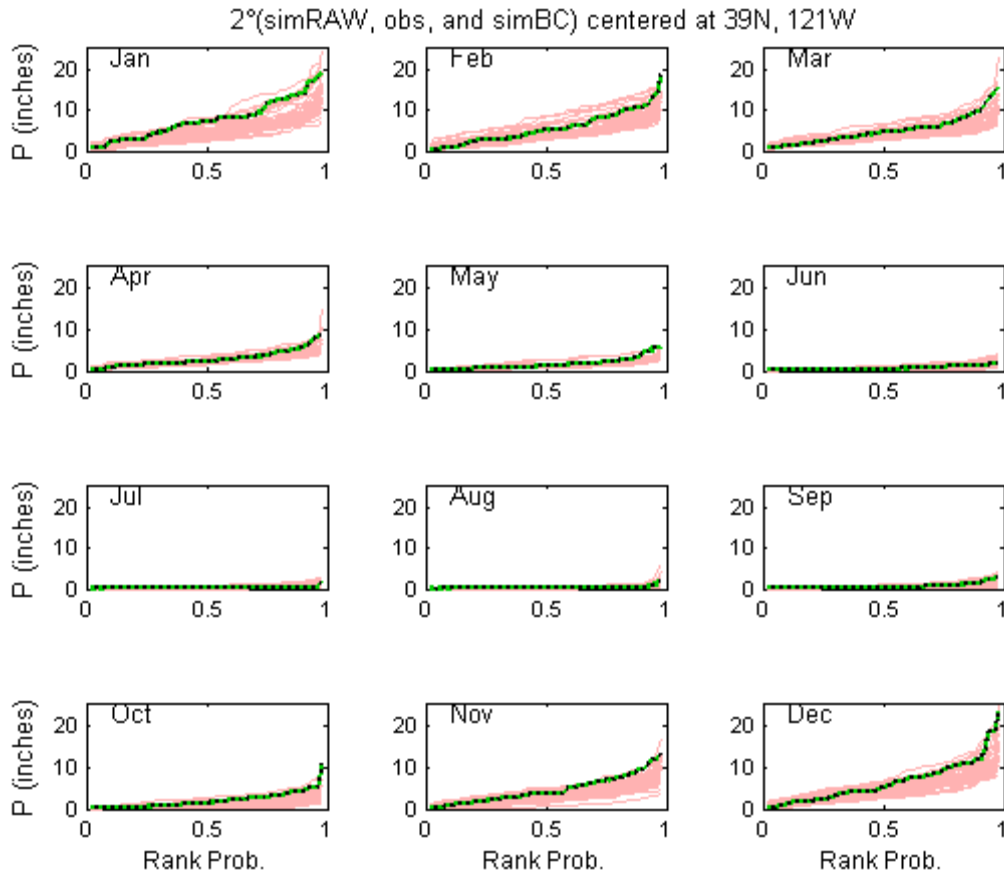


Figure 6. Climate Projection Bias Correction Example: Monthly Precipitation.

Figure 6 shows month-specific panels, where each panel shows a single 1950–1999 distribution of 2° obs (heavy black line), 112 simulation-specific 1950–1999 distributions of 2° Raw (red lines), and 112 simulation-specific 1950–1999 distributions of 2° BC (dashed green lines, all superimposed on one another by design of the bias correction procedure).

West-Wide Climate Risk Assessments:
BCSD Surface Water Projections

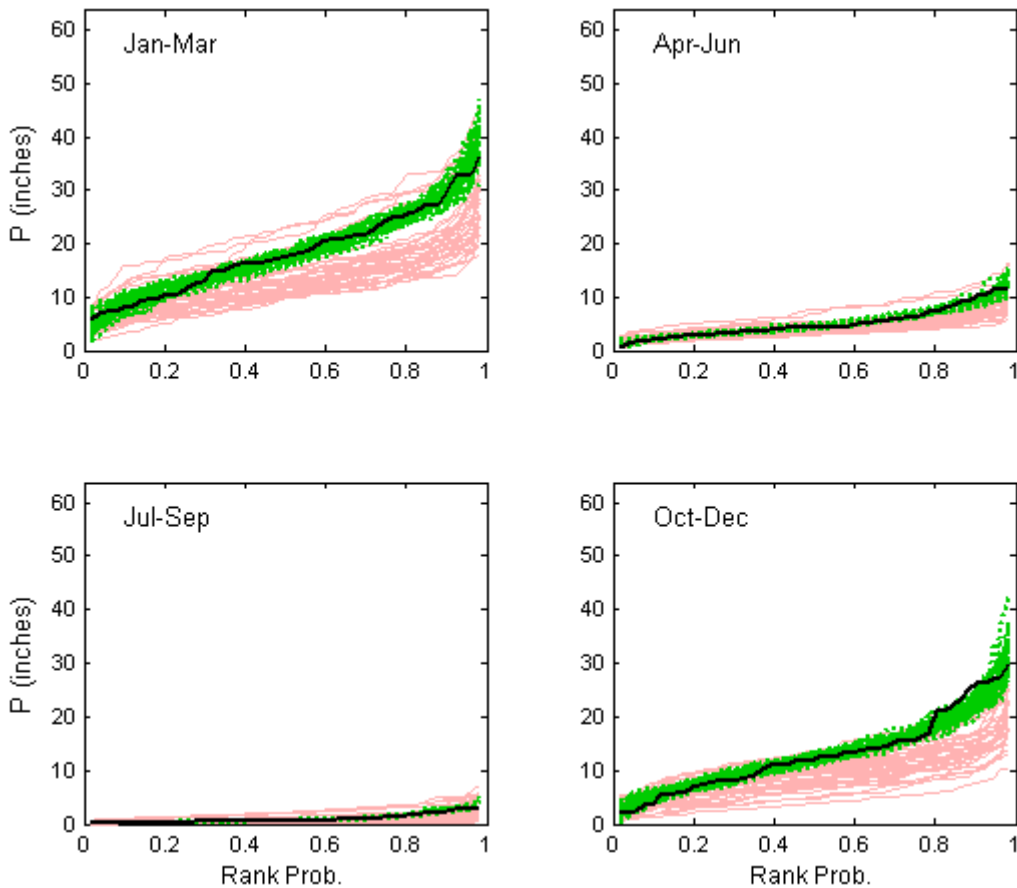


Figure 7. Climate Projection Bias Correction Example: Seasonal Precipitation.

Figure 7 shows season-specific panels, where each panel shows a single 1950–1999 distribution of 2° obs (heavy black line), 112 simulation-specific 1950–1999 distributions of 2° Raw (red lines), and 112 simulation-specific 1950–1999 distributions of 2° BC (dashed green lines, free to vary by design of the bias correction procedure).

Note that the foregoing analysis of figures 4–7 shows that the monthly bias correction does afford an incidental bias correction effect at the seasonal (and presumably annual) time scales. A similar result was found by Maurer et al. (2010) where quantile mapping bias correction applied to daily data removed the majority of the bias in monthly aggregated data as well. For temperature, the residual biases appear to be of second order importance relative to the incidental seasonal bias correction. For precipitation, however, the residual seasonal biases are relatively larger and can approach the magnitude of incidental seasonal bias correction, particularly for extremes. The seasonal biases likely reflect differences in monthly autocorrelation found in observed climate and in model

climates, but the extent to which they affect downscaled change statistics (i.e., differences between future and present climates within a model) is not known. A model lacking observed autocorrelation for 20th century climate also may lack it for 21st century climate, such that extreme seasons are biased low in both time periods with reduced effect on change statistics. The effect of residual biases at nonmonthly time scales is, thus, an area for further study.

On the issue of differences in how bias correction is applied to temperature and precipitation, the chief difference is that for temperature, before applying bias correction to 21st century projected values, the 21st century trend in 2° Raw is identified and set aside. Subsequently, bias correction is applied to the trend-removed values, and then the trend that was removed is added back to these values to produce 2° BC temperatures. As discussed in Wood et al. (2004), this is important during the temperature bias correction step to prevent rising future temperatures from falling disproportionately on the extreme tail of the 2° obs monthly distribution and requiring frequent extrapolation of the empirical distributions used in the quantile-mapping bias correction. An important side effect of this procedure is that the 2° BC is forced to have the same trend as 2° Raw. For precipitation, this trend-removal and re-insertion step has not been implemented in past studies, though ongoing work is using this approach for precipitation as well as temperature. Consequently, 21st century trends in precipitation are not forced to be the same for 2° Raw and 2° BC as they are for temperature.

The decision to omit the trend-preservation step for precipitation in Wood et al. (2004) arose from the observation that most trends in the pre-CMIP3 model runs for precipitation, in western North America, were not statistically significant. Consequently, future precipitation monthly distributions aligned sufficiently with those for current climate so that the need for extrapolation during the quantile-mapping step was minimal. Where extrapolation is applied for temperature, a normal distribution is used. For precipitation, a Weibull distribution is used where minimal values are needed; whereas a Gumbel distribution is used to extrapolate maximal values.

This second issue may bear influence on the third issue, which involves the relative effects of bias correction and spatial disaggregation on assessing changes in temperature or precipitation from the BCSD climate projections. An example is illustrated on figure 8. The figure results are from a BCSD 1/8° location within the 2° location just discussed (i.e., blue 1/8° pixel on figure 3 within the 2° red box). First, focus on temperature and precipitation projection ensembles for this pairing of 1/8° and 2° grid-cells (figure 8, left column showing ensembles of 2° Raw (red), 2° BC (green) and 1/8° BCSD (blue)). These time series ensembles show that bias correction can affect the spread and central tendency of projection

values as they evolve through time (red ensemble versus green ensemble). It's evident that spatial downscaling also can have an effect (e.g., green ensemble versus blue ensemble). In this example, downscaling to the given 1/8° grid cell leads to a cooler and wetter ensemble, which is understandable since the 1/8° grid cell is at a higher elevation in the Sierra Nevada and subject to orographic enhancement of precipitation relative to the lower Central Valley areas contained within the 2° grid cell.

The right column of figure 8 illustrates to the latter aspects of the third issue: how bias correction may affect the interpretation of precipitation changes. Focusing on a historical and future period (1970–1999 to 2040–2069, gray column areas in left column of figure 8), changes in mean-annual temperature (degree Fahrenheit [°F]) and mean-annual precipitation (%) are assessed within each of BCSD projections (i.e., 112 projections leading to distributions of 112 changes). These changes then are shown (figure 8, right column) as rank-distributions and for each ensemble (2° Raw [red], 2° BC [green] and 1/8° Raw [blue]). The effect of *bias correction* on this “climate change assessment” is represented through comparison of quantile differences between the 2° Raw (red) and 2° BC (green) distributions. The effect of *spatial disaggregation* on this “climate change assessment” is represented through comparison of quantile differences between the 2° BC (green) and 1/8° BCSD (blue) distributions. For both temperature and precipitation, it's clear that the spatial disaggregation generally doesn't affect the climate change assessment as shown in these distributional views. For temperature, it's also clear that bias correction doesn't substantially affect the assessment of temperature change told by this distributional view. However, for precipitation, the bias correction procedure has affected the precipitation change possibilities, because the distribution of changes from 2° Raw to 2° BC becomes wetter (e.g., roughly 2% wetter at the 50th percentile and roughly 3% wetter at the 75th percentile). What likely happens is that the mapping goes towards a more positively skewed distribution from a normal distribution. This makes the extrapolation issue worse at the high end than at the lower end, where precipitation is bounded. The bias correction for precipitation really wasn't envisioned for situations where a lot of extrapolation would occur, but this plot (figure 8, lower right), for this cell, suggests that this is the case. It is clear that the mapping of a positively skewed variable leads to some changes in the extremes that have a noticeable effect on the mean, and likely exacerbates the wetting problem. This extrapolation behavior is important to the hydrologic projection results in this report, but the issue requires further investigation.

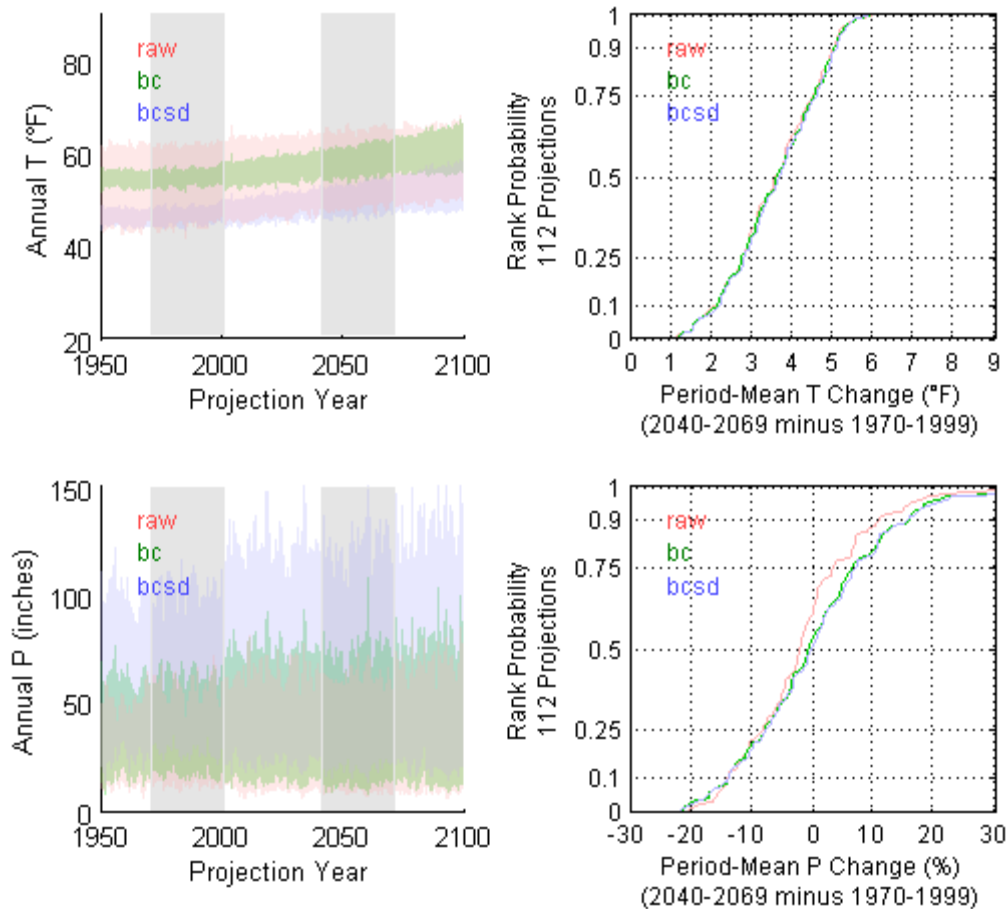


Figure 8. Climate Projections: Effects of Bias Correction and Spatial Downscaling, One Location.

Figure 8 shows the effect of *bias correction* on this “climate change assessment” through comparison between the 2° Raw (red), and 2° BC (green). The effect of *spatial disaggregation* on this “climate change assessment” is represented through comparison of 2° BC (green) and 1/8° BCSD (blue).

Broadening the view to the contiguous United States and doing a similar assessment, but focused on (a) only bias correction effects on climate change assessment, and (b) at three of the quantiles in the distribution (i.e., 25th, 50th, and 75th), it’s clear that the procedure generally leads to a similar effect over much of the United States (figure 9). The effect of quantile temperature changes are minor, generally within +/- 0.1 degree Celsius (°C) as shown.

West-Wide Climate Risk Assessments:
BCSD Surface Water Projections

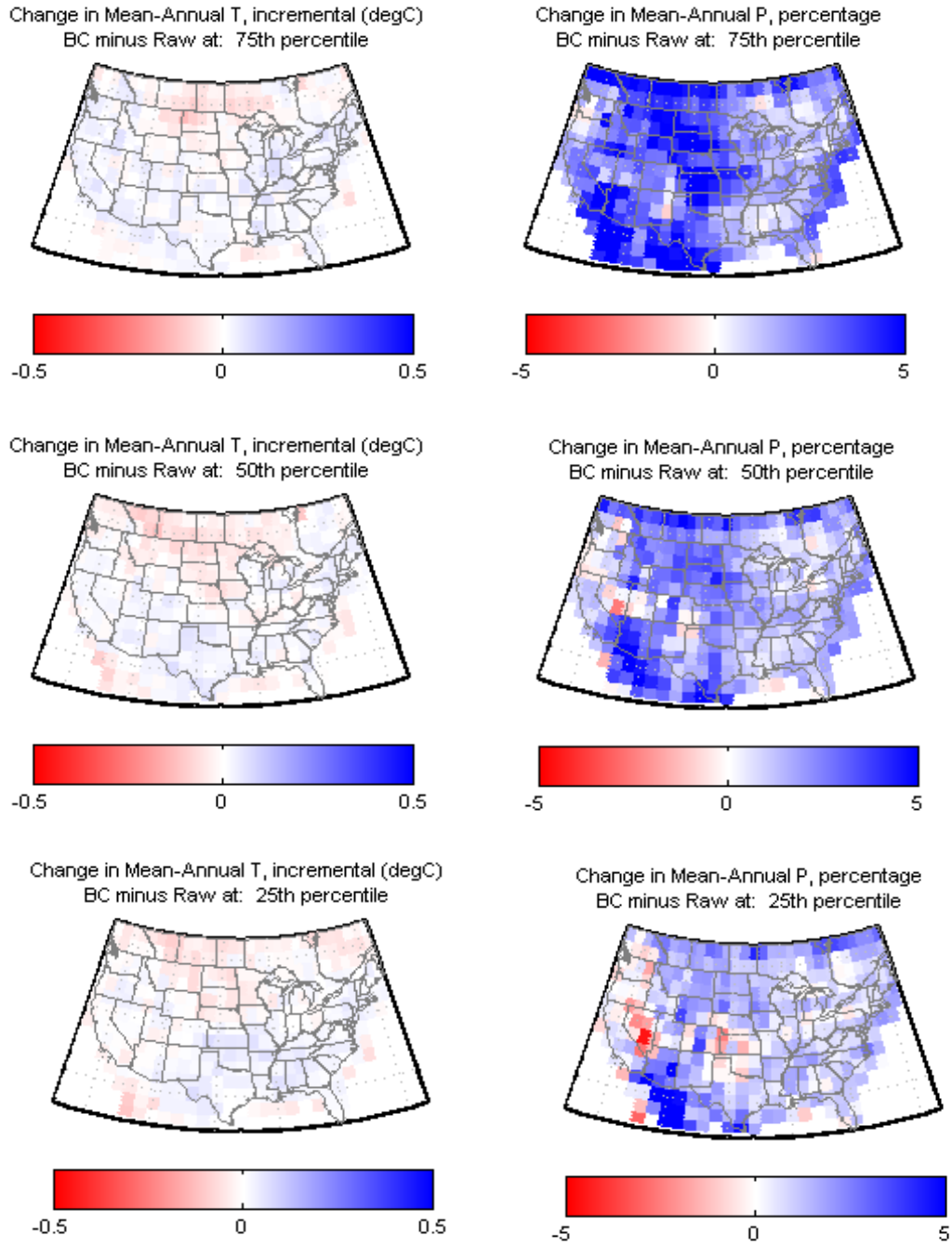


Figure 9. Climate Projections: Effects of Bias Correction, Contiguous United States Locations.

Figure 9 shows difference in the “climate change assessment” conducted at each 2°grid cell for simulated 2040–2069 climate changed from 1970–1999 climate. The percentiles in each panel title correspond to

the change distribution quantile being assessed (e.g., figure 8, right panel, showing all quantiles, but here only focusing on three quantiles).

The effect on quantile precipitation changes is more significant, with large regions experiencing a shift toward wetter changes, particularly at wetter quantiles. The wetting tendency is smaller in the wetter areas (such as the Pacific Northwest) than the drier areas (such as the Southwest United States). Given information from recent studies suggesting that the percentage change in annual runoff of a 1% increase in precipitation may be 2% or greater for many Western United States basins, this finding bears significant implication for the hydrologic assessment that follows in this study. The methodological induced “wetting” of the precipitation projections leads to a portrayal of less adverse hydrologic impacts than if they had been based on the precipitation changes expressed by raw GCM precipitation results.

Despite some methodological issues described here, the BCSD climate projections data used in this activity are useful because:

- They represent a large collection of available CMIP3 climate projection information.
- They reflect climate projection bias correction and spatial downscaling that has been consistently conducted over the Western United States, which is necessary for hydrologic analysis.

That said, there are aspects of the BCSD algorithm that can modulate the climate *change* signal expressed by CMIP3 dataset (prior to bias correction and spatial downscaling), and these aspects should be considered when interpreting hydrologic simulations conducted under BCSD climate conditions. Also note that, BCSD can be applied easily with BC being done on trend-removed or with-trend GCM precipitation.

CHAPTER 4

Developing Hydrologic Projections from Climate Projections

Surface water hydrology models have been used frequently to study climate change impacts on hydrology and water resources (Vicuna and Dracup 2007). Several types of models have been applied in Western United States basins; some examples are:

- Variable Infiltration Capacity model (Liang et al. 1994) applied to investigate impacts in California's Central Valley (Van Rheen et al. 2004; Maurer 2007), Colorado River Basin (Christensen et al. 2004; Christensen and Lettenmaier 2007), the Columbia-Snake Basin (Payne et al. 2004), and numerous others.
- National Oceanic and Atmospheric Administration-National Weather Service's (NOAA-NWS) Sacramento Soil Moisture Accounting model (Burnash et al. 1973) coupled to the Snow17 snow accumulation and ablation model (Anderson 1973) (i.e., SacSMA/Snow17) applied to investigate impacts in the California Sierra Nevada (Miller et al. 2003; Maurer et al. 2010; Brekke et al. 2009b).
- Water Evaluation and Planning model's hydrologic module (Yates et al. 2005) also applied to study California hydrologic impacts (Purkey et al. 2007).
- U.S. Geological Survey's Precipitation Runoff Modeling System (Leavesley et al. 1983) applied in Washington's Yakima River Basin (Mastin 2008) among other locations.
- The Soil and Water Assessment Tool (SWAT) was applied in the San Joaquin basin in California (Ficklin et al. 2009), the Arkansas-Red basin, and the Missouri basin (Rosenberg et al. 1999; Stone et al. 2001).

Application of these hydrologic model types to a study basin generally involves the following types of decisions (not an exhaustive list):

- Spatial structure and resolution at which water balance will be calculated (i.e., gridded area elements or irregular areas defined by topography).
- Soil classes and characteristics that govern infiltration, soil water-holding capacity, etc.

West-Wide Climate Risk Assessments:
BCSD Surface Water Projections

- Land cover classes and characteristics that describe rooting depth access to soil moisture and, in turn, affect potential evapotranspiration.
- Meteorological variables forcing the simulation such as precipitation, temperature, and potentially other weather variables depending on model type.
- Routing scheme for aggregating runoff from subareas to downstream streamflow locations.
- Model structure and physics (e.g., whether and how the snow accumulation and melt cycle is represented).
- Time step for simulating water balance.
- Calibration objectives defining which historical hydrologic aspects the model is developed to reproduce when forced by historical weather (e.g., monthly to annual runoff statistics) and *where* these aspects are to be reproduced (e.g., a menu of locations scattered from upstream to downstream in a larger basin).

This chapter summarizes various aspects of developing hydrologic projections for this effort, including:

- Considerations for Hydrologic Model Selection, including survey of available hydrologic model-*applications* for use in this analysis and the ultimate selection of available VIC model-*applications*.
- Description of selected VIC hydrologic model applications.
- Description of how these model-*applications* were used to develop BCSD surface water hydrologic projections, including simulation setup and generation of daily VIC input weather consistent with monthly BCSD climate projections.
- Discussion of VIC model-*application* biases when simulating historical hydrologic conditions.
- Discussion of bias correction of VIC-simulated runoff and whether such bias correction affects assessment of percentage runoff impacts under climate change.

4.1 Hydrologic Model Selection Considerations

Considerations were focused on available hydrologic model-applications in the Western United States. Model-application availability was defined as being a given runoff model type (e.g., VIC or SacSMA/Snow17), applied to basins *spanning* the Western United States, and where basin-specific applications were verified of subjected model calibration. Among available model-applications, there were two types that generally satisfied these criteria:

- The University of Washington applications of VIC, which have served as seasonal water supply forecasting tools in an experimental Western United States hydrologic forecasting system.¹¹
- NOAA NWS applications of SacSMA/Snow17 (Burnash and Ferral (1996) and Anderson 2006), which currently serve operational hydrologic forecasting purposes in NWS river forecast centers.

Structure and application differences between these model applications, and others not considered (e.g., WEAP, PRMS), introduce some uncertainties when assessing hydrologic response under climate change. Briefly:

- **Structural comparison:** VIC and SacSMA/Snow17 are consistent in that they each simulate surface water balance for a spatial distribution of subareas and then route runoff from these subareas to aggregate runoff locations specified by the user. The two models differ in a variety of ways, including:
 - Required meteorological variables (precipitation and potential evapotranspiration [PET] for SacSMA, average daily temperature and precipitation for Snow17; VIC requiring precipitation, minimum daily temperature, maximum daily temperature, and wind speed).
 - Disaggregation of soil moisture zones (six soil water “tanks” per area element in SacSMA; two or three tanks in typical VIC applications).
 - Treatment of PET (pre-processed input to SacSMA; computed in VIC).

¹¹ Applications described at “University of Washington Westwide Streamflow Forecasting System” formerly featured at <http://www.hydro.washington.edu/forecast/westwide/>; documented in Wood and Lettenmaier 2006, Wood et al. 2005, and also Maurer et al. 2002. Applications were obtained from University of Washington personnel and from Dr. Andrew Wood, now at NOAA NWS Colorado Basin River Forecast Center, formerly at University of Washington.

Snow17 is a temperature-index based model, whereas VIC's snow model is an energy balance model that is applied for up to five elevation zones within each grid cell.

- **Application comparison:** Both sets of west-wide networks of model-applications have been calibrated to reproduce observed streamflow conditions at various locations and for various streamflow aspects (e.g., minimize error in monthly streamflow variability, reproduce mean-monthly runoff, and reproduce mean-annual runoff). SacSMA/Snow17 is calibrated to daily flow, whereas VIC is less extensively calibrated—typically to monthly flows only. Both model-applications portray precipitation fate as either runoff or evapotranspiration and assume no deep percolation loss from the surface balance over time. In other words, both model-applications largely ignore ground water interaction with surface waters, except in the case of unconfined aquifers with shallow depth-to-ground water. The applications differ in terms of time step choice and how subareas are defined. The VIC applications simulate water balance for each area element in a $1/8^\circ$ spatial grid (coincident with BCSD climate projections' $1/8^\circ$ spatial grid) and on a daily time step, with an hourly time step for the snow model. The NWS SacSMA/Snow17 applications simulate water balance on a 6-hour time step for irregular-area elevation zones within subbasins defined by topography. The NWS SacSMA/Snow17 application in the mountainous Western United States usually features two to three elevation zones per subbasin (versus VIC's one to five zones).

This activity utilized the suite of VIC applications primarily because VIC computes potential evapotranspiration internally, and it is expected that potential evapotranspiration (ET) should change under climate change and have a significant effect on future surface water balance. Treatment of increasing PET with the available SacSMA/Snow17 applications would be less straightforward and require an offline assessment of how PET should respond to climate changes, whereby findings from that assessment would be used as a basis for adjusting the climatological mean-monthly PET inputs typically featured in NWS SacSMA/Snow17 model-applications. PET considerations aside, the SacSMA/Snow17 model-applications have received substantial and comprehensive calibration attention and model-maintenance given that they support operational hydrologic forecasting services for flood and water supply prediction. The VIC applications, by comparison, were produced in an experimental setting in the context of graduate student efforts at the University of Washington during recent years. The degree of model calibration is certain to affect hydrologic sensitivities to climate change, but the size of this effect is not known. However, it is possible for hydrologic simulation outputs to be corrected for biases before using in water resources and reservoir operations assessments.

4.2 About the VIC Hydrology Model-Applications

4.2.1 Model Description

The VIC model (Liang et al. 1994; Liang et al. 1996; Nijssen et al. 1997) is a spatially distributed hydrologic model that solves the water balance at each model grid cell. The model initially was designed as a land-surface model to be incorporated in a GCM so that land-surface processes can be more accurately simulated. However, the model now is run almost exclusively as a stand-alone hydrology model (not integrated with a GCM) and has been widely used in climate change impact and hydrologic variability studies, as indicated earlier in this chapter. For climate change impact studies, VIC is run in what is termed the water balance mode that is less computationally demanding than an alternative energy balance mode, in which a surface temperature that closes both the water and energy balances is solved for iteratively. A schematic of the VIC¹² hydrology and energy balance model is given in figure 10.

Using the University of Washington VIC applications, the water balance mode is driven by daily weather forcings of precipitation, maximum and minimum air temperature, and wind speed. Additional model forcings that drive the water balance, such as solar (short-wave) and long-wave radiation, relative humidity, vapor pressure, and vapor pressure deficit, are calculated within the model. The VIC model contains a subgrid-scale parameterization of the infiltration process (based on the Nanjing model), which impacts the vertical distribution of soil moisture in, typically, a three-layer model grid cell (Liang et al. 1994). The VIC model also represents subgrid-scale vegetation variability using multiple vegetation types and properties per grid cell. Potential evapotranspiration is calculated using a Penman Monteith approach (e.g., Maidment (ed.) 1993). VIC also contains a subdaily (1-hour time step) snow model (Cherkauer and Lettenmaier 2003; Wigmosta et al. 1994; Andreadis et al. 2009). The VIC outputs are configurable but typically include grid cell moisture and energy states through time (i.e., soil moisture, snow water content, snowpack cold content) and water leaving the basin either as evapotranspiration, baseflow, sublimation, or runoff, where the latter represents the combination of faster-response surface runoff and slower-response baseflow.

To calculate streamflow results at a given location, a two-step simulation process is used. The first step is to run VIC independently for each grid cell in the watershed, producing surface runoff and base flow. The second step involves

¹² For information on the VIC model structure, see <http://www.hydro.washington.edu/Lettenmaier/Models/VIC/>.

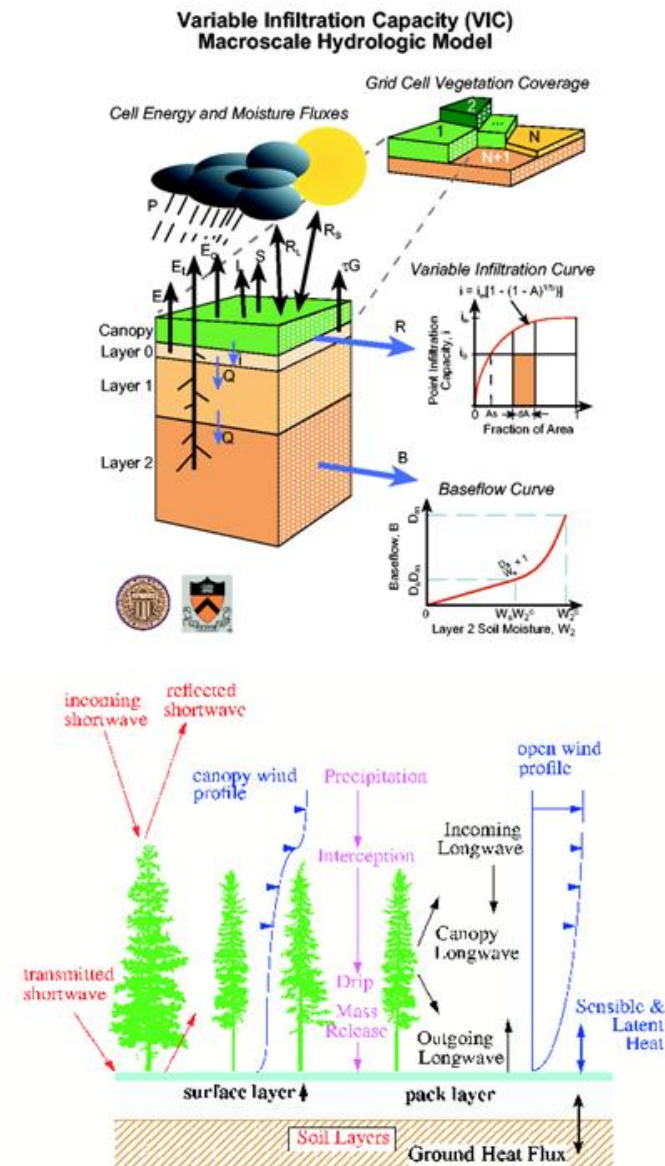


Figure 10. Schematic of VIC Hydrologic Model and Energy Balance Snow Model.

hydraulic routing where the runoff from the grid cells are transported to streamflow gauges or locations of interest in a stream or river channel network. The routing model used in this second step is from Lohmann et al. (1996), and is part of the VIC model setup described in this section. A schematic of the VIC routing model is given in figure 11.

The routing model has two steps. First, surface runoff and baseflow simulated by the hydrology model at the centre of the VIC grid cell are moved to the edge of the cell where it enters the channel network. The runoff then is routed through the

VIC River Network Routing Model

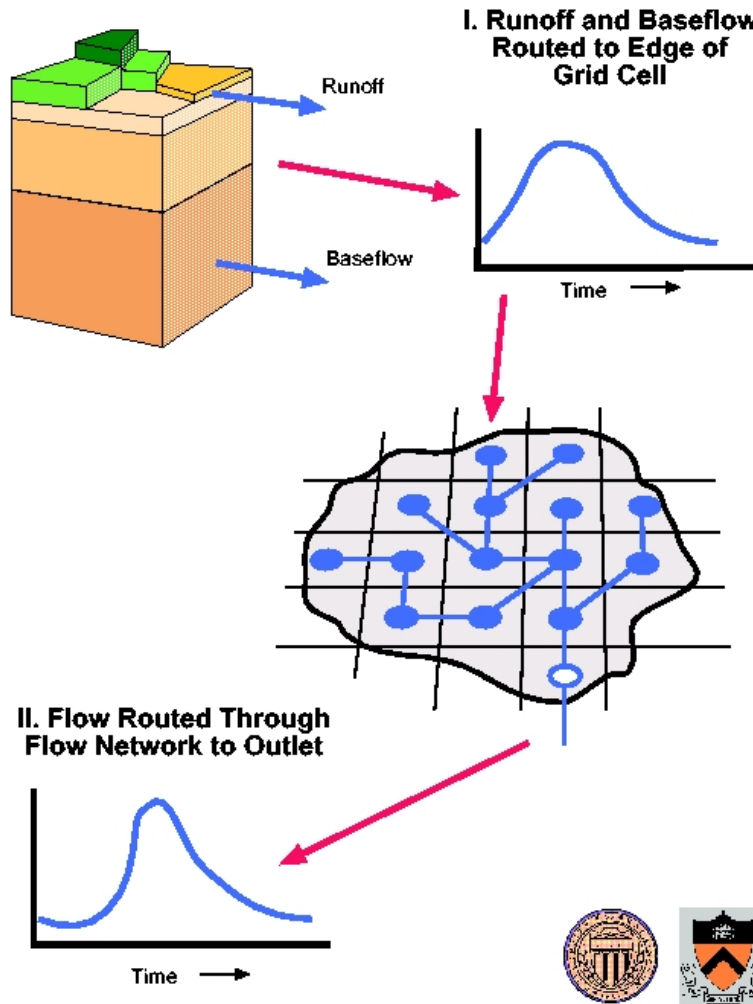


Figure 11. Schematic of VIC River Network Routing Model.

channel network specified above a streamflow location of interest. Such setup requires specifying the coordinates of the streamflow location within the basin grid, identifying tributary grid cells and flow directions through these grid cells, and ultimately fraction-area contribution from tributary grid cells to streamflow at the location of interest.

4.2.2 Applications Description

VIC model applications were obtained from the University of Washington and other experienced VIC model developers, as footnoted earlier.¹¹ For this activity, VIC version 4.0.7 and 32-bit executables were utilized. The VIC applications had been developed for several Western United States river basins that collectively

encompass the Western United States, including the eight “major Reclamation river basins” listed in the SECURE Water Act as well as most of Reclamation’s administrated area (excluding the Red River basin in North Dakota).

Streamflow reporting from these VIC applications was specified for a menu of locations relevant to WWCRA purposes. These include 152 locations from the USGS Hydroclimatic Data Network (HCDN) (Slack et al. 1993) and 43 additional locations that coincide with runoff locations of interest within Reclamation’s managed river systems (i.e., 43 WWCRA locations). It is worthwhile to note that, where calibrated, the VIC models were calibrated to data not from HCDN but from several natural flow datasets.¹³

The geographic distribution of the routing locations is shown on figure 12. A description of the WWCRA routing locations is given in table 1.

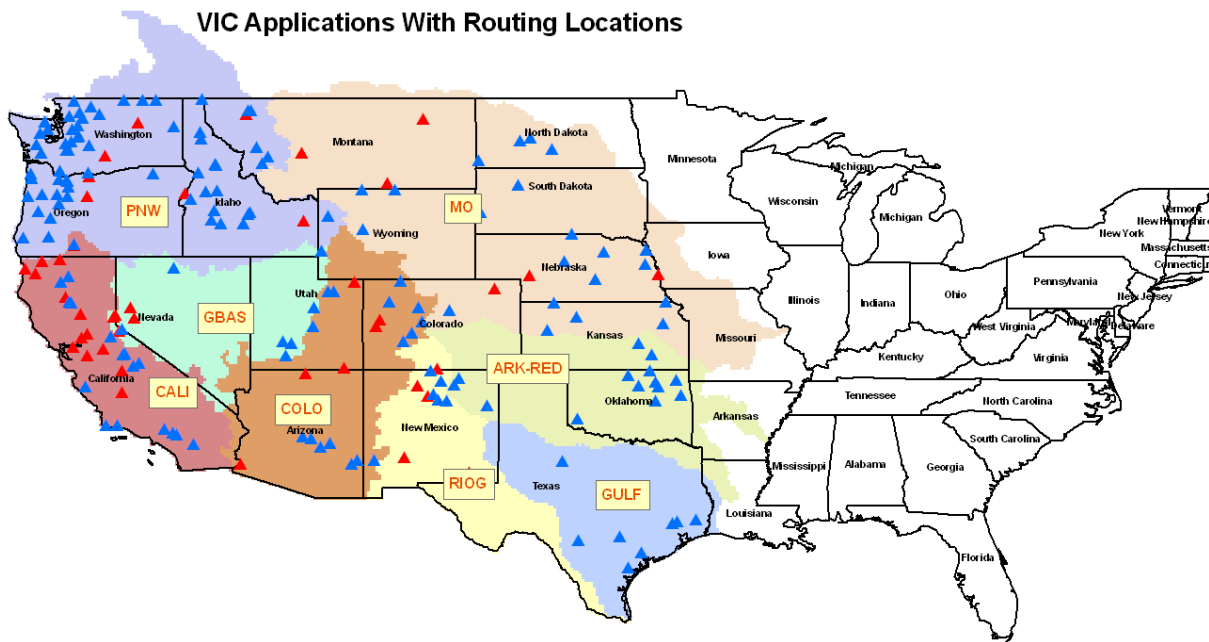


Figure 12. VIC Applications at 1/8° Resolution with the Two Sets of Routing Locations—HCDN (Blue Triangles, Total 152) and WWCRA Locations (Red Triangles, Total 43) Used in the Study.

¹³ For example (Andy Wood, personal communication), for calibrating the Colorado River basin VIC application, natural flows in the Colorado River Basin from Reclamation (<http://www.usbr.gov/lc/region/g4000/NaturalFlow/index.html>) were used. The California VIC applications (covering the Sacramento, San Joaquin, and Klamath River basins) were calibrated using natural flow time series from the California Data Exchange Center (CDEC) at California Department of Water Resources (<http://www.water.ca.gov/>). The Columbia River Basin was calibrated using natural flow data from Bonneville Power Administration (BPA), (<http://www.bpa.gov>) reports. The Missouri River basin was calibrated using natural flow data from the Natural Resources Conservation Service and NWS.

Table 1. Station description for the 43 WWCRA reporting locations

Count	Site Name and Description	Latitude	Longitude	State	SWA Basin
1	Williamson R. below the Sprague River	42.5577	-121.8442	OR	Klamath
2	Klamath River below Iron Gate Dam	41.9281	-122.4431	CA	Klamath
3	Klamath River near Seiad Valley	41.8529	-123.2311	CA	Klamath
4	Klamath River at Orleans	41.3036	-123.5336	CA	Klamath
5	Klamath River near Klamath	41.5111	-123.9783	CA	Klamath
6	Snake River at Brownlee Dam	44.8389	-116.8995	ID	Columbia
7	Columbia River at Grand Coulee	47.9656	-118.9817	WA	Columbia
8	Columbia River at the Dalles	45.6075	-121.1722	OR	Columbia
9	Yakima River at Parker	46.5061	-120.4519	WA	Columbia
10	Deschutes River near Madras	44.7261	-121.2465	OR	Columbia
11	Snake River near Heise	43.6128	-111.6600	ID	Columbia
12	Flathead R at Columbia Falls	48.3619	-114.1839	MT	Columbia
13	Colorado River at Lees Ferry	36.8647	-111.5875	AZ	Colorado
14	Colorado River above Imperial Dam	32.8834	-114.4685	CA-AZ	Colorado
15	Green R near Greendale	40.9086	-109.4224	UT	Colorado
16	Colorado R near Cameo	39.2392	-108.2656	CO	Colorado
17	Gunnison R near Grand Junction	38.9766	-108.4562	CO	Colorado
18	San Juan R near Bluff UT	37.1469	-109.8642	UT	Colorado
19	Sacramento River at Freeport	38.4561	-121.5003	CA	Sacramento
20	Sacramento R at Bend Bridge near Red Bluff	40.2642	-122.2219	CA	Sacramento
21	Feather R at Oroville	39.5217	-121.5467	CA	Sacramento
22	San Joaquin River near Vernalis	37.6761	-121.2653	CA	SanJoaquin
23	Stanislaus R at New Melones Dam	37.9472	-120.5292	CA	SanJoaquin
24	Missouri River at Canyon Ferry Dam	46.6494	-111.7275	MT	Missouri
25	Milk River at Nashua	48.1297	-106.3639	MT	Missouri
26	S.F. Platte River near Sterling	40.6192	-103.1886	CO	Missouri
27	Missouri River at Omaha	41.2589	-95.9222	NE	Missouri
28	Rio Grande near Lobatos	37.0786	-105.7564	CO	RioGrande
29	Rio Chama near Abiquiu	36.3183	-106.5972	NM	RioGrande
30	Rio Grande near Otowi	35.8762	-106.1433	NM	RioGrande
31	Rio Grande at Elephant Butte Dam	33.1563	-107.1905	NM	RioGrande
32	Pecos R at Damsite No 3 nr Carlsbad	32.5114	-104.3342	NM	RioGrande
33	Little Truckee R below Boca Dam	39.3883	-120.0950	CA	Truckee
34	W.F. Carson R at Woodfords	38.7697	-119.8328	CA	Truckee
35	Sacramento-San Joaquin Rivers at Delta	38.0645	-121.8567	CA	Sacramento and San Joaquin
36	San Joaquin R at Millerton Lake (Friant Dam)	36.9981	-119.7066	CA	SanJoaquin
37	Truckee R at Farad Gage (just above CA stateline)	39.4540	-120.0063	CA	Truckee
38	Truckee R. at Nixon Gage	39.7780	-119.3392	NV	Truckee
39	Carson R. at Ft Churchill Gage	39.3272	-119.1508	NV	Truckee
40	Big Horn River at Yellowtail Dam	45.3079	-107.9567	MT	Missouri
41	N.F. Platte River at Lake McConaughy	41.2145	-101.6434	NE	Missouri
42	American River at Fair Oaks	38.6366	-121.2284	CA	Sacramento
43	Tulare-Buena Vista Lakes	36.0524	-119.7187	CA	NA

Routing model inputs were developed for the 43 WWCRA locations from 15 arc-second (~ 450 meters) DEM (Digital Elevation Model), flow accumulation, and flow direction data available from the USGS HydroSHEDS (hydrological data and maps based on Shuttle Elevation Derivatives at Multiple Scales) archive using ArcGIS.

4.3 Use of VIC Model Applications To Develop BCSD Surface Water Hydrologic Projections

The application described in this section follows the methodology originally introduced in Wood et al. 2004 and featured in various subsequent efforts (e.g., Payne et al. 2004; Christensen et al. 2004; Christensen and Lettenmaier 2007; Barnett et al. 2008; Maurer 2007; McGuire and Hamlet 2010). The common requirement among these applications is that monthly BCSD climate projections of precipitation and average temperature had to be converted into VIC weather inputs. Spatially, the monthly BCSD climate projections were specified on the same grid as the VIC hydrology model-applications, so no spatial reconciliation was necessary. Temporally, the monthly two-variable climate projections had to be converted into consistent sequence of daily VIC weather forcings (precipitation, minimum temperature, maximum temperature, and wind speed).

The approach to do this temporal translation generally follows the historical resampling and scaling technique introduced in Wood et al. 2002. The procedure involves proceeding month by month through a monthly BCSD projection and doing the following three-step procedure:

- **Step 1.** Get the monthly total precipitation and mean temperature at every grid cell of the VIC domain for each projection month.
- **Step 2.** Conditionally select a historical observed month from the reference historical weather data (in this case, from the period of 1950–1999 from daily dataset of Maurer et al. 2002). The month selection is conditioned by applying two criteria: 1) if the domain-average precipitation for a downscaled month is in the top half (wet), be sure to select a historical month from the top half (wet); 2) otherwise, choose a historical month with higher precipitation.
- **Step 3.** Preserving the daily sequence from the sample month selected in Step 2 at every location, adjust each grid cell's historical observed daily sequence so that the adjusted historical month value matches the projection month value. For precipitation, apply a scaling ratio to the sequence. For temperature, apply an incremental adjustment to the sequence. However, for precipitation, there are some difficulties to surmount when applying this monthly-to-daily translation scheme. The difficulties primarily arise on precipitation scaling issues. To address occurrences of overly high values of daily precipitation, an additional criteria is imposed during scaling, which limits daily precipitation to 150% of the daily historical maximum precipitation for a cell for a given month. Precipitation in excess of 150% is spread evenly across the other days in the month. Similar constraints were imposed in Payne et al. 2004 and

Maurer et al. 2007 and are necessary to avoid pathological combinations of dry samples with wet target months (i.e., large scaling of insufficient numbers of precipitation days). Such cases are found more frequently in dry locations or seasons, such as the Southwest United States or parts of the Pacific Northwest during summer.

As an example, consider making synthetic daily weather for a single month in a given climate projection at a given grid cell. Step 1 involves recognizing the projection month for which synthetic weather is being developed (e.g., January 2031 of the given climate projection). Step 2 involves conditionally sampling a historical month (e.g., select January 1979's sequence of 31 daily values from the Maurer et al. 2002 dataset). The observed January 1979 provides a realistic spatial-temporal sequence of daily weather variability over the entire basin (e.g., occurrence of precipitation, progression of synoptic weather events across the basin, spells of warmer to cooler days). Step 3 involves scaling for precipitation or shifting for temperature, such that the adjusted daily precipitation or temperature series matches the monthly value for the projection month (January 2031).

The steps and constraints described above for monthly to daily disaggregation was implemented following the University of Washington Climate Impacts Group's recent development of hydrologic projections for the Pacific Northwest.¹⁴ However, different constraints have been used in other efforts—for example, the VIC modeling done for the WaterSMART Colorado River Basin Study. Finally, the forcings development for this effort was done uniquely for big basins and that across big basin boundaries, the daily sequences within a month will differ, but that monthly sequences across boundaries will be consistent.

4.4 Assessment of VIC Model-Applications' Historical Simulations

Before proceeding to performing hydrologic projections under climate change, the performance of the VIC applications were analyzed to evaluate how well the models simulate historical flows at selected streamflow sites. Results were found to vary, suggesting that where the VIC model-applications received calibration attention, they were found to do reasonably well at reproducing historical monthly and annual runoff. However, for locations that had not been calibrated, the VIC simulated runoff bias could be significant.

¹⁴ WA HB 2860 at <http://www.hydro.washington.edu/2860/>.

To illustrate these findings, discussion focuses on 2 of the 43 WWCRA reporting locations, which are shown in figures 13–16. These three sites were selected to represent the following types of historical simulation conditions:

- **Small bias example** – where seasonality and annual mean flows are closely reproduced (e.g., Colorado River above Imperial Dam).
- **Large bias example** – where seasonality is out of phase and there is annual bias (e.g., Deschutes River near Madras).

Two sets of plots are presented for each location. First, a time series plot of monthly volumes covering the period water years 1951–1999. The second plot shows the mean annual hydrograph estimated from the 49 water years data (water years 1951–1999) along with the mean annual bias—difference in the mean annual volumes between the simulated and observed annual hydrographs.

Summary of annual biases for 10 WWCRA locations are given table 2. The annual biases are expressed as a percentage difference of the mean annual simulated volume from the mean annual observed volume over the 49 water years, 1951–1999. Therefore, positive bias implies that the simulated flows over this period (water years, 1951–1999) are greater than the observed flow volumes over this same period. From table 2 and bias calculations, the point to note is that

Table 2. Bias in historical flow simulations for selected WWCRA locations

<i>Station Name</i>	<i>Observed Annual Mean Volume (TAF)</i>	<i>Simulated Annual Mean Volume (TAF)</i>	<i>Bias (%)</i>	<i>Correlation</i>
Williamson R. below the Sprague River	887.55	360.65	-59.37	0.9742
Feather R at Oroville	4783.30	4412.20	-7.76	0.9749
San Joaquin River near Vernalis	6630.50	7197.60	8.55	0.9642
San Joaquin R at Friant Dam	1852.80	1729.10	-6.67	0.9909
Colorado River above Imperial Dam	16035.00	16968.00	5.81	0.9789
Little Truckee R below Boca Dam	11.90	188.74	1486.00	0.4168
W.F. Carson R at Woodfords	78.81	81.08	2.88	0.9856
Deschutes River near Madras	4040.30	3195.90	-20.90	0.6593
Snake River near Heise	5354.10	3843.40	-28.22	0.9849
Rio Grande near Lobatos	309.56	1804.20	482.81	0.9146

the model biases are high for smaller basins with very low annual flow volumes. For flows accumulated over a larger contributing area, for example, the locations on the Sacramento-San Joaquin, Colorado and Columbia River systems, the biases are significantly lower.

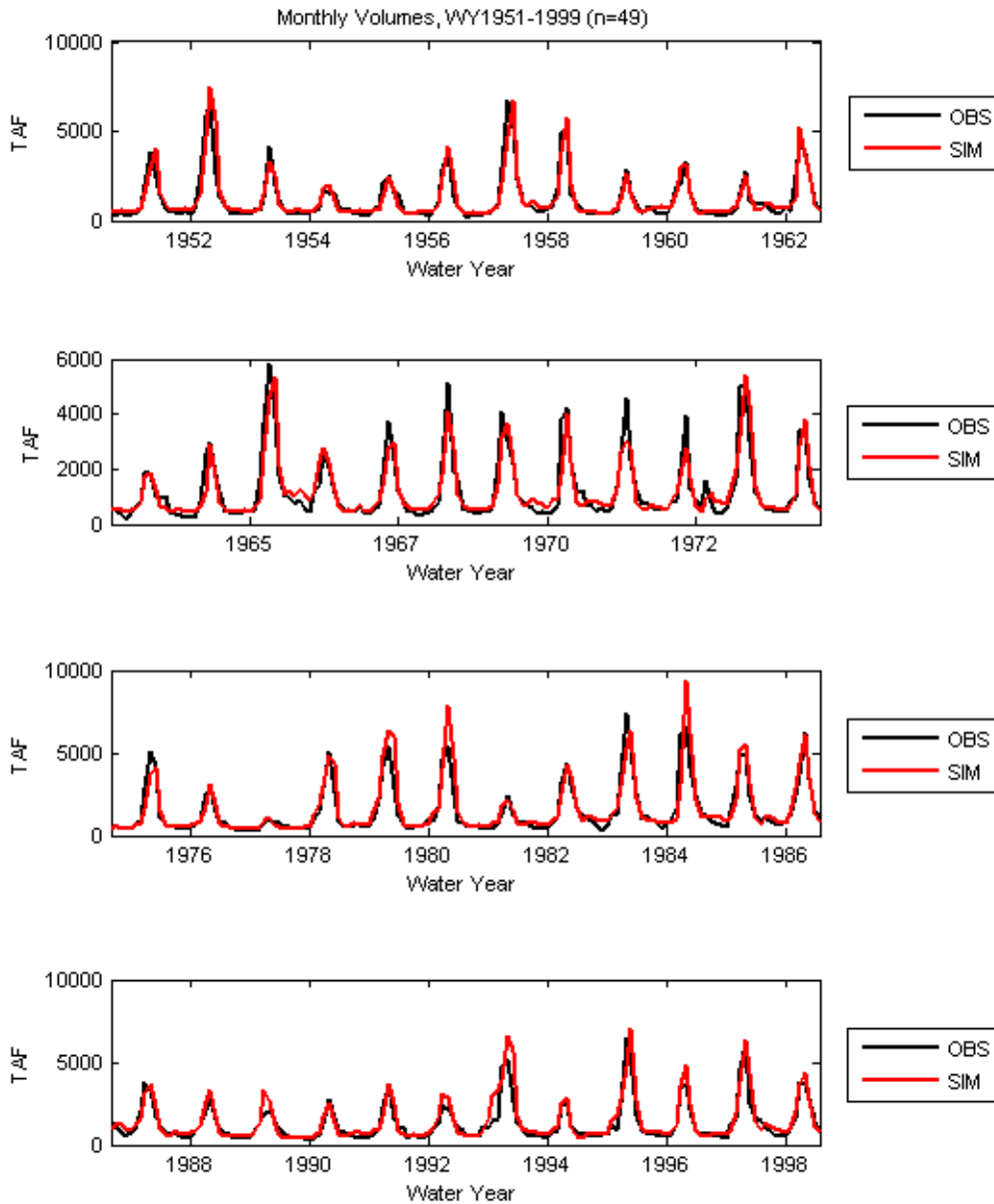


Figure 13. Historical Simulated Runoff, Small-Bias Example: Monthly Time Series.

Figure 13 shows monthly observed (black line) and simulated (red line) flow volumes for water years 1951–1999 for the site Colorado River above Imperial Dam.

West-Wide Climate Risk Assessments:
BCSD Surface Water Projections

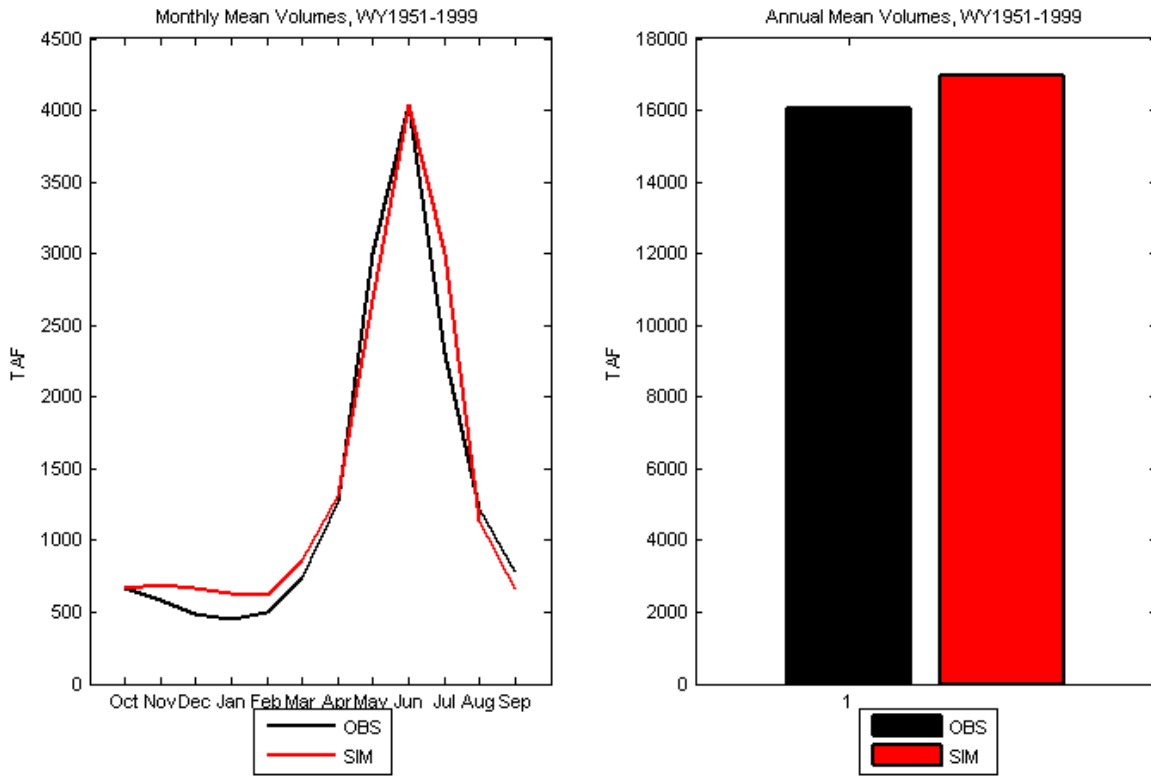


Figure 14. Historical Simulated Runoff, Small-Bias Example: Monthly and Annual Means.

Figure 14 shows monthly mean volume (left panel) and annual mean volumes (right panel) calculated from water years 1951–1999 for the site Colorado River above Imperial Dam.

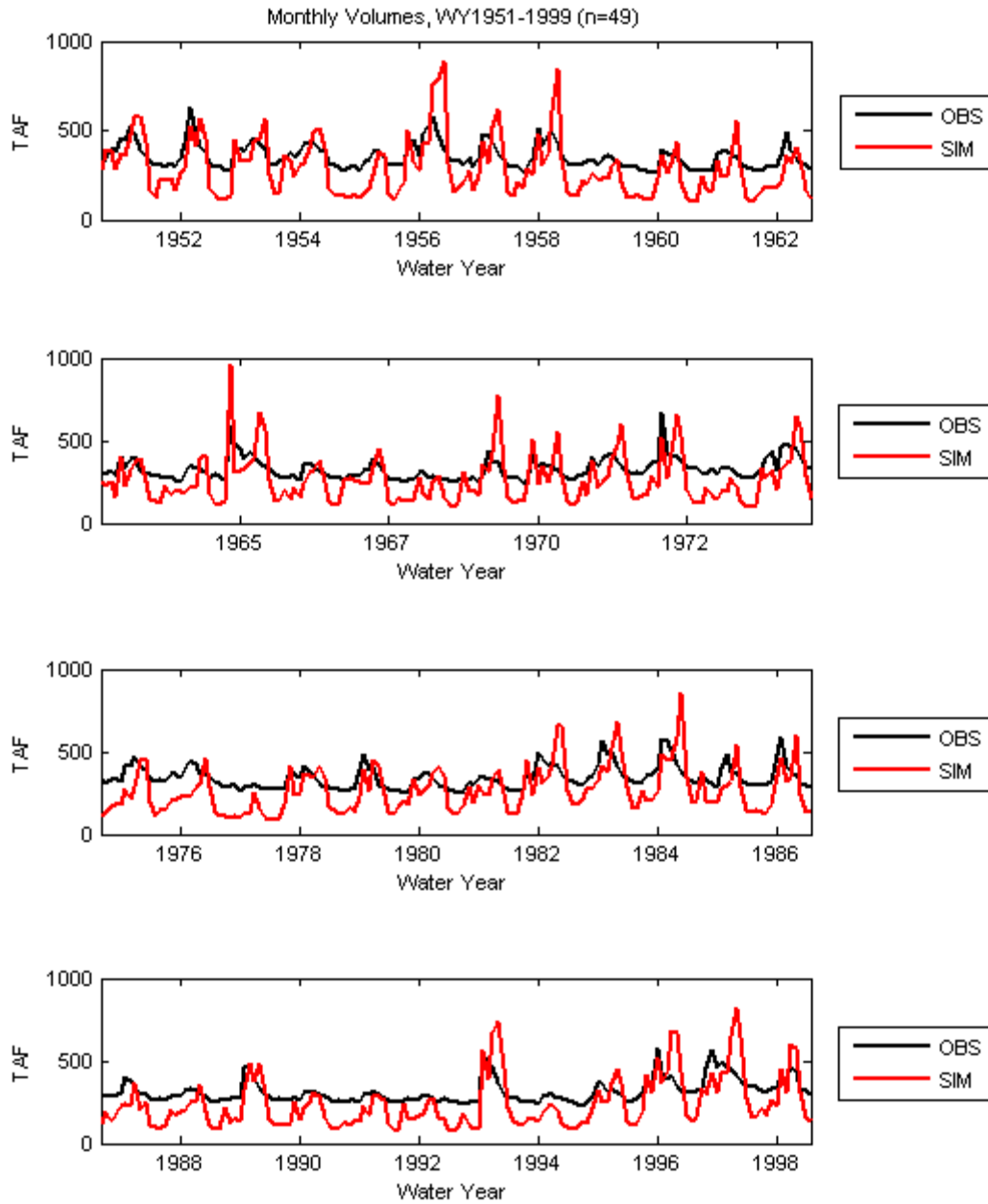


Figure 15. Historical Simulated Runoff, Large-Bias Example: Monthly Time Series.

Figure 15 shows monthly observed (black line) and simulated (red line) flow volumes for water years 1951–1999 for the site Deschutes River near Madras.

West-Wide Climate Risk Assessments:
BCSD Surface Water Projections

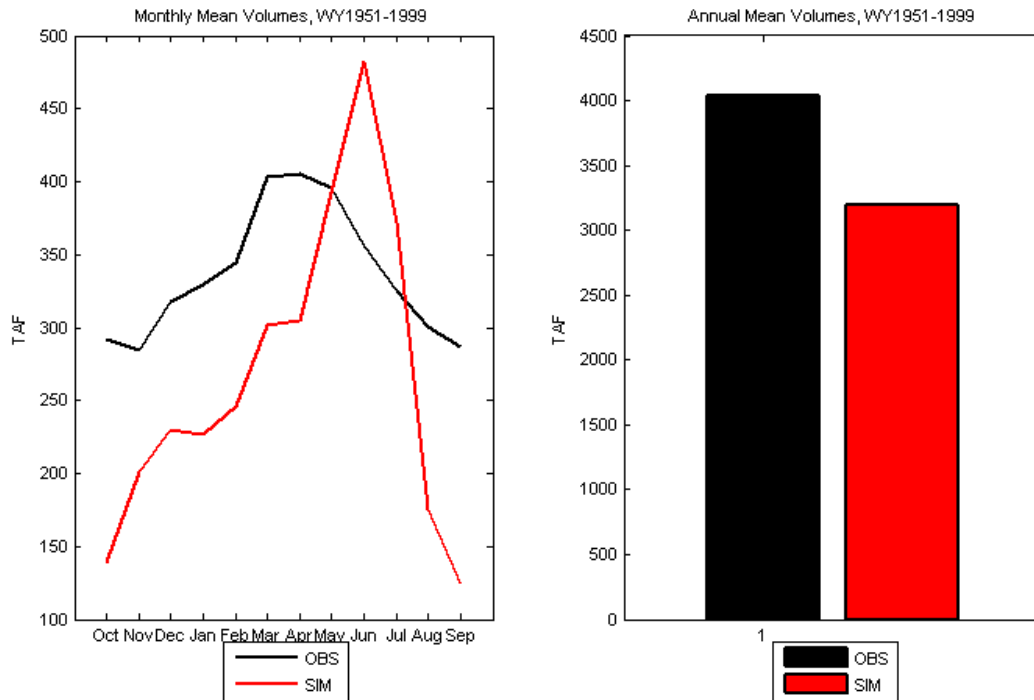


Figure 16. Historical Simulated Runoff, Large-Bias Example: Monthly and Annual Means.

Figure 16 shows monthly mean volume (left panel) and annual mean volumes (right panel) calculated from water years 1951–1999 for the site Deschutes River near Madras

Figure 17 shows how bias in simulated historical mean-annual streamflow varied at the 152 HCDN locations considered in this activity.¹⁵ Note that the size of HCDN basins varies considerably, as the reported HCDN sites range in annual mean volumes from about 1,500 acre-feet to 8.5 million acre-feet (MAF). The median observed annual mean flow across the HCDN sites is about 235 thousand acre-feet (TAF). Dividing the HCDN sites into two groups—basins with flows less than or equal to (\leq) the median observed annual mean flow (i.e., all basins with annual observed mean flow $\leq \sim 235$ TAF) and basins with observed annual

¹⁵ HCDN flow time series were obtained from Tom Piechota (personal communication 2010) and are available online at <http://faculty.unlv.edu/piechota/DataSets3.htm> (accessed December 2010). The dataset is described in the paper, Coupled Interdecadal and Interannual Oceanic/Atmospheric Variability and United States Streamflow, Water Resources Research, 41(W12408), by G.A. Tootle, T.C. Piechota, and A.K. Singh, 2005. This dataset is an extension of the work described in USGS Open File Report 92-129, Hydro-Climatic Data Network (HCDN): A U.S. Geological Survey Streamflow Data Set for the United States for the Study of Climate Variations, 1874–1988 by J.R. Slack and J.M. Landwehr.

mean flows greater than ($>$) ~ 235 TAF—the absolute median bias in the annual simulated flow volumes was estimated to be nearly 26 and 15%, respectively. The absolute bias statistics jointly covers the cases where the simulated flow may either be higher or lower than the observed flows (i.e., both positive and negative biases in simulated flow). Also, the median correlation of monthly means from the 152 HCDN locations is about 0.9, suggesting an overall good representation of variability of monthly means across the sites. Similar to the WWCRA locations, we find that flows from larger contributing areas, in the case of the HCDN sites, also result in lower simulation biases. As noted earlier, the HCDN sites were not used for calibrating the VIC model applications.

Bias in Simulated Annual Mean Flow, WY 1951-1999

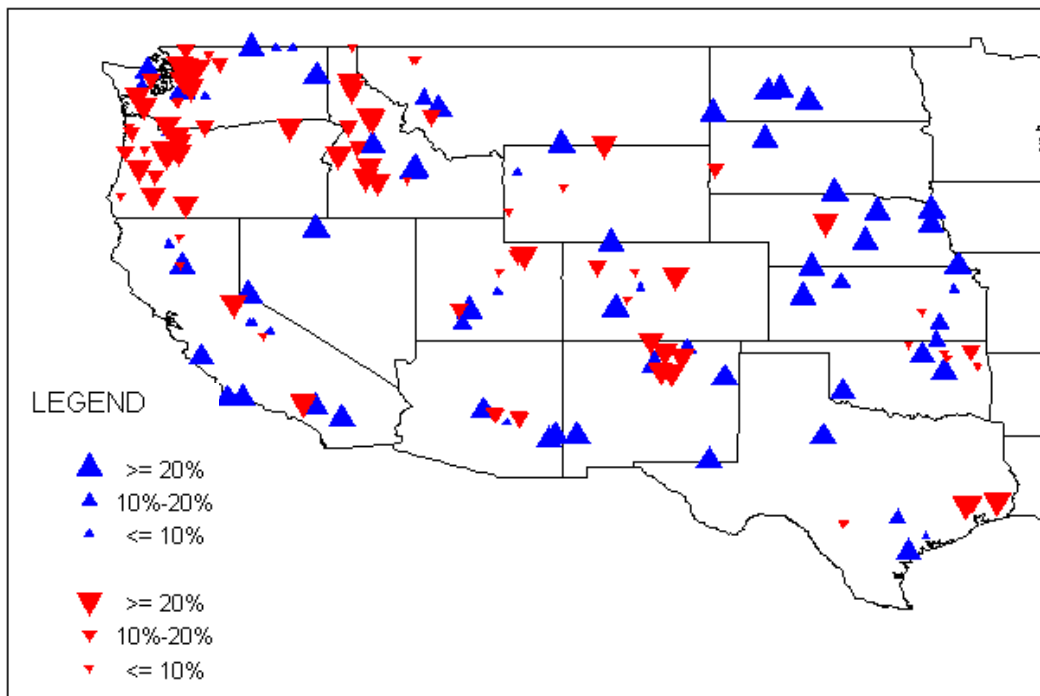


Figure 17. Historical Simulated Runoff, West-wide Bias Summary: Annual Mean.

Figure 17 shows bias in simulated mean annual flow for the 152 HCDN locations. Upward pointing blue triangles imply positive bias (simulated flow $>$ observed flow), and downward pointing red triangles are locations with negative bias (simulated flow less than [$<$] observed flow).

4.5 Flow Bias and Bias Correction

In section 4.4, biases in the simulated flow at the selected locations, both the WWCRA sites and at the HCDN sites, were presented. The general observation is that the biases—difference between simulated and observed flows—tend to be relatively higher for smaller basins (i.e., basins with smaller annual flows is a function of the drainage area contributing to the flow). Snover et al. (2003) point out that, even after calibration, there could be residual bias attributed to model structure and model forcings. One of the methods to alleviate the discrepancy between the simulated and observed flows is to follow a post-processing step to adjust simulated runoff results to be consistent with monthly to annual aspects of runoff from observed datasets (Snover et al. 2003). Shi et al. (2008) contrast the benefits of calibration versus post-processing for VIC model predictions, concluding that post-processing can reduce errors associated with poor calibration but with lesser effectiveness for shorter time scale metrics (e.g., daily flows versus seasonal runoff volumes). Smith et al. (1992) recommend bias correction of flows to reduce hydrologic model errors in an ensemble seasonal forecasting context.

In the post-processing adjustment process of observed and simulated flows, the first step is to identify the bias over an analysis period. Years 1950–1999 (total of 50 years) was used as the bias identification period to do the post-VIC bias correction of simulated runoff. This bias is characterized using a quantile map (similar to the monthly bias correction featured in the development of monthly BCSD climate projections, discussed in chapter 3), where the quantile map features two empirical cumulative distribution functions (CDFs), one of simulated flows during the bias identification period and another of the reference observed flows during this period. The CDFs are constructed at a given runoff location, first on month-specific basis to characterize bias in monthly mean flows and then on an annual basis to characterize bias in the annual mean flow.

After defining these maps, simulated runoff bias correction ensues. The quantile maps are interpreted to reveal VIC runoff simulation bias for a given simulated runoff magnitude. For example, consider a VIC runoff location where the simulated January 2021 runoff magnitude happens to equal the 10th percentile magnitude within the VIC simulated-historical January CDF, fit to simulated 1950–1999 January runoff values. Switching from simulated- to observed-historical CDF and keeping the view on the 10th percentile, the observed-historical 10th percentile value is identified. This latter value is accepted as the new “bias-corrected” magnitude for January 2021. Because the bias correction is magnitude-based, the correction can be viewed as ignorant of climate condition and permits the maps to be applied to correct runoff from any climate-specific

VIC simulation. Note however, that, when simulated flows exist outside of the range of simulated flows informing the quantile map, assumptions have to be made on how to extrapolate the map. In this discussion, assumptions are made that the ratio of observed to simulated flows at the maximum quantile is applied for any simulated magnitudes exceeding the quantile map at this maximum quantile (amounting to a linear extrapolation). Likewise, the ratio of observed to simulated flows at the minimum quantile is applied for any simulated magnitudes less than the quantile map at the minimum quantile.

For the historical period, water years 1951–1999, the quantile mapping technique can eliminate successfully much of the simulated runoff bias, almost completely if the focus is on monthly mean and annual mean runoff. This is demonstrated on figures 18–21, which correspond to the same two WWCRA runoff locations used to illustrate small and large simulated runoff biases (figures 13–16). For each location, time series of observed historical flow (labeled OBS), VIC simulations (labeled SIM) and bias-corrected VIC (labeled BCF) are shown (figure 18 and figure 20) as well as summaries of monthly and annual means (figure 19 and figure 21). Note that, in following the Snover et al. 2003 technique for runoff bias correction, a higher priority is placed on matching the historical annual flow distribution at the expense of some mismatch with the historical month-specific distributions. In other words, for the historical condition, the resultant bias-corrected runoff features annual period-statistics and CDFs that exactly match those from the observed historical runoff dataset and monthly period-statistics and CDFs that closely match those from the observed historical dataset.

In the context of assessing future hydrologic impacts within these BCSD hydrologic projections, runoff impacts (chapter 5) have been calculated using the raw or nonbias-corrected VIC simulations. However, it should be recognized that (1) the biases in simulated mean-annual runoff (as a %) are rather large in some places, and (2) although section 4.3 highlighted a concern about the climate projection bias correction procedure wettening the mean-annual precipitation changes, it would appear that the imperfect calibrations of the hydrology models may be a larger contributor to impacts uncertainty (or bias) in many locations. Moving forward, lack of calibration of the hydrologic models is a real issue that needs to be addressed, and should be addressed before these models are used in future assessments. Reclamation will (a) refine the VIC application and/or (b) introduce more appropriate hydrologic models. However, before implementing west-wide calibration efforts, it is also important to assess the fitness of the chosen model structure for some geographic situations, particularly basins where ground water interactions with surface water may be an important process and not well-simulated in VIC.

West-Wide Climate Risk Assessments:
BCSD Surface Water Projections

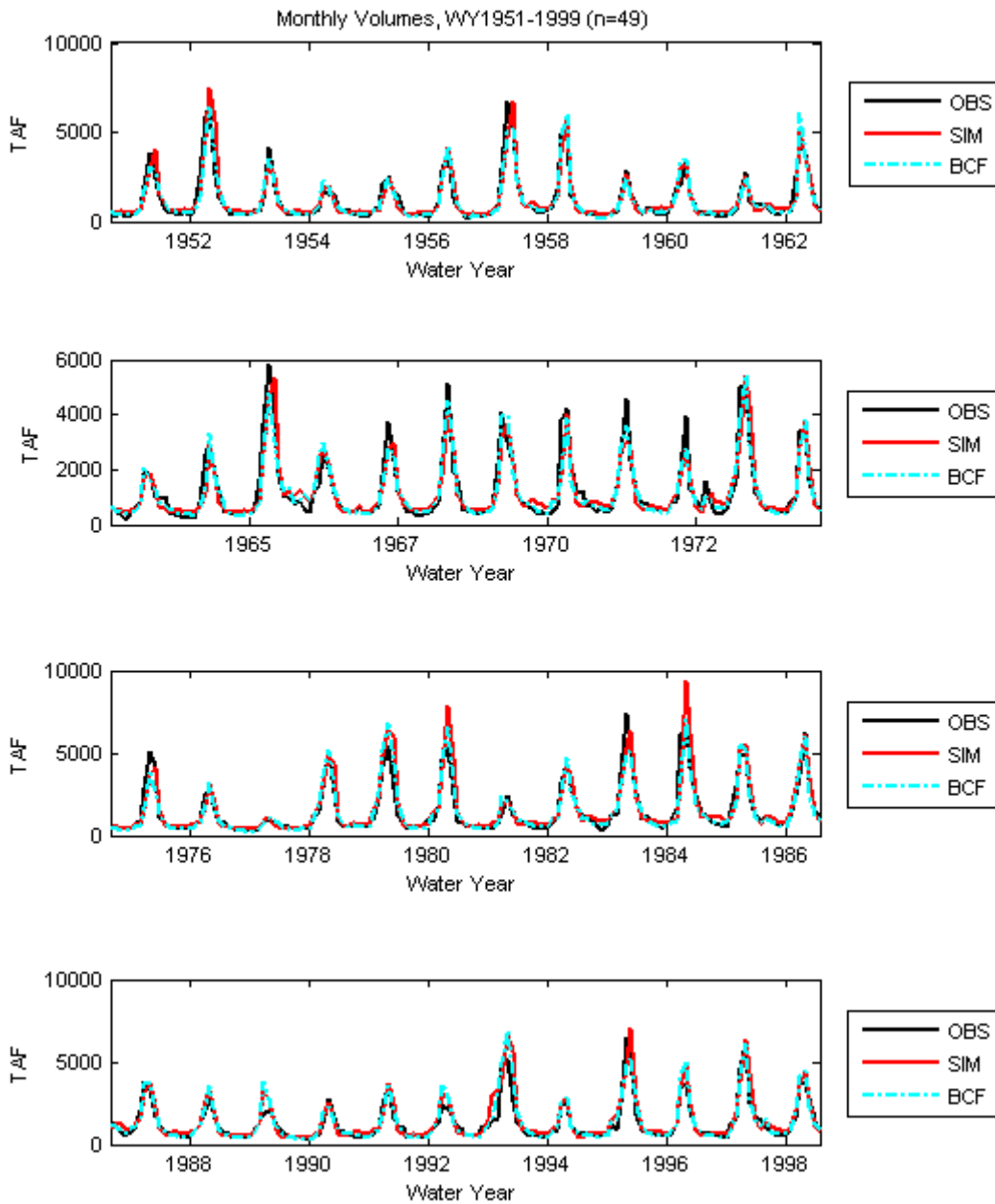


Figure 18. Historical Simulated Runoff, Small-Bias Example: Monthly Time Series Before and After Bias Correction.

Figure 18 shows monthly observed (black line), simulated (red line), and bias-corrected simulated (cyan line) flow volumes for water years 1951–1999 for the site Colorado River above Imperial Dam.

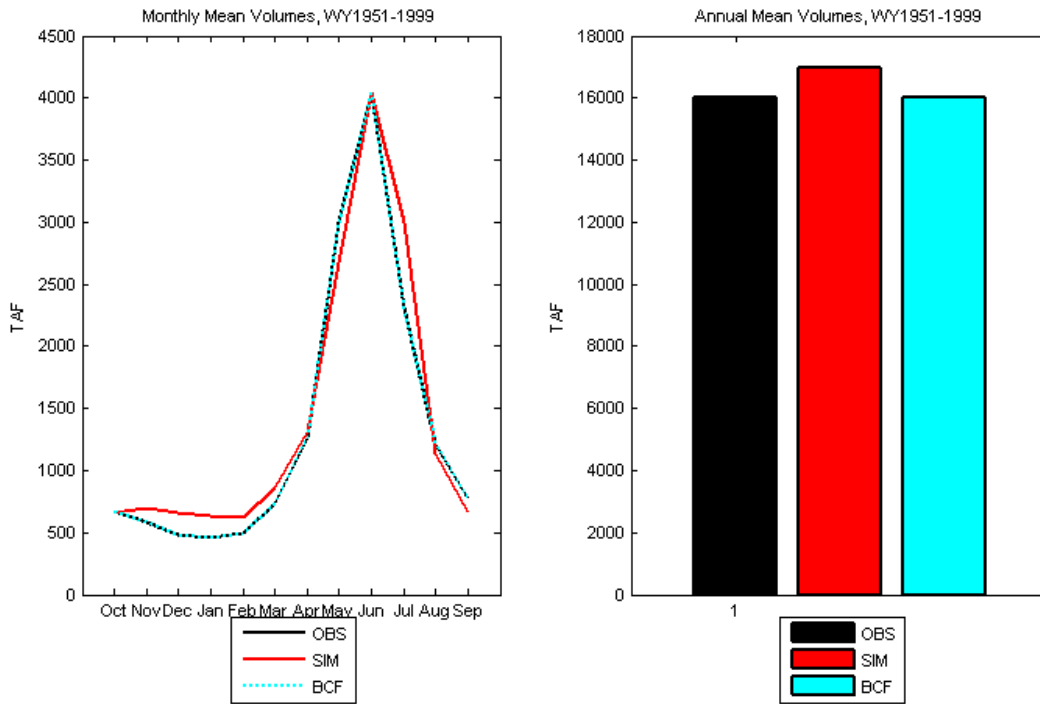


Figure 19. Historical Simulated Runoff, Small-Bias Example: Monthly and Annual Means Before and After Bias Correction.

Figure 19 shows monthly mean volume (left panel) and annual mean volumes (right panel) including bias-corrected simulated flow (BCF) calculated from water years 1951–1999 for the site Colorado River above Imperial Dam.

West-Wide Climate Risk Assessments:
BCSD Surface Water Projections

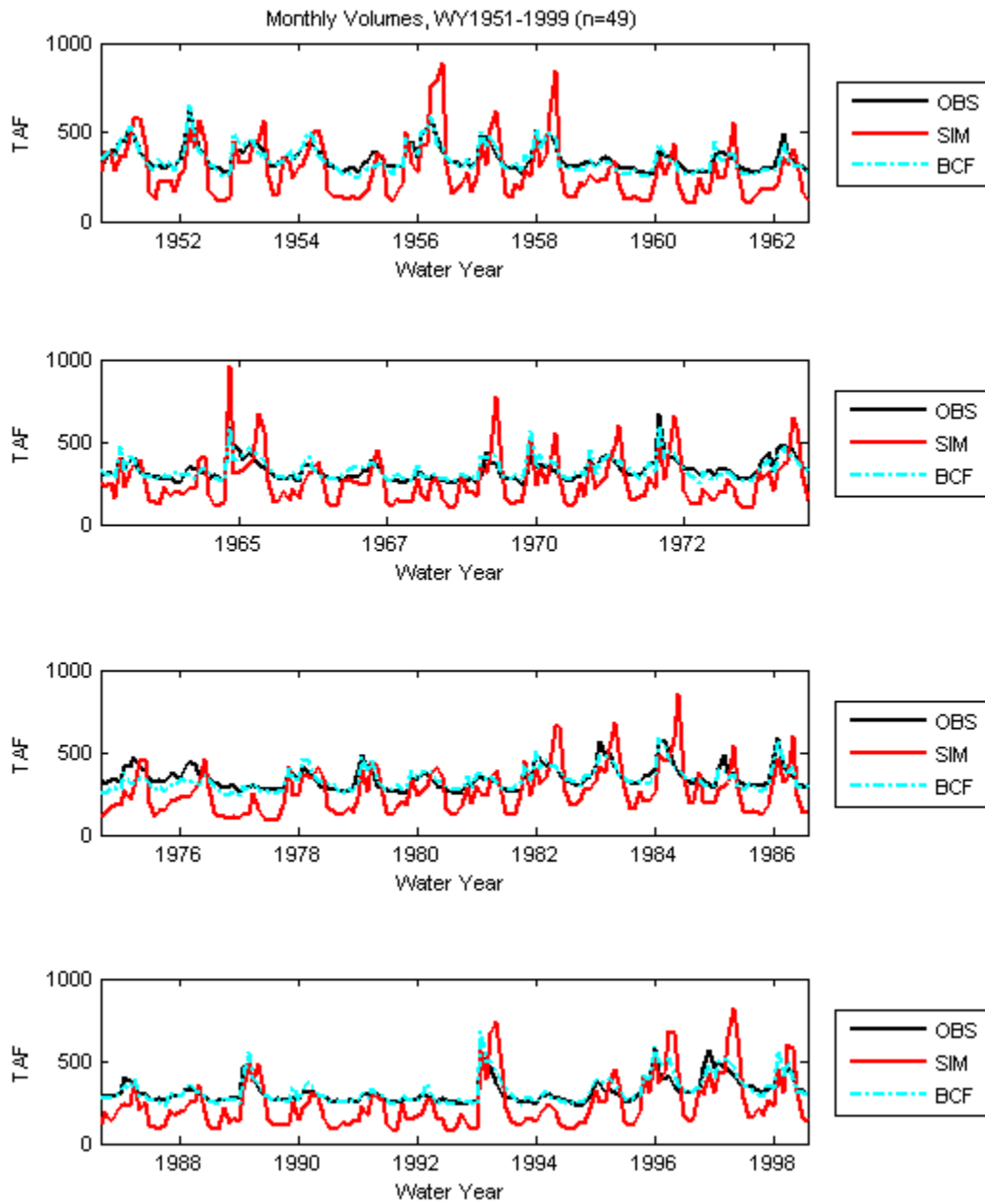


Figure 20. Historical Simulated Runoff, Large-Bias Example: Monthly Time Series Before and After Bias Correction.

Figure 20 shows monthly observed (black line), simulated (red line), and bias-corrected simulated (cyan line) flow volumes for water years 1951–1999 for the site Deschutes River near Madras.

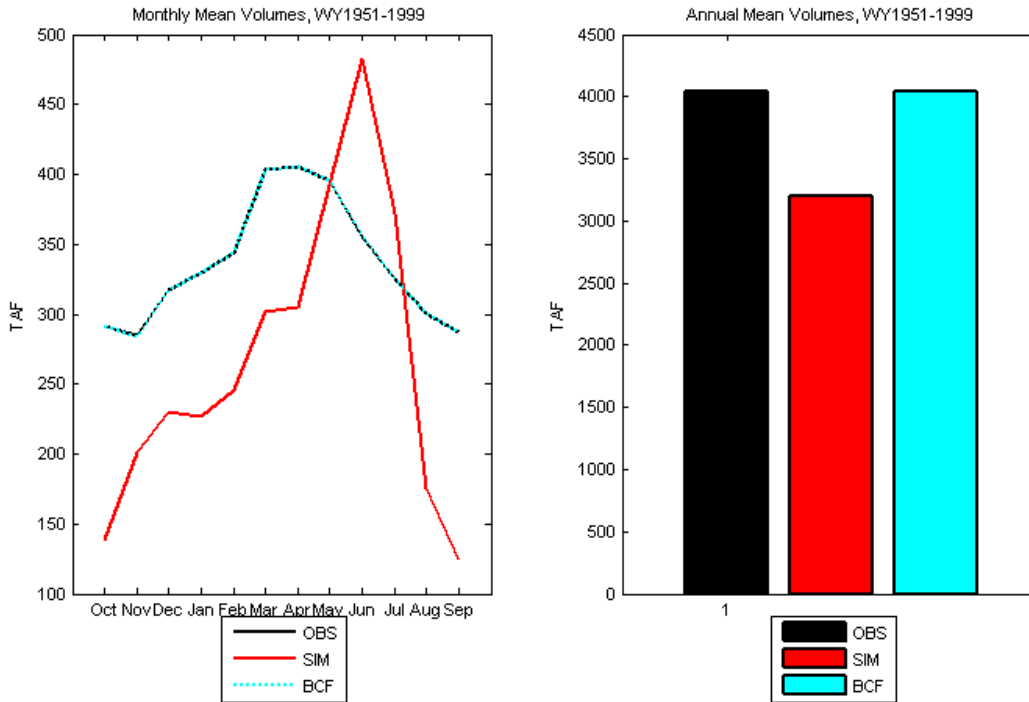


Figure 21. Historical Simulated Runoff, Large-Bias Example: Monthly and Annual Means Before and After Bias Correction.

Figure 21 shows monthly mean volume (left panel) and annual mean volumes (right panel) including bias-corrected simulated flow (BCF) calculated from water years 1951–1999 for the site Deschutes River near Madras.

CHAPTER 5

Hydroclimate Projections for Major Reclamation River Basins Under Climate Change

5.1 Evaluation Approach

In this chapter, surface water hydroclimate projections for the major Reclamation river basins are presented. These include distributions and changes in precipitation, mean temperature, snow water equivalent, and runoff. The figures and analysis for each major Reclamation river basin is grouped under two sections. The first section is referred to as hydroclimate projections and in each case provides an overview for each of the major Reclamation river basins. The overview locations in each of the eight¹⁶ major Reclamation river basins, and the sections below that describe them, are:

- Colorado River Basin – Colorado River at Imperial Dam (section 5.2)
- Columbia River Basin – Columbia River at Dalles (section 5.3)
- Klamath River basin – Klamath River near Klamath (section 5.4)
- Missouri River basin – Missouri River at Omaha (section 5.5)
- Rio Grande basin – Rio Grande at Elephant Butte Dam (section 5.6)
- Sacramento and San Joaquin River basins – Sacramento and San Joaquin Rivers at the Delta (section 5.7)
- Truckee and Carson River basins – Truckee River at Nixon gauge (section 5.8)

The second section presents climate change impacts on annual runoff and seasonal cycles for selected runoff locations within each of the major basins. Runoff impacts are reported at 43 locations (refer to table 1) covering all the major Reclamation river basins.

¹⁶ The Sacramento and San Joaquin River basins are considered together as part of Reclamation's Central Valley operations, as are the Truckee and Carson River basins. The SWA specifies the Sacramento and San Joaquin as separate river basins and only specifies the Truckee River basin. Also, the Tulare Lake hydrologic region is included as a WWCRA reporting location.

Under the hydroclimate projections section, two plot types—time series plots and spatial plots are presented for each major river basin.

5.1.1 Time Series Plots

This set includes basin and projection specific annual time series plots for six hydroclimate indicator variables covering the period 1950–2099.

- Annual Total Precipitation
- Annual Mean Temperature
- April 1st Snow Water Equivalent
- Annual Runoff
- December–March Runoff
- April–July Runoff

The three variables—annual total precipitation, annual mean temperature, and April 1st snow water equivalent—vary spatially (at 1/8° or ~ 12-km-grid resolution) across the basins. To estimate total annual precipitation for a given basin, basin-wide average precipitation (average across the grid cells in the basin) was first calculated for each month of the years 1950–2099. These monthly precipitation values then were summed for each year (1950–2099) to obtain the annual total precipitation.

To estimate basin mean temperature, average temperature was calculated from all the grid cells in the basin for each month of the years 1950–2099. These monthly temperatures for any given year next were averaged to estimate the basin-wide annual mean temperature.

Snow water equivalent (SWE) on April 1 of a given year is a widely used measure to assess snowpack and subsequent spring–summer runoff conditions in the snowmelt dominated basins of the Western United States. SWE is a State variable and output from the VIC hydrology model. For each of the simulation years, 1950–2099, April 1st SWE was saved from the simulations for the model grid cells in a given basin. This gridded SWE on April 1st was averaged over all the grid cells for the given basin to calculate the basin-wide April 1st SWE in each of the simulation years, 1950–2099.

Runoff for each of the locations listed above was calculated for the annual timescale and for two seasonal timescales—December–March (DJFM) total runoff depicting winter season runoff conditions and April–July (AMJJ) total runoff depicting spring–summer runoff conditions. For each of the simulation

years 1950–2099, monthly runoff was aggregated on a water year¹⁷ basis to calculate water year specific total annual runoff, DJFM runoff, and AMJJ runoff.

The annual time series plots for the six hydrologic indicator variables for all the 112 projections were calculated, and the results are presented to reflect ensemble central tendency and ensemble spread. The central tendency is measured using the ensemble median and the 5th and 95th percentile bounds from the 112 projections provides the lower and upper uncertainty bounds in the envelope of hydroclimatic possibility through time.

5.1.2 Spatial Plots

The second sets of plots include spatial plots of decade-mean precipitation, temperature and April 1st SWE. These plots show the spatial distribution for the variables across the contributing basins for the overview locations (a total of seven¹⁸) in each of the eight major Reclamation river basins. The spatial plots are developed on a water year basis (affects calculations for only precipitation and temperature averaging) for the reference decade, 1990s (water years, 1990–1999).

Spatial distribution of precipitation for the 1990s' decade is presented as an ensemble median of the 112 projections. At each grid cell in a given basin and for each of the 112 projections, average total precipitation was calculated by averaging total precipitation from the 10 water years, 1990–1999. Next, for each grid cell, the ensemble median of the decade average total precipitation was calculated and used in developing the spatially varying precipitation plots.

Estimation of precipitation changes, in each of the future decades, 2020s, 2050s, and 2070s was calculated as follows. At each grid cell in a given basin and for each of the 112 projections, average total precipitation was calculated by averaging total precipitation from the 10 water years in the respective future decades. That is, water years 2020–2029 for the 2020s' decade, water years 2050–2059 for the 2050s' decade, and water years 2070–2079 for the 2070s' decade. Then, for a given projection and at a given grid cell, percentage difference between a given future decade average total precipitation and the reference 1990s' decade average total precipitation was calculated. This percentage difference for a given cell was calculated only if the 1990s' average total precipitation for that cell was greater than 0.01 millimeter. This step is

¹⁷ Water year t is defined as the period from October 1 of year $(t - 1)$ to September 30 of year t . For example, water year 1951 will span from October, 1950 through September 1951. So there are 149 water years spanning the calendar years 1950–2099. For time series plotting of runoff, values from water year 1951 was repeated for 1950.

¹⁸ Seven locations from eight major Reclamation basins because of the combined delta inflow location from both the Sacramento and San Joaquin Rivers.

necessary to threshold division by a small value, which would result in a numerically large change magnitude. Also, positive percentage change implies wetter conditions, while negative percentage change implies drier conditions from the 1990s' reference decade.

After all projection-specific changes were calculated for a given future decade; three percentiles of change were calculated. These are the 25th percentile, the 50th percentile (or median), and the 75th percentile change. Estimating these different change percentiles for a given future decade provides a measure of the uncertainty in the projected precipitation change estimates in the three decades. The median or 50th percentile change provides a measure of the central tendency of change in decade average total precipitation in a given future decade from the 1990s' decade.

The estimation of decadal SWE distribution for the 1990s' reference decade and the change in SWE calculations for the future decades, 2020s, 2050s, and 2070s, are exactly similar. For SWE, the 25th percentile, the 50th percentile (or median), and the 75th percentile change in future decades are presented. The calculations for the spatial distribution of mean temperature are also similar to the spatial distribution of precipitation calculation for the 1990s' reference decade. The difference being, in case of temperature, mean annual temperature is first calculated from the 12 monthly values (in case of precipitation, it is the total precipitation) for each of the 10 water years and, subsequently, averaged to calculate the decade average mean annual temperature. The changes in mean annual temperature for the future decades are presented as magnitude changes and not as percentage change (precipitation changes in future decades are expressed as a percentage). The uncertainty in the distribution of the change in decade-mean temperature for the 2020s, 2050s, and 2070s are characterized using the 25th and 75th percentile with the median (50th percentile) representing the central tendency in decade-mean temperature distribution.

5.1.3 Impacts on Runoff Annual and Seasonal Cycles

Runoff at selected subbasin locations within the major Reclamation basins is presented under this section heading. The first set of plot demonstrates annual cycle variation and climate change impacts on the annual cycle at each of the selected locations. Mean annual hydrograph—plot of mean monthly flows from the 112 projections—is shown for the reference decade 1990s, covering water years 1990–1999. Similar mean annual hydrographs are developed for the three future decades 2020s (water years 2020–2029), 2050s (water years 2050–2059), and 2070s (water years 2070–2079). Uncertainty bounds—5th and 95th percentiles in the flow projections also are presented for the earliest (2020s) and latest (2070s) future decades.

The second set of plots shows the shift in the DJFM (December–March) total winter season runoff and AMJJ (April–July) total spring–summer season runoff for the three future decades from the reference 1990 decade. These seasonal shifts are presented as boxplots. The box in the boxplots is defined by the 25th and 75th percentiles of the respective time-series data (e.g., DJFM runoff)—interquartile range (IQR). The horizontal line within the box is the median of the time-series data, and the whiskers (horizontal bars at the end of vertical lines on either side of the box) are the approximate 5th and 95th percentiles of the time-series data. Points beyond the whiskers are referred to as the outliers. The boxplots are developed from the 112 projection specific decadal change values (change from the reference 1990s’ decade) for the winter and spring–summer runoff seasons.

In subsequent sections, 5.2 through 5.8, the plots described in sections 5.1.1 and 5.1.2 for each of the major Reclamation basins are presented. The results are presented in the following order of the basins.

- Colorado River Basin (section 5.2)
- Columbia River Basin (section 5.3)
- Klamath River Basin (section 5.4)
- Missouri River Basin (section 5.5)
- Rio Grande Basin (section 5.6)
- Sacramento and San Joaquin River Basins (section 5.7)
- Truckee and Carson River Basins (section 5.8)

5.2 Colorado River Basin

5.2.1 Hydroclimate Projections

Figure 22 shows six ensembles of hydroclimate projections for the basin above Colorado River at Imperial Dam: annual total precipitation (top left), annual mean temperature (top right), April 1st SWE (middle left), annual runoff (middle right), December–March runoff season (bottom left), and April–July runoff season (bottom right). The heavy black line is the annual time series of 50 percentile values (i.e., ensemble-median). The shaded area is the annual time series of 5th to 95th percentiles.

Total annual precipitation over the basin is seen to have a very nominal decline over the transient period going out to 2099. The uncertainty envelope appears to be largely constant over time, implying that there is no increase or decrease in the uncertainty envelope from the present for total annual precipitation magnitudes

through time. The mean annual temperature over the basin shows an increasing trend and a diverging uncertainty envelope over time. April 1st SWE also shows a decreasing trend. The annual runoff has a nominal declining trend. The December–March runoff volume shows no trend, but portrays divergence over time in the upper limit of its uncertainty bound.

Figure 23 shows spatial distribution of simulated decadal precipitation in the basin above the Colorado River at Imperial Dam: simulated 1990s' distribution of ensemble-median decadal mean condition (upper middle) and changes in decadal mean condition for three look ahead periods (2020s, 2050s, 2070s relative to 1990s) and at three change percentiles within the ensemble (25, 50, and 75). The change values are scaled from -20% (red, decrease) to +20% (blue, increase). For the 2020s' decade, there appears to be an increase in precipitation in the southern parts of the basin, some increase in the headwater areas of the basin on the west, and no change in the central portions of the basin. By the middle of the 21st century (2050s' decade), most of the basin shows a decline in precipitation volumes, except in the headwater areas. By the latter part of the 21st century (2070s' decade), the basin shows to become wetter mostly in the upper areas, but the lower regions of the basin shows decline persisting from the 2050s' decade.

Figure 24 shows spatial distribution of simulated decade mean temperature in the basin above the Colorado River at Imperial Dam: simulated 1990s' distribution of ensemble-median decadal mean condition (upper middle) and changes in decadal mean condition for three look ahead periods (2020s, 2050s, 2070s relative to 1990s) and at three change percentiles within the ensemble (25, 50, and 75). The change in temperature distribution is scaled from 0 to 6 °F. The median change for the 2020s', 2050s', and 2070s' decades relative to the 1990s shows an increasing temperature value throughout the basin.

Figure 25 shows spatial distribution of April 1st SWE in the basin above the Colorado River at Imperial Dam: simulated 1990s' distribution of ensemble-median decadal mean condition (upper middle) and ensemble-median change in decadal mean condition for the three look ahead periods (2020s, 2050s, 2070s relative to 1990s). The April 1st SWE shows persistent decline through the future decades from the 1990s' distribution.

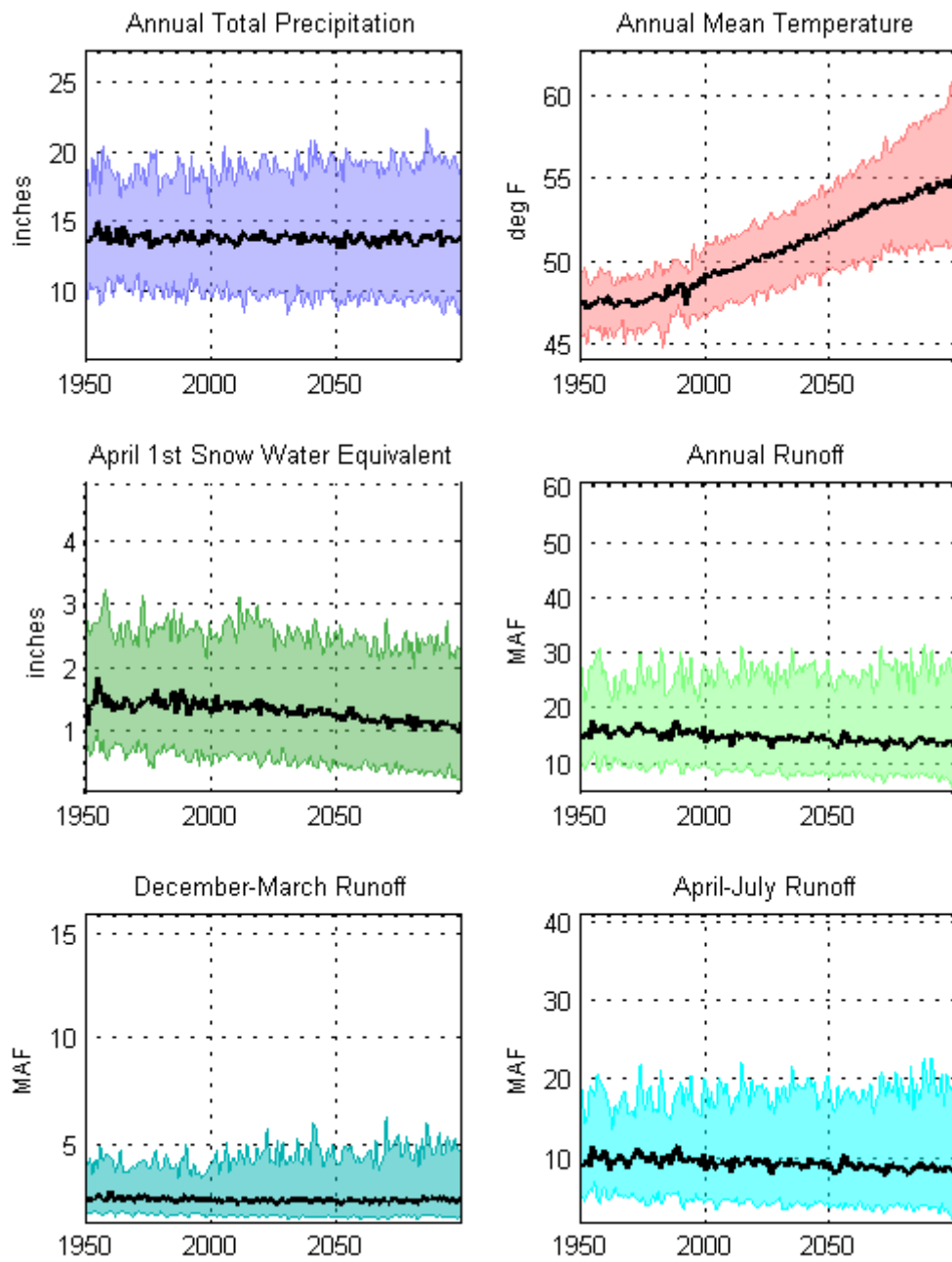


Figure 22. Colorado Basin – Projections Ensembles for Six Hydroclimate Indicators.

West-Wide Climate Risk Assessments:
BCSD Surface Water Projections

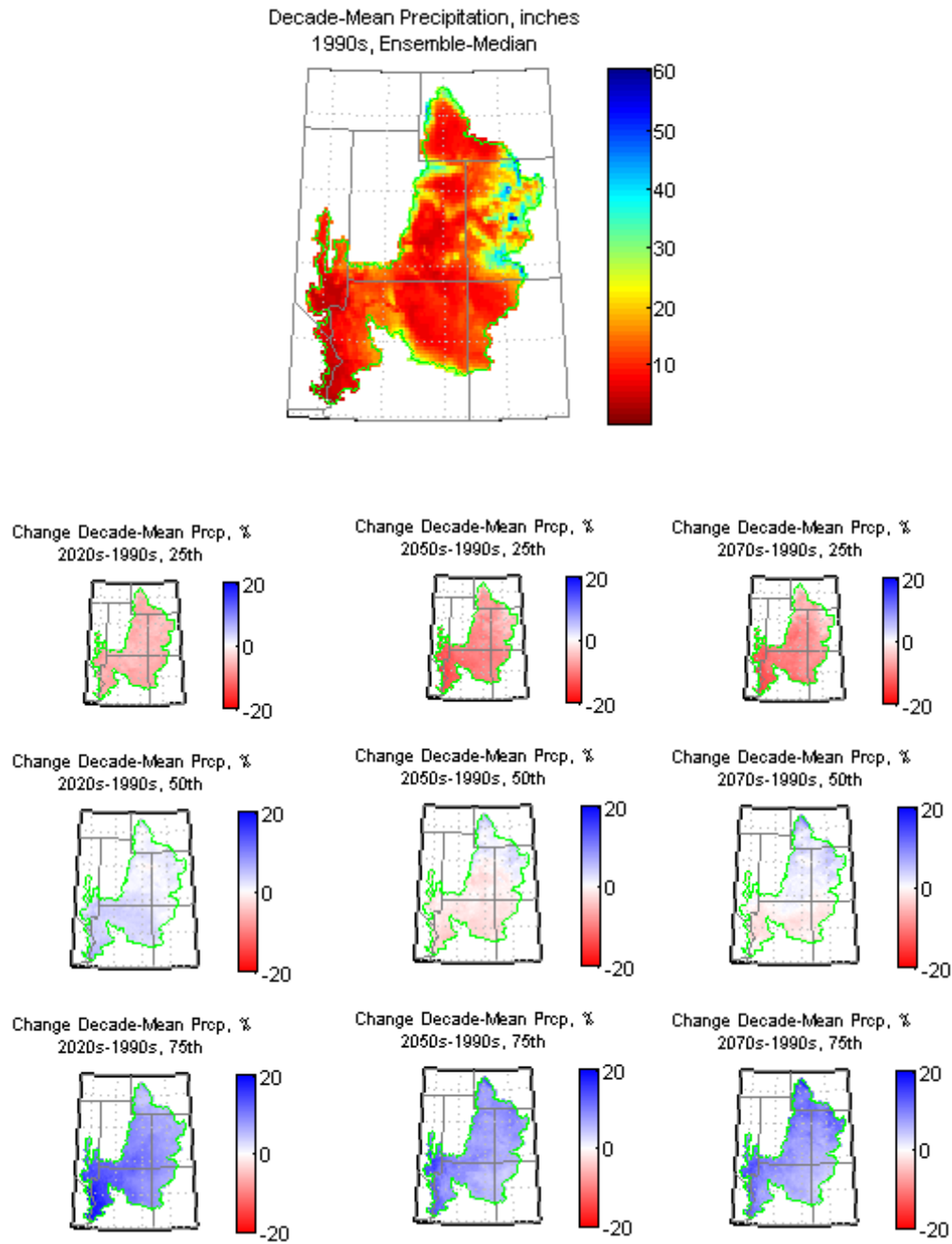


Figure 23. Colorado Basin – Spatial Distribution of Simulated Decadal Precipitation.

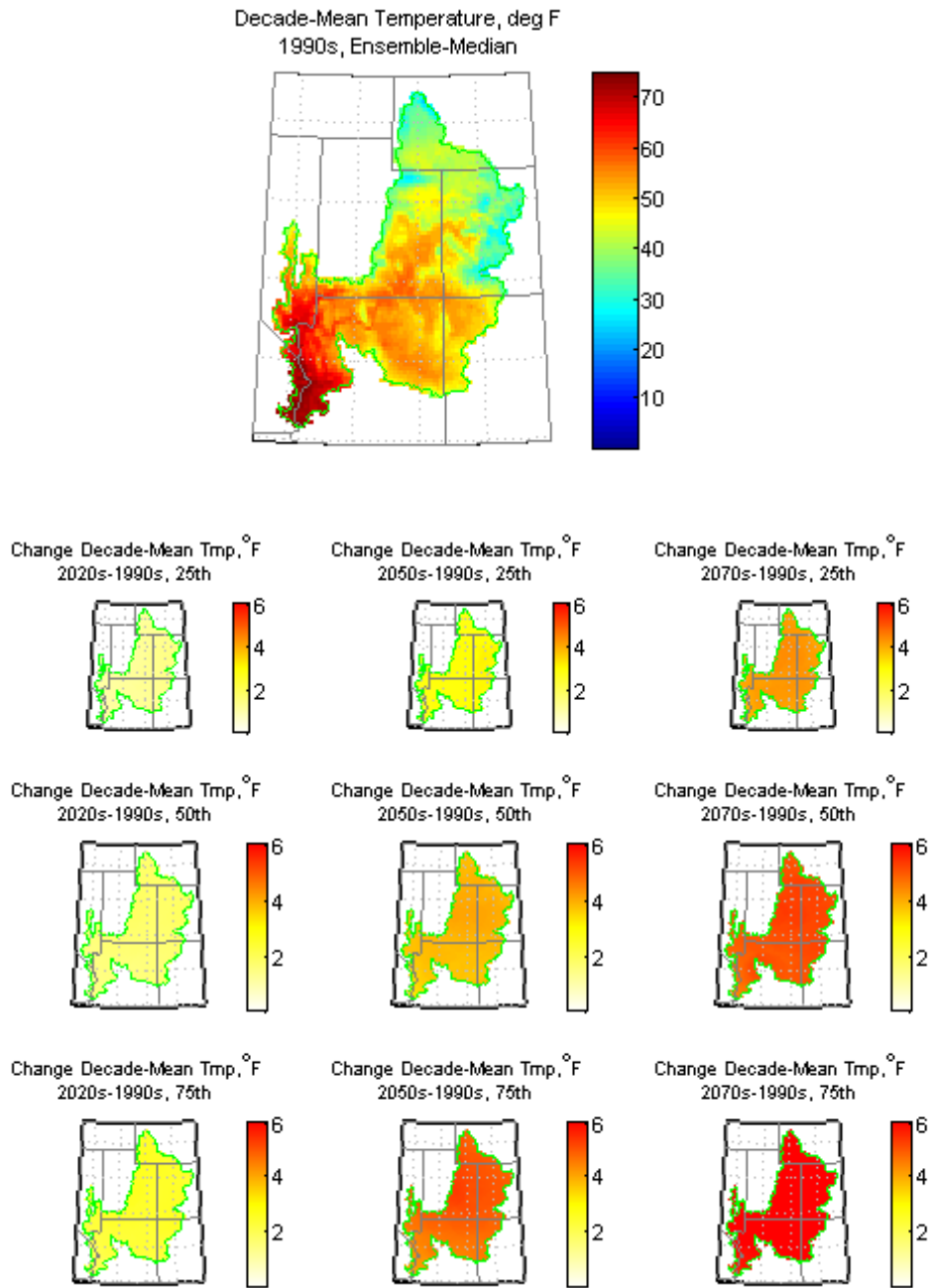


Figure 24. Colorado Basin – Spatial Distribution of Simulated Decadal Temperature.

West-Wide Climate Risk Assessments:
BCSD Surface Water Projections

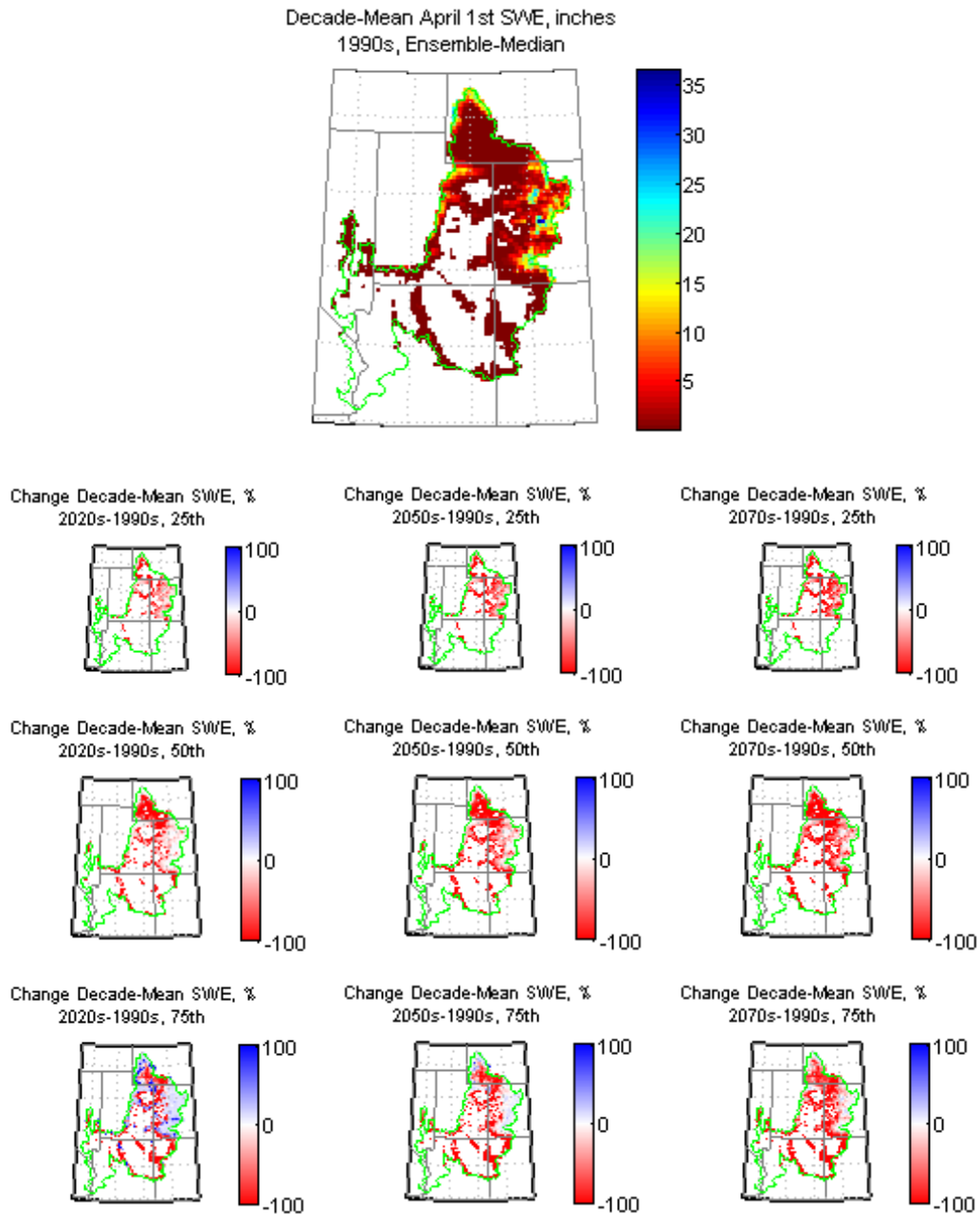


Figure 25. Colorado Basin – Spatial Distribution of Simulated Decadal April 1st SWE.

5.2.2 Impacts on Runoff Annual and Seasonal Cycles

Figure 26 shows ensemble-median mean-monthly values (heavy lines) for the 1990s, 2020s, 2050s, and 2070s, and the decadal-spread of mean-monthly runoff for the 1990s (black shaded area) and 2070s (magenta shaded area) where spread is bound by the ensemble's 5th to 95th percentile values for each month. Overall,

the shift to earlier runoff peaks—most prominent for the 2070s’ decade over the other decades for the Colorado River at Lees Ferry and at Cameo, Gunnison River near Grand Junction and for the San Juan River near Bluff.

Figure 27 shows the ensemble-distribution (boxplot) of changes in mean-seasonal values (heavy lines) for the 2020s, 2050s, and 2070s relative to the 1990s, where the boxplots’ box represents the ensemble’s interquartile range and the box-midline represents ensemble-median. There is no appreciable difference between the decades, except for the 2070s’ decade where there is some decrease in the median April–July runoff for the Gunnison River near Grand Junction and the San Juan River near Bluff location.

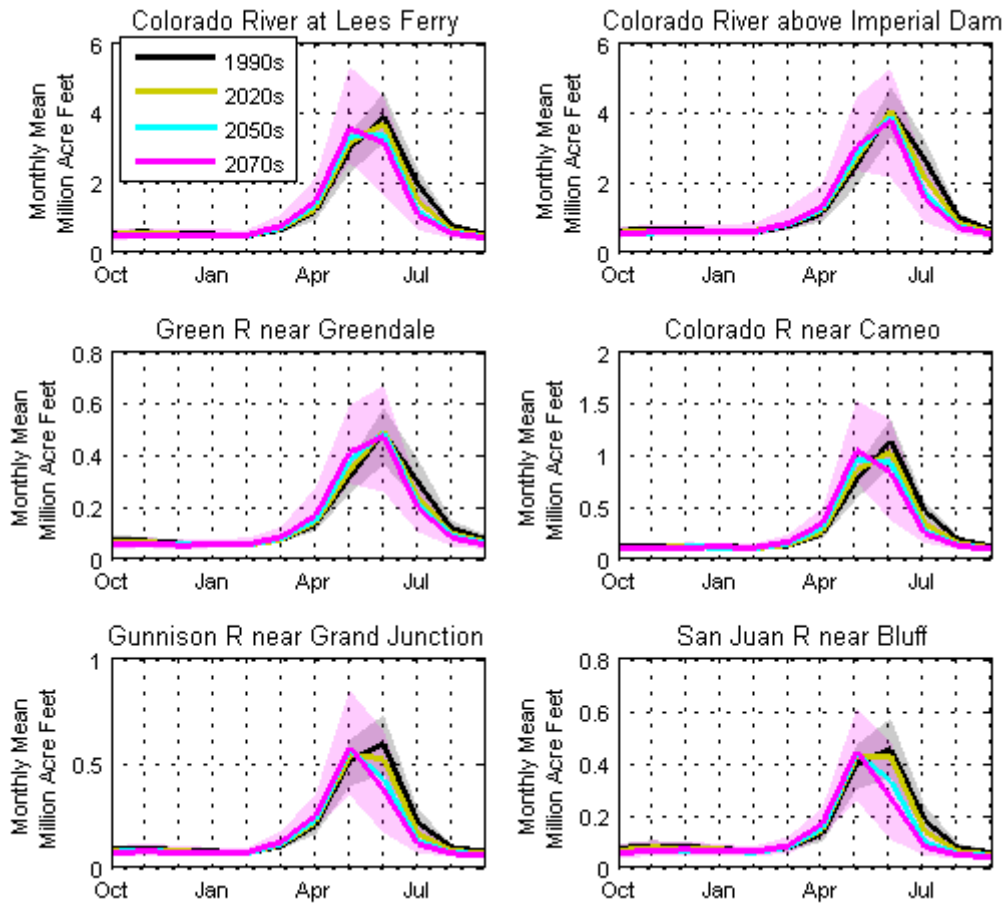


Figure 26. Colorado Basin – Simulated Mean-Monthly Runoff for Various Subbasins.

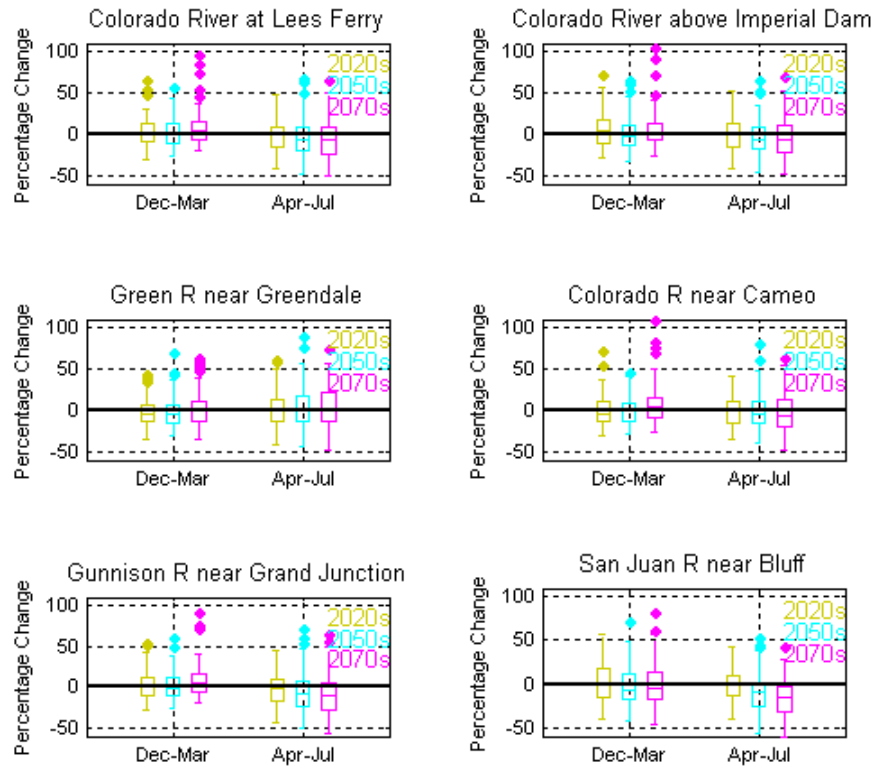


Figure 27. Colorado Basin – Simulated Mean-Seasonal Runoff for Various Subbasins.

5.3 Columbia River Basin

5.3.1 Hydroclimate Projections

Figure 28 shows six ensembles of hydroclimate projections for the basin above the Columbia River at The Dalles: annual total precipitation (top left), annual mean temperature (top right), April 1st SWE (middle left), annual runoff (middle right), December–March runoff season (bottom left), and April–July runoff season (bottom right). The heavy black line is the annual time series of 50 percentile values (i.e., ensemble-median). The shaded area is the annual time series of 5th to 95th percentiles.

There is an increasing trend of total annual precipitation across the basin through time. The uncertainty envelope for precipitation is also somewhat diverging. Mean annual temperature shows an increasing trend with an expanding uncertainty envelope through time. The April 1st SWE appears to have a nonlinear trend. The SWE has a nominal increasing trend going out to 2050 but appears to decline in the post-2050 period. The annual runoff has a nominal increasing trend, with expanding uncertainty bounds. The winter runoff

(December–March) also shows an increasing trend, and the upper uncertainty bound shows divergence over time. The April–July runoff season has a nominal increasing trend.

Figure 29 shows spatial distribution of simulated decade-mean precipitation in the basin above the Columbia River at The Dalles: simulated 1990s' distribution of ensemble-median decadal mean condition (upper middle) and changes in decadal mean condition for three look aheads (2020s, 2050s, 2070s relative to 1990s) and at three change percentiles within the ensemble (25, 50, and 75). The ensemble-median change for all the future decades shows increase in the spatial distribution of decade-mean precipitation relative to the 1990s. The ensemble-median precipitation also shows an increase in intensity relative to the 1990s for each successive look ahead decade.

Figure 30 shows spatial distribution of simulated decade-mean temperature in the basin above the Columbia River at The Dalles: simulated 1990s' distribution of ensemble-median decadal mean condition (upper middle) and changes in decadal mean condition for three look aheads (2020s, 2050s, 2070s relative to 1990s) and at three change percentiles within the ensemble (25, 50 and 75). The median change for the 2020s', 2050s', and 2070s' decades relative to the 1990s shows an increasing temperature value throughout the basin.

Figure 31 shows spatial distribution of April 1st SWE in the basin above the Columbia River at The Dalles: simulated 1990s' distribution of ensemble-median decadal mean condition (upper middle) and ensemble-median change in decadal mean condition for three look aheads (2020s, 2050s, 2070s relative to 1990s). The April 1st SWE shows persistent decline through the future decades from the 1990s' distribution.

West-Wide Climate Risk Assessments:
BCSD Surface Water Projections

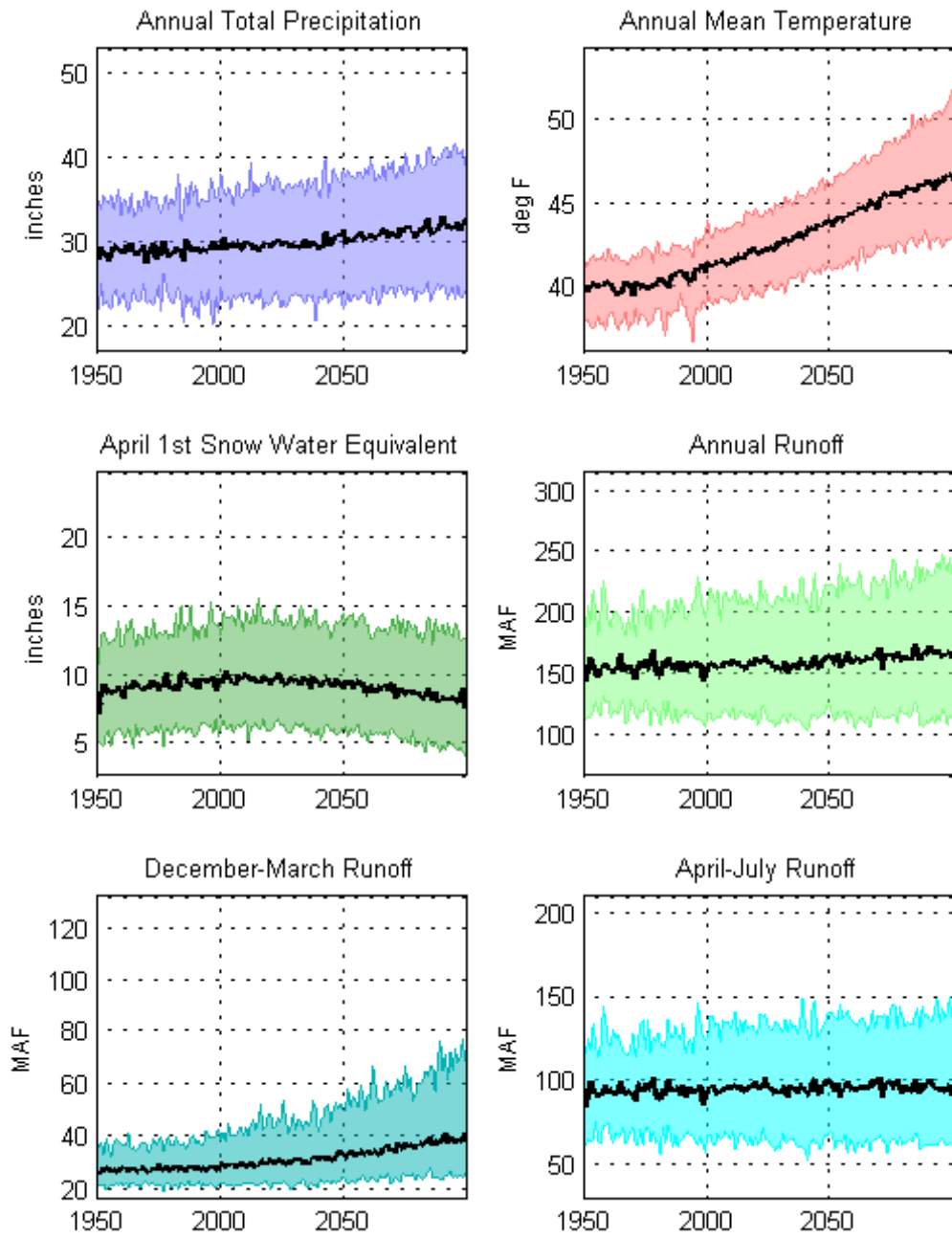


Figure 28. Columbia Basin – Projections Ensembles for Six Hydroclimate Indicators.

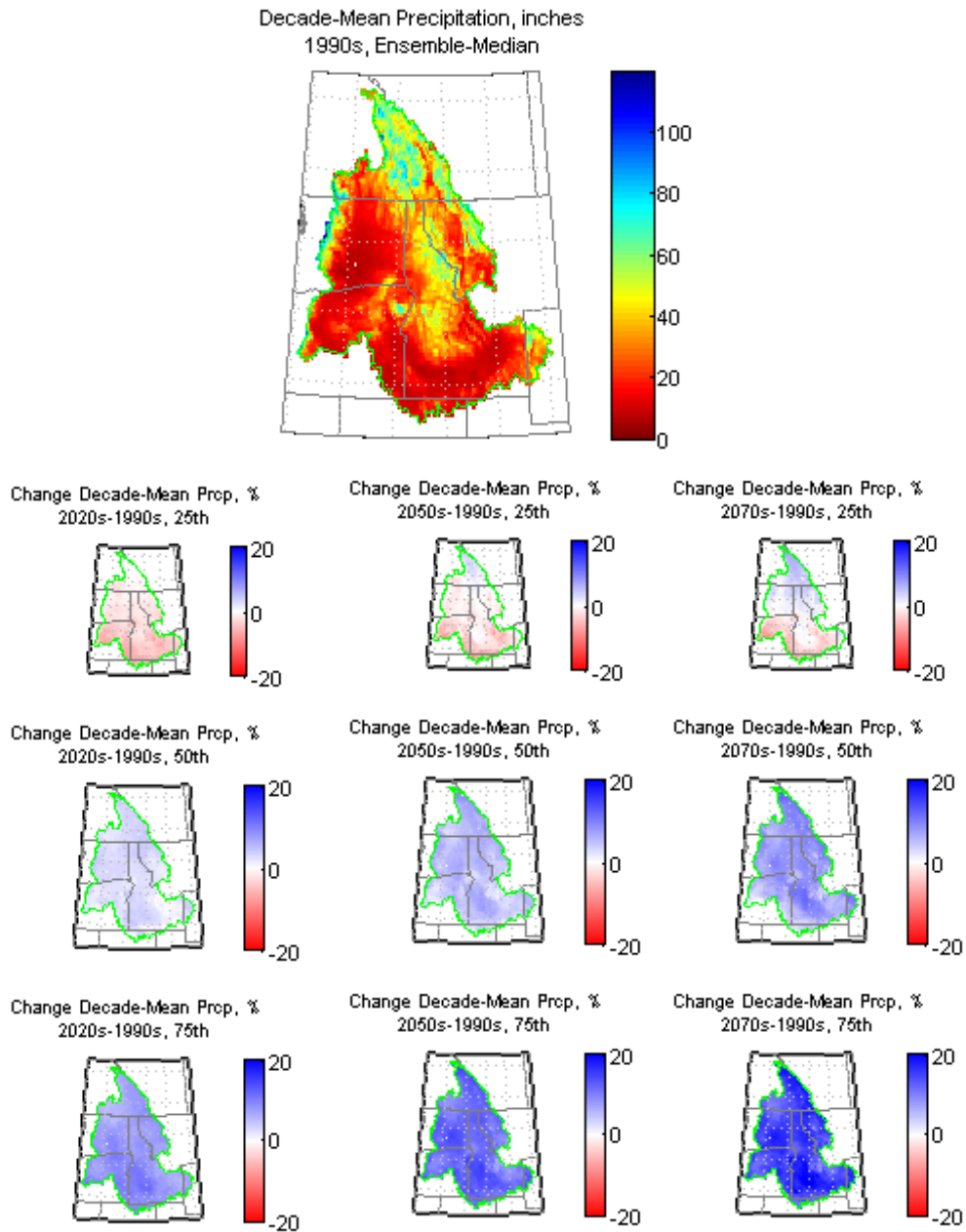


Figure 29. Columbia Basin – Spatial Distribution of Simulated Decadal Precipitation.

West-Wide Climate Risk Assessments:
BCSD Surface Water Projections

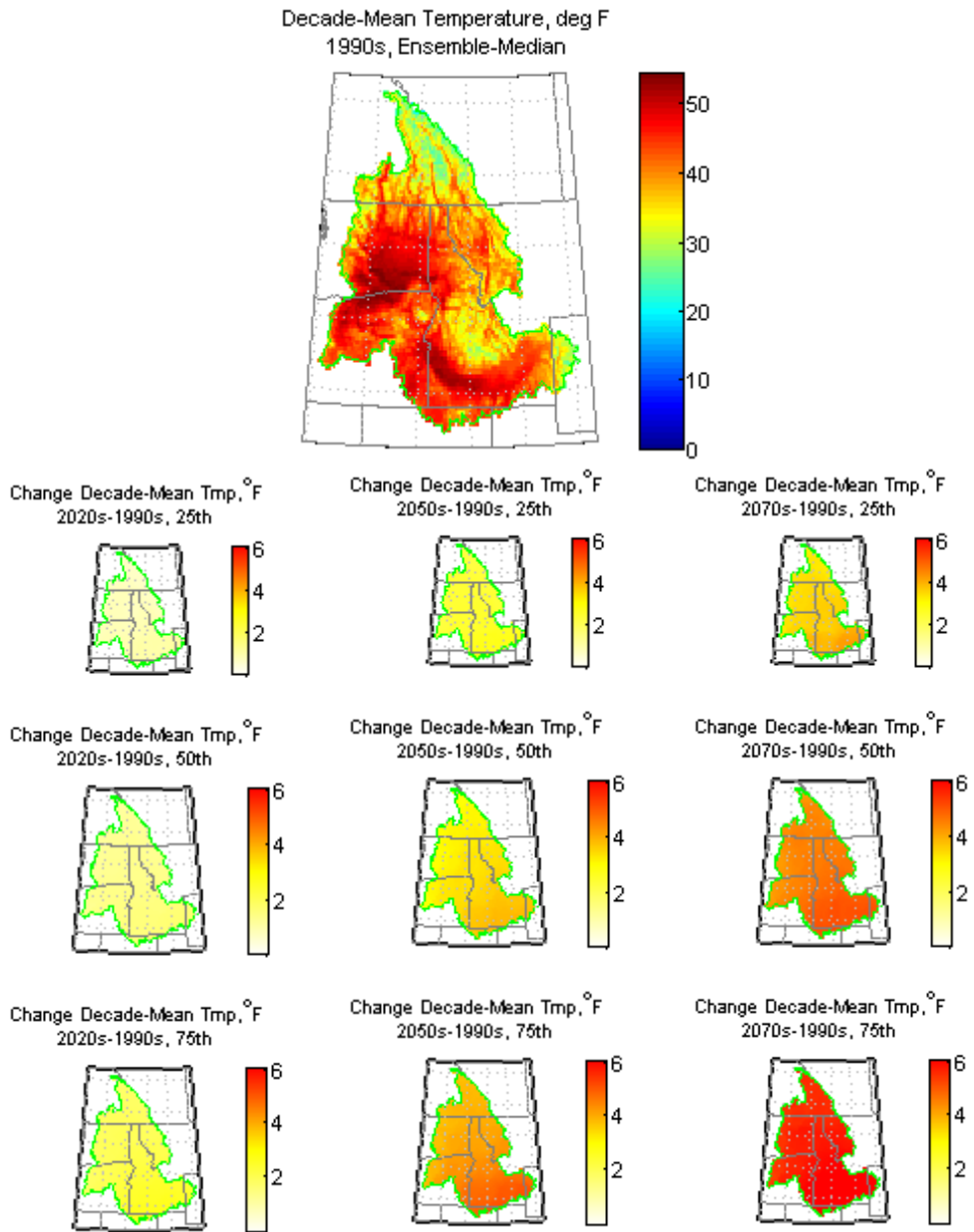


Figure 30. Columbia Basin – Spatial Distribution of Simulated Decadal Temperature.

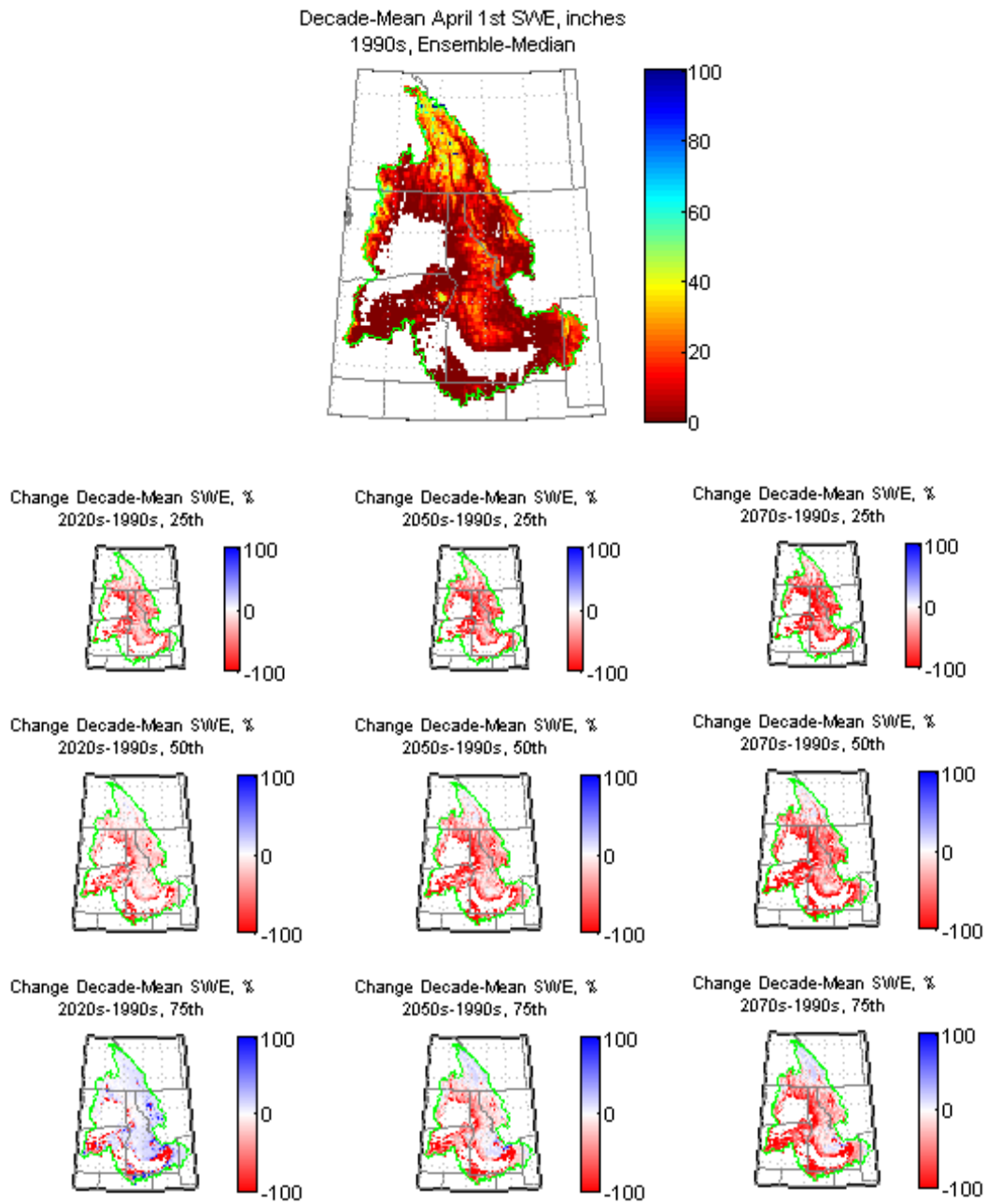


Figure 31. Columbia Basin – Spatial Distribution of Simulated Decadal April 1st SWE.

5.3.2 Impacts on Runoff Annual and Seasonal Cycles

Figure 32 shows ensemble-median mean-monthly values (heavy lines) for the 1990s, 2020s, 2050s, and 2070s, and the decadal-spread of mean-monthly runoff for the 1990s (black shaded area) and 2070s (magenta shaded area) where spread is bound by the ensemble's 5th to 95th percentile values for each month. There appears to be, overall, little shift in the peak runoff timing over the decades from the 1990s' reference.

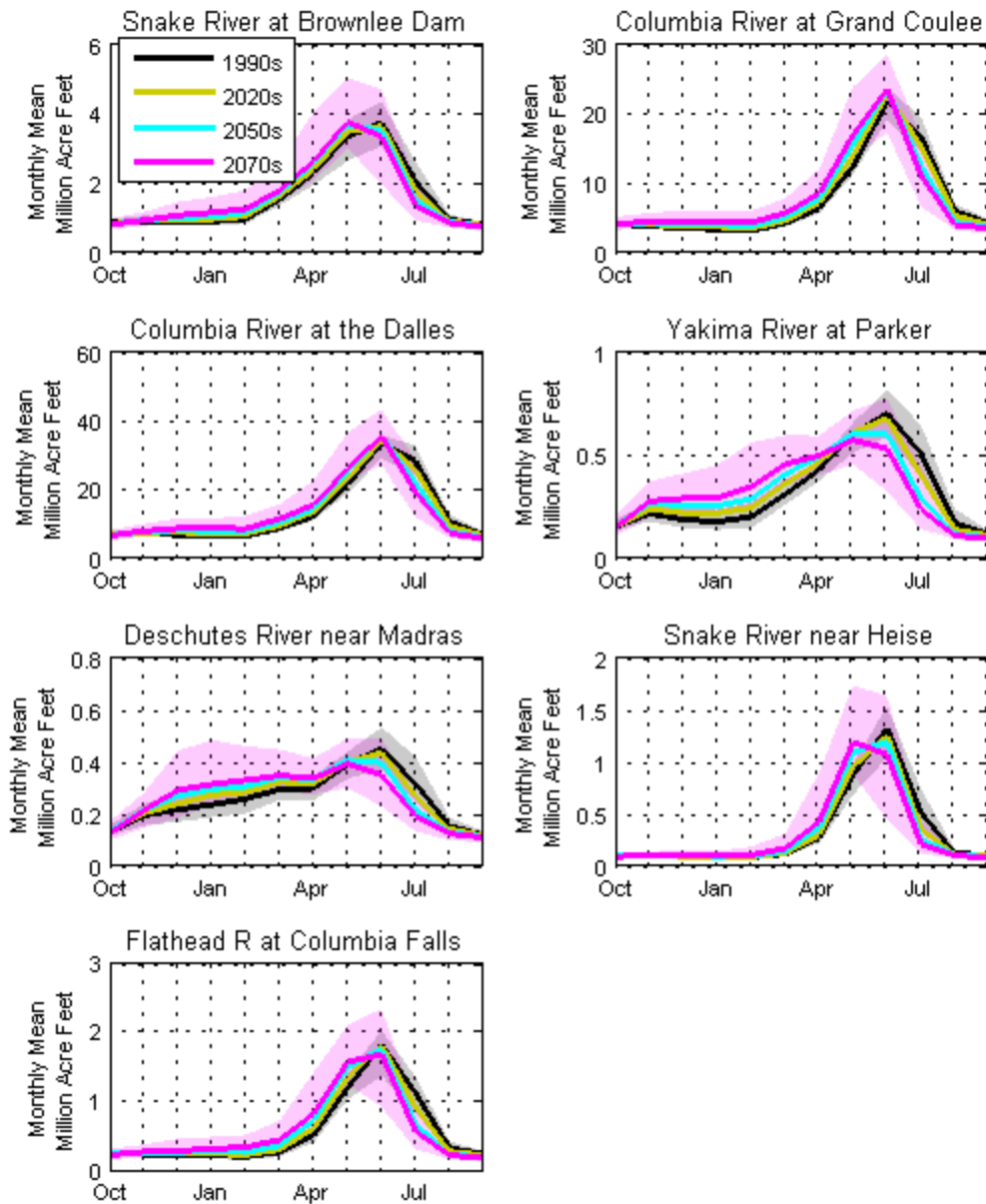


Figure 32. Columbia Basin – Simulated Mean-Monthly Runoff for Various Subbasins.

Figure 33 shows ensemble-distribution (boxplot) of changes in mean-seasonal values (heavy lines) for the 2020s, 2050s, and 2070s relative to the 1990s, where the boxplots box represents the ensemble’s interquartile range and the box-midline represents ensemble-median. For all the locations, there is increase in the winter (DJFM) runoff in all the future decades from the 1990s’ reference.

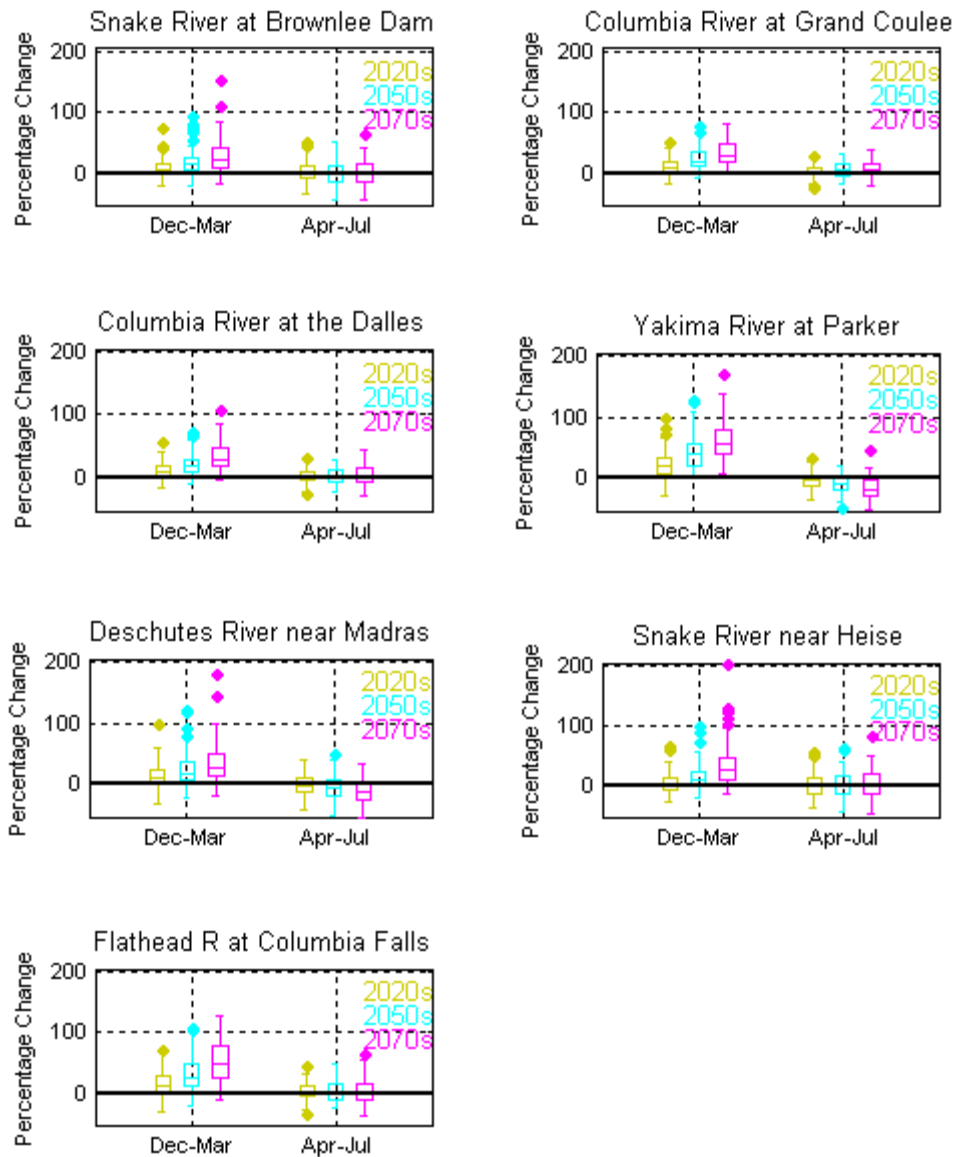


Figure 33. Columbia Basin – Simulated Mean-Seasonal Runoff for Various Subbasins.

5.4 Klamath River Basin

5.4.1 Hydroclimate Projections

Figure 34 shows six ensembles of hydroclimate projections for the basin above the Klamath River near Klamath: annual total precipitation (top left), annual mean temperature (top right), April 1st SWE (middle left), annual runoff (middle right), December–March runoff season (bottom left), and April–July runoff season (bottom right). The heavy black line is the annual time series of 50 percentile values (i.e., ensemble-median). The shaded area is the annual time series of 5th to 95th percentile.

Annual total precipitation shows no trend. Annual mean temperature shows an increasing trend. April 1st SWE shows a decreasing trend. Annual runoff shows no trend over time. Winter runoff shows an increasing trend, but the spring–summer runoff shows a decreasing trend.

Figure 35 shows spatial distribution of simulated decadal precipitation in the basin above the Klamath River near Klamath: simulated 1990s' distribution of ensemble-median decadal mean condition (upper middle) and changes in decadal mean condition for three look aheads (2020s, 2050s, 2070s relative to 1990s) and at three change percentiles within the ensemble (25, 50, and 75). The ensemble-median change for the 2020s' and 2050s' future decades shows increase in the spatial distribution of decade-mean precipitation relative to the 1990s. The 2070s' decade show a decrease in precipitation distribution over the 1990s' reference.

Figure 36 shows spatial distribution of simulated decadal temperature in the basin above the Klamath River near Klamath: simulated 1990s' distribution of ensemble-median decadal mean condition (upper middle) and changes in decadal mean condition for three look aheads (2020s, 2050s, 2070s relative to 1990s) and at three change percentiles within the ensemble (25, 50, and 75). The median change for the 2020s', 2050s', and 2070s' decades relative to the 1990s shows an increasing temperature value throughout the basin.

Figure 37 shows spatial distribution of April 1st SWE in the basin above the Klamath River near Klamath: simulated 1990s' distribution of ensemble-median decadal mean condition (upper middle) and ensemble-median change in decadal mean condition for three look aheads (2020s, 2050s, 2070s relative to 1990s). The April 1st SWE shows persistent decline through the future decades from the 1990s' distribution. The decrease in April 1st SWE shows a progressive increase in snowpack loss over the three decades and has a north to south trajectory.

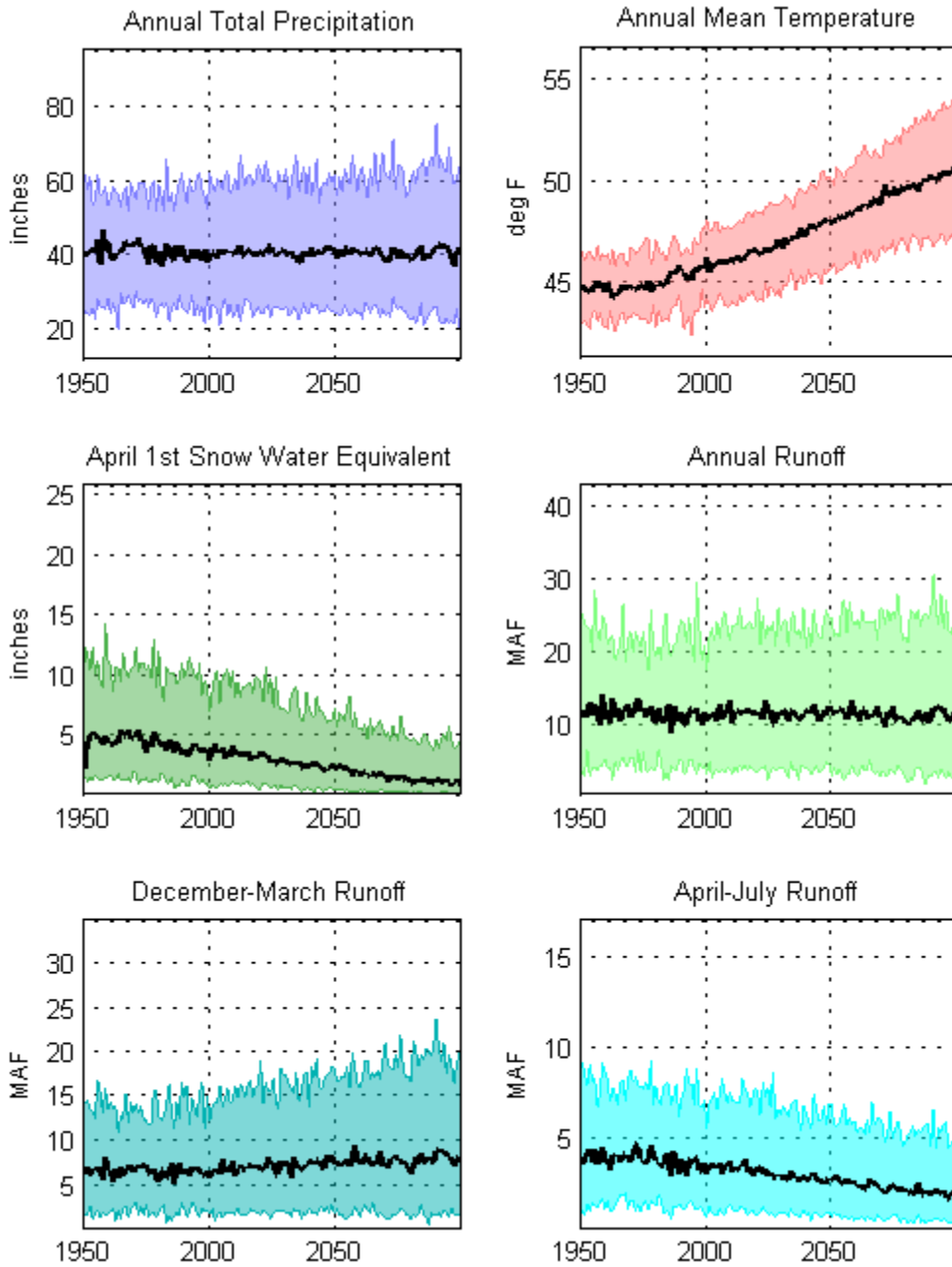


Figure 34. Klamath Basin – Projections Ensembles for Six Hydroclimate Indicators.

West-Wide Climate Risk Assessments:
BCSD Surface Water Projections

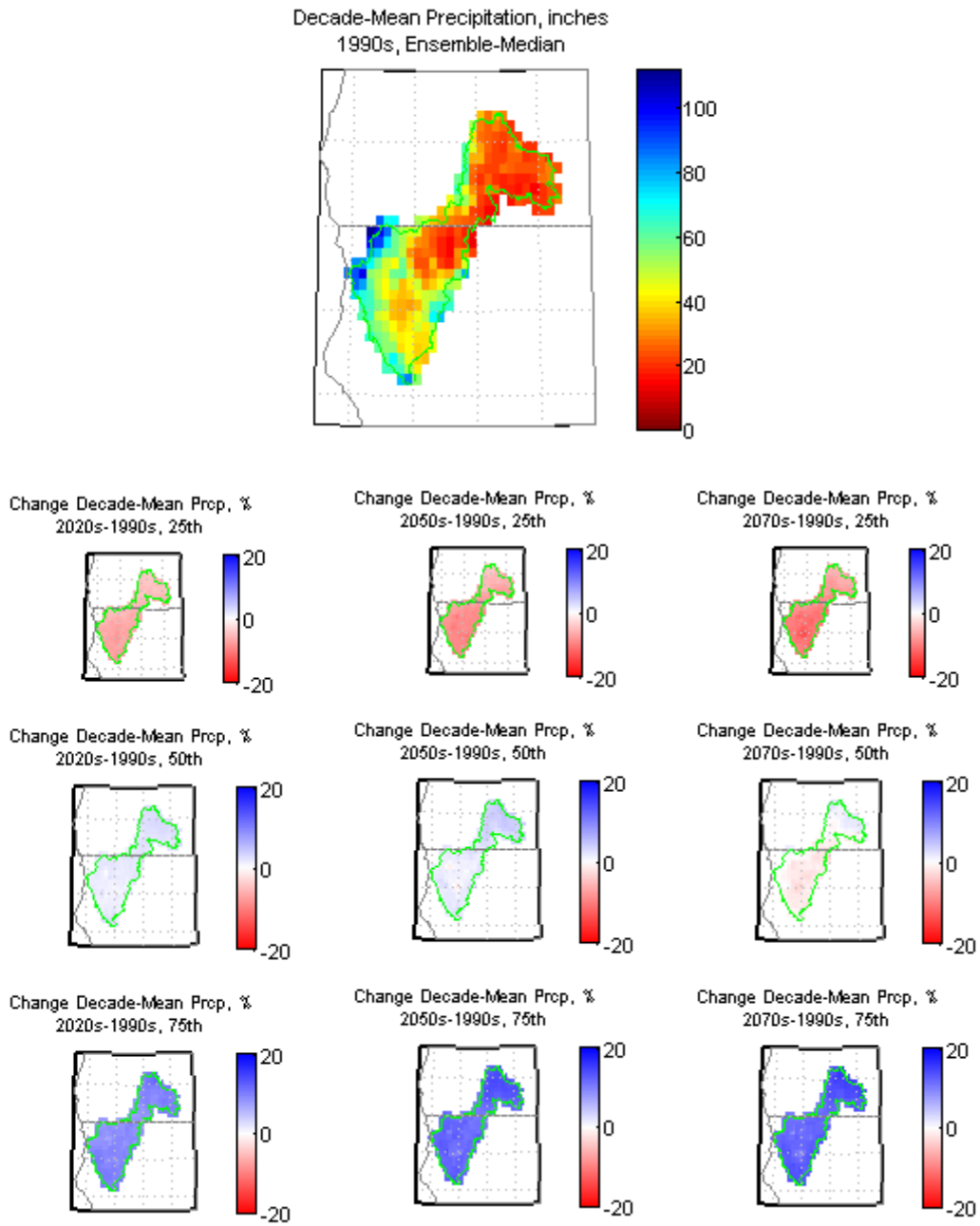


Figure 35. Klamath Basin – Spatial Distribution of Simulated Decadal Precipitation.

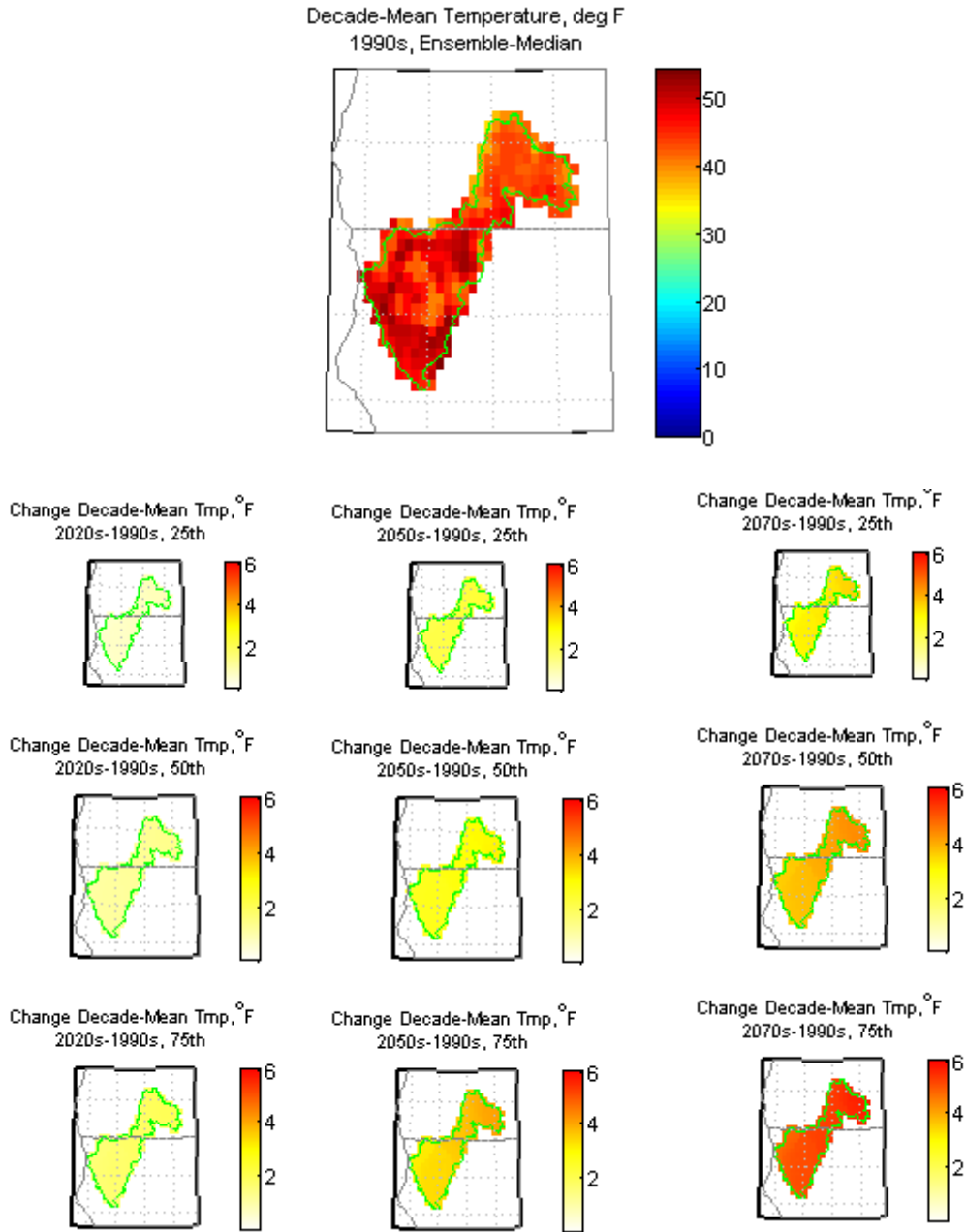


Figure 36. Klamath Basin – Spatial Distribution of Simulated Decadal Temperature.

West-Wide Climate Risk Assessments:
BCSD Surface Water Projections

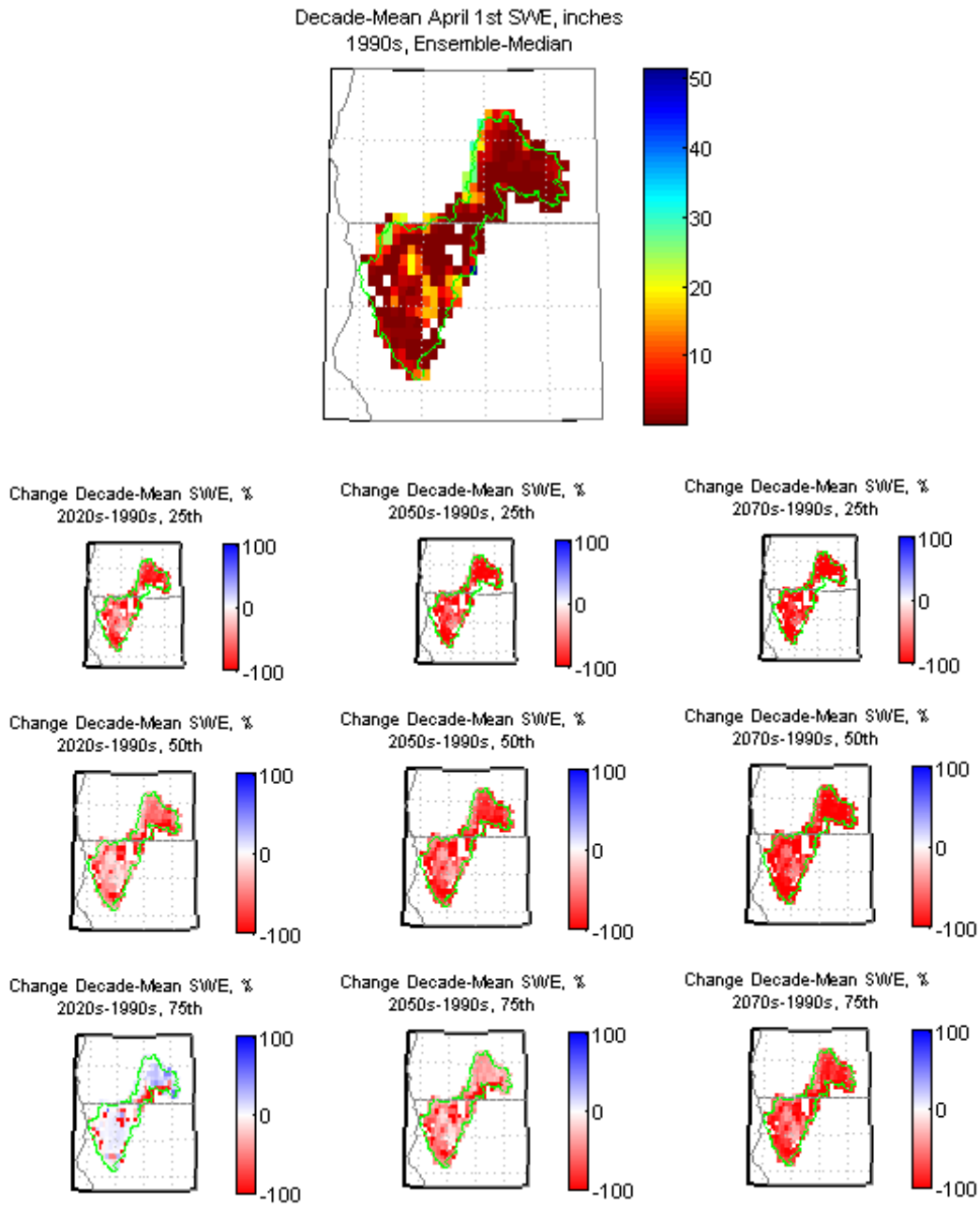


Figure 37. Klamath Basin – Spatial Distribution of Simulated Decadal April 1st SWE.

5.4.2 Impacts on Runoff Annual and Seasonal Cycles

Figure 38 shows ensemble-median mean-monthly values (heavy lines) for the 1990s, 2020s, 2050s, and 2070s, and the decadal-spread of mean-monthly runoff for the 1990s (black shaded area) and 2070s (magenta shaded area) where spread is bound by the ensemble's 5th to 95th percentile values for each month. For all the five sites in this basin, the shift in peak runoff in all the future decades is clearly visible.

Figure 39 shows ensemble-distribution (boxplot) of changes in mean-seasonal values (heavy lines) for the 2020s, 2050s, and 2070s relative to the 1990s, where the boxplots box represents the ensemble's interquartile range and the box-midline represents ensemble-median. For all the sites, there are large increases in the December–March runoff from the 1990s and decreases in April–July runoff.

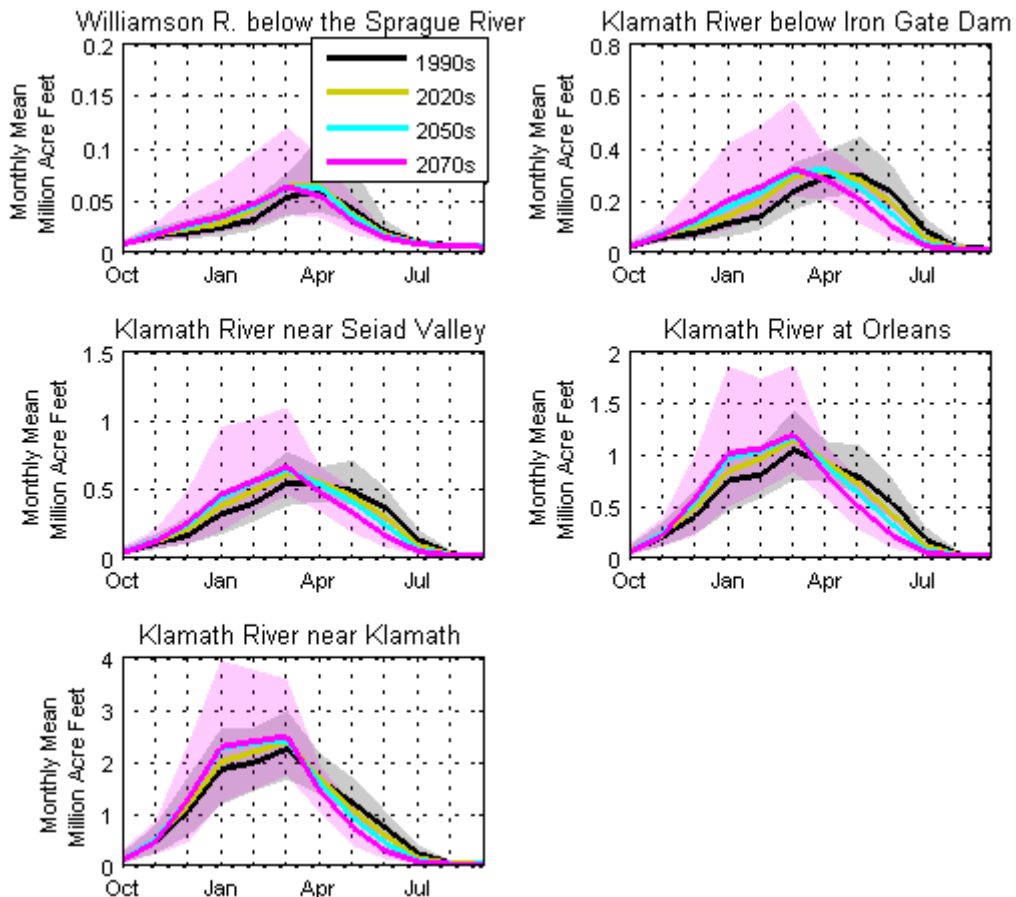


Figure 38. Klamath Basin – Simulated Mean-Monthly Runoff for Various Subbasins.

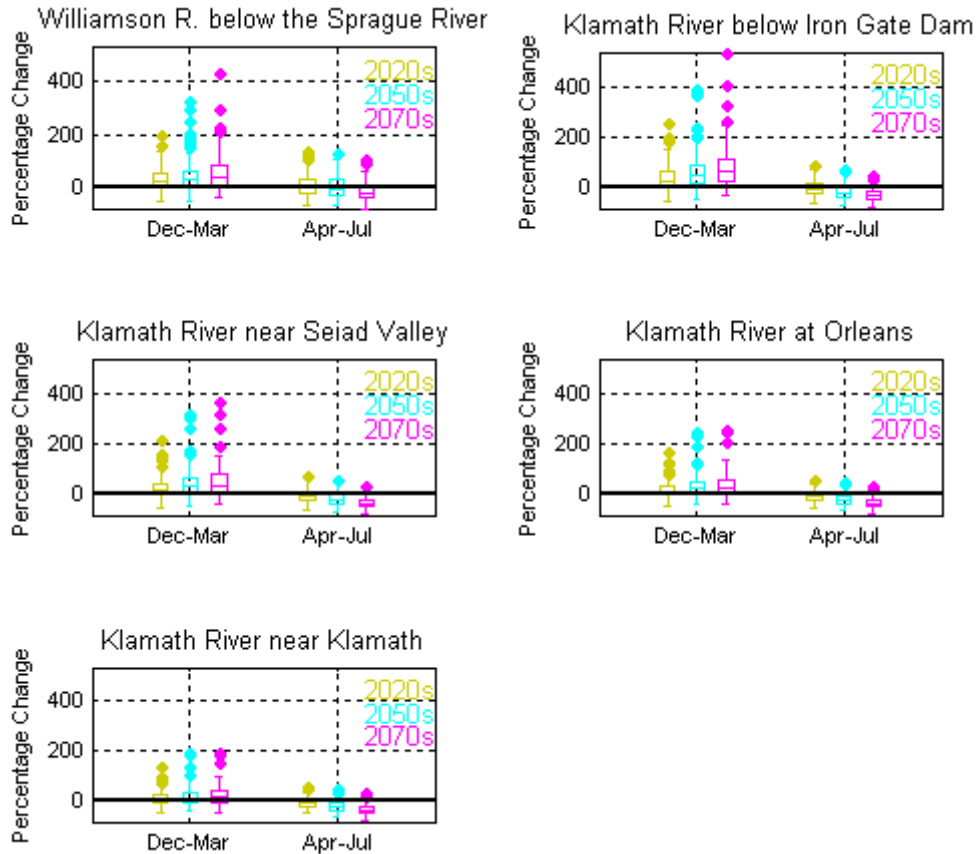


Figure 39. Klamath Basin – Simulated Mean-Seasonal Runoff for Various Subbasins.

5.5 Missouri River Basin

5.5.1 Hydroclimate Projections

Figure 40 shows six ensembles of hydroclimate projections for the basin above the Missouri River at Omaha: annual total precipitation (top left), annual mean temperature (top right), April 1st SWE (middle left), annual runoff (middle right), December–March runoff season (bottom left), and April–July runoff season (bottom right). The heavy black line is the annual time series of 50 percentile values (i.e., ensemble-median). The shaded area is the annual time series of 5th to 95th percentile.

Annual total precipitation shows an increasing trend. Annual mean temperature shows an increasing trend. April 1st SWE show a decreasing trend. Annual runoff shows an increasing trend. December–March runoff shows an increasing trend, and April–July runoff also shows an increasing trend. It is interesting

to note the increase in spring–summer season runoff in spite of a decreasing April 1st SWE. The fact that annual total precipitation has an increasing trend contributes to the increased April–July runoff.

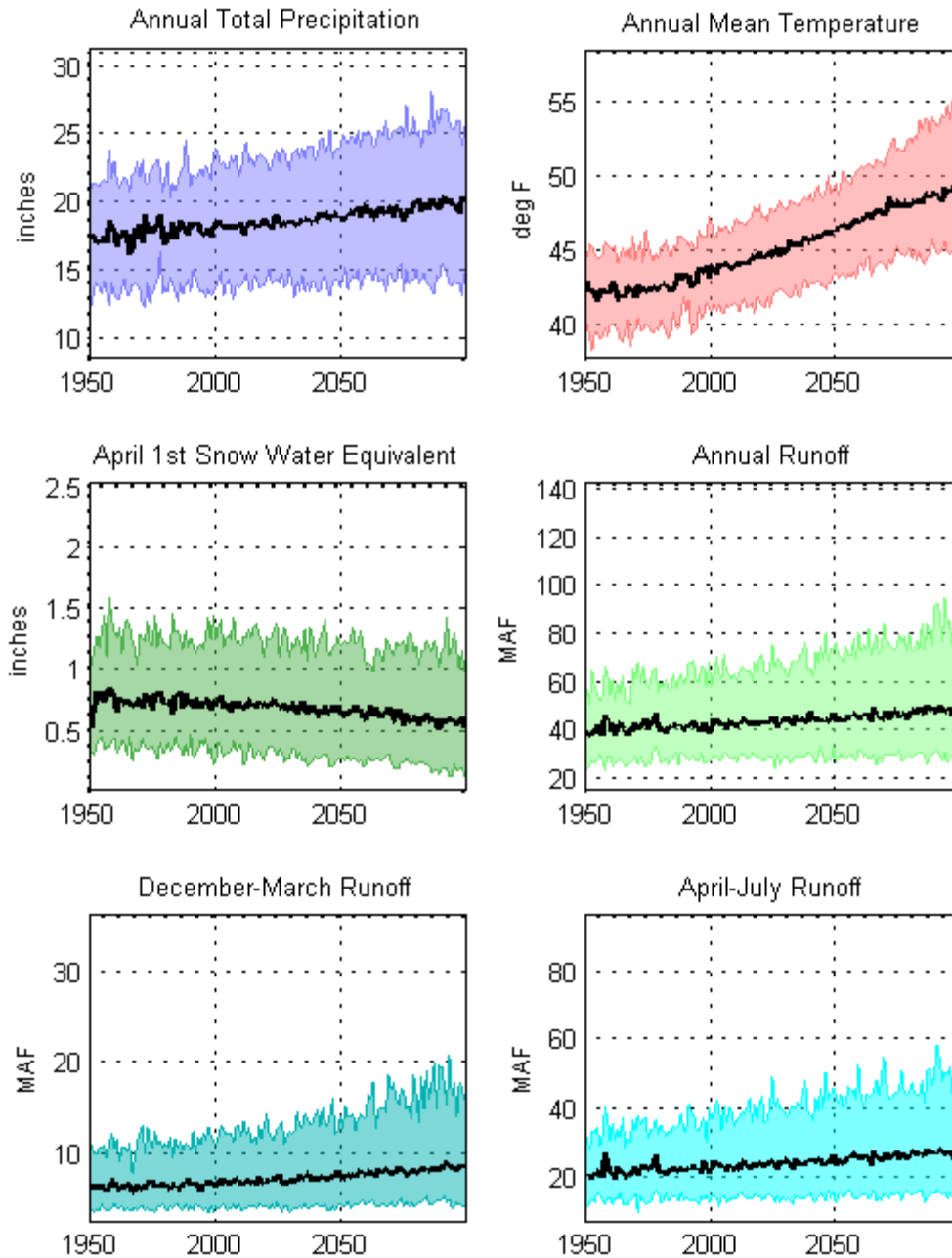


Figure 40. Missouri Basin – Projections Ensembles for Six Hydroclimate Indicators.

Figure 41 shows a spatial distribution of simulated decadal precipitation in the basin above the Missouri River at Omaha: simulated 1990s' distribution of ensemble-median decadal mean condition (upper middle) and changes in decadal mean condition for three look aheads (2020s, 2050s, 2070s relative to 1990s) and at three change percentiles within the ensemble (25, 50, and 75). The ensemble-median change for all the future decades shows an increase in the spatial distribution of decade-mean precipitation relative to the 1990s. The ensemble-median precipitation also shows an increase in intensity relative to the 1990s for each successive look ahead decade.

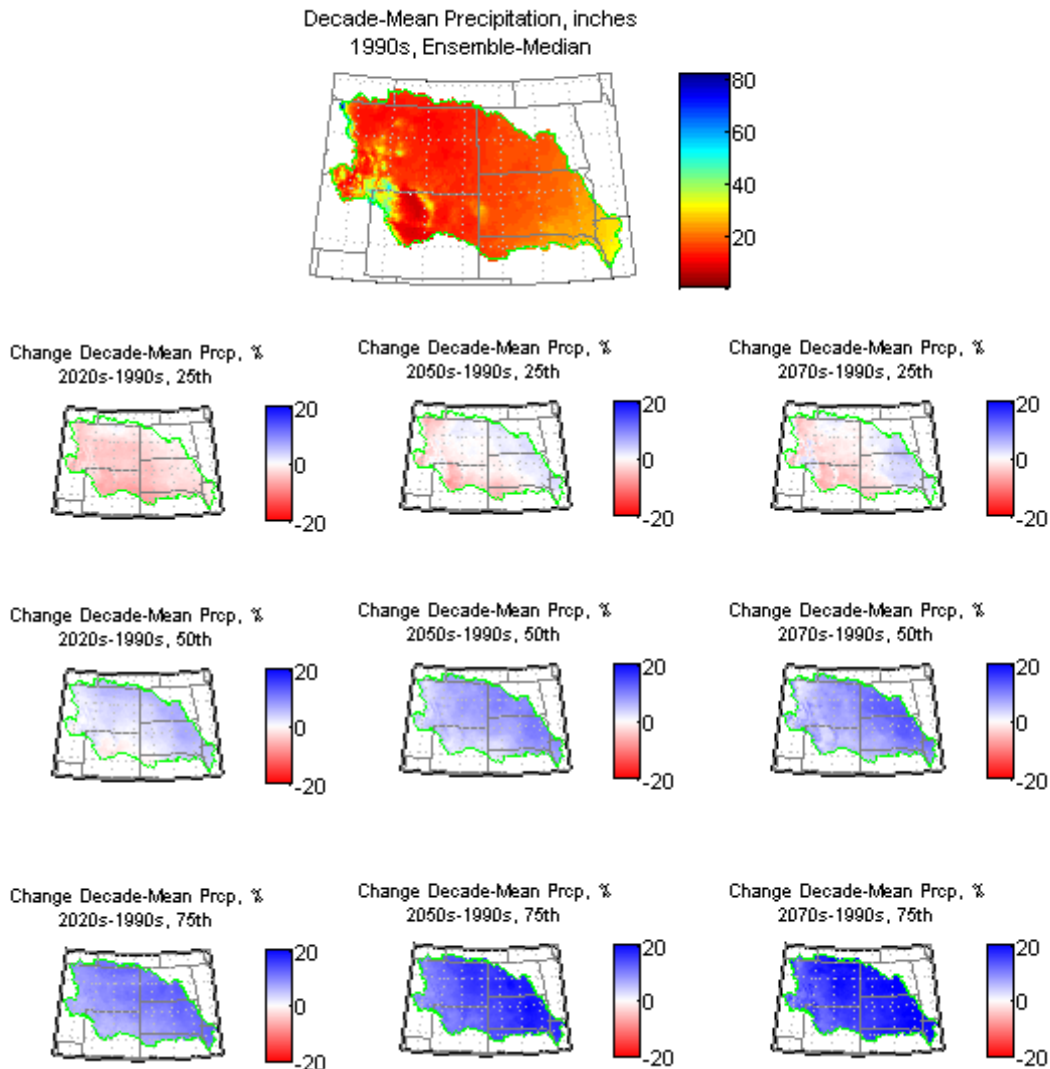


Figure 41. Missouri Basin – Spatial Distribution of Simulated Decadal Precipitation.

Figure 42 shows a spatial of simulated decadal temperature distribution in the basin above the Missouri River at Omaha: simulated 1990s' distribution of ensemble-median decadal mean condition (upper middle) and changes in decadal mean condition for three look aheads (2020s, 2050s, 2070s relative to 1990s) and at three change percentiles within the ensemble (25, 50, and 75). The median change for the 2020s', 2050s', and 2070s' decades relative to the 1990s shows an increasing temperature value throughout the basin.

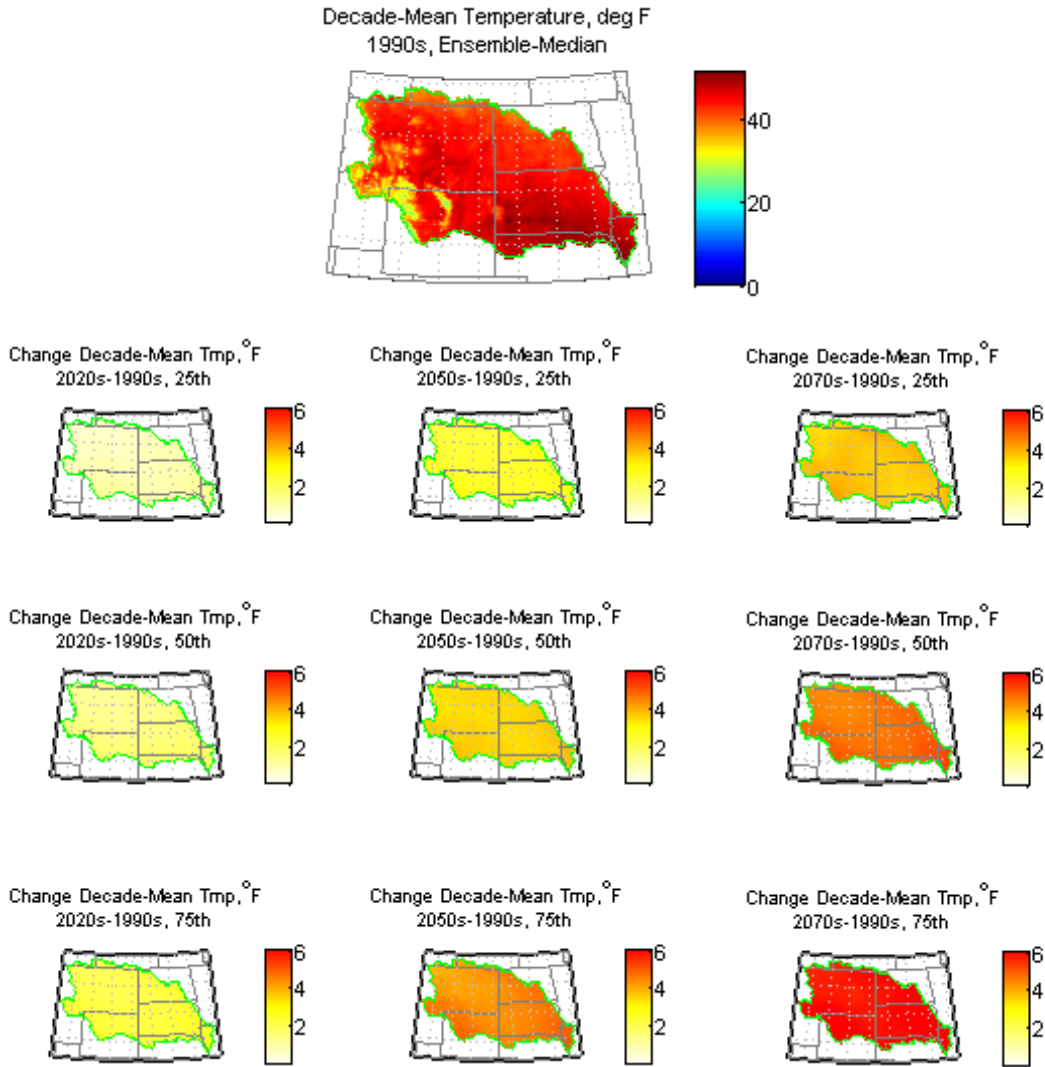


Figure 42. Missouri Basin – Spatial Distribution of Simulated Decadal Temperature.

Figure 43 shows a spatial distribution of April 1st SWE in the basin above the Missouri River at Omaha: simulated 1990s' distribution of ensemble-median decadal mean condition (upper middle) and ensemble-median change in decadal mean condition for three look aheads (2020s, 2050s, 2070s relative to 1990s). The April 1st SWE shows persistent decline through the future decades from the 1990s' distribution.

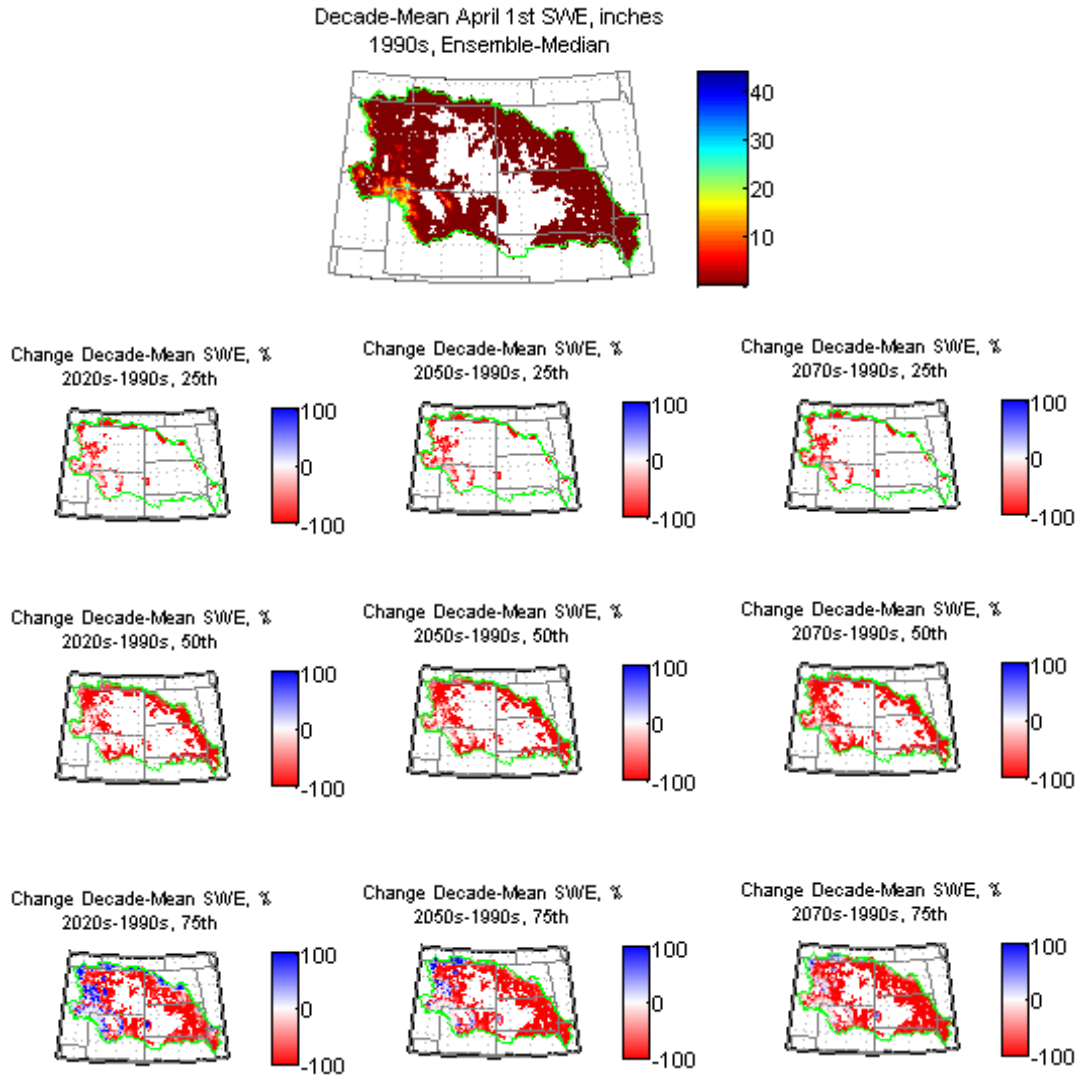


Figure 43. Missouri Basin – Spatial Distribution of Simulated Decadal April 1st SWE.

5.5.2 Impacts on Runoff Annual and Seasonal Cycles

Figure 44 shows ensemble-median mean-monthly values (heavy lines) for the 1990s, 2020s, 2050s, and 2070s, and the decadal-spread of mean-monthly runoff for the 1990s (black shaded area) and 2070s (magenta shaded area) where spread is bound by the ensemble’s 10th to 90th percentile values for each month. There is a shift in peak runoff timing between the 2020s’ and 2070s’ decades.

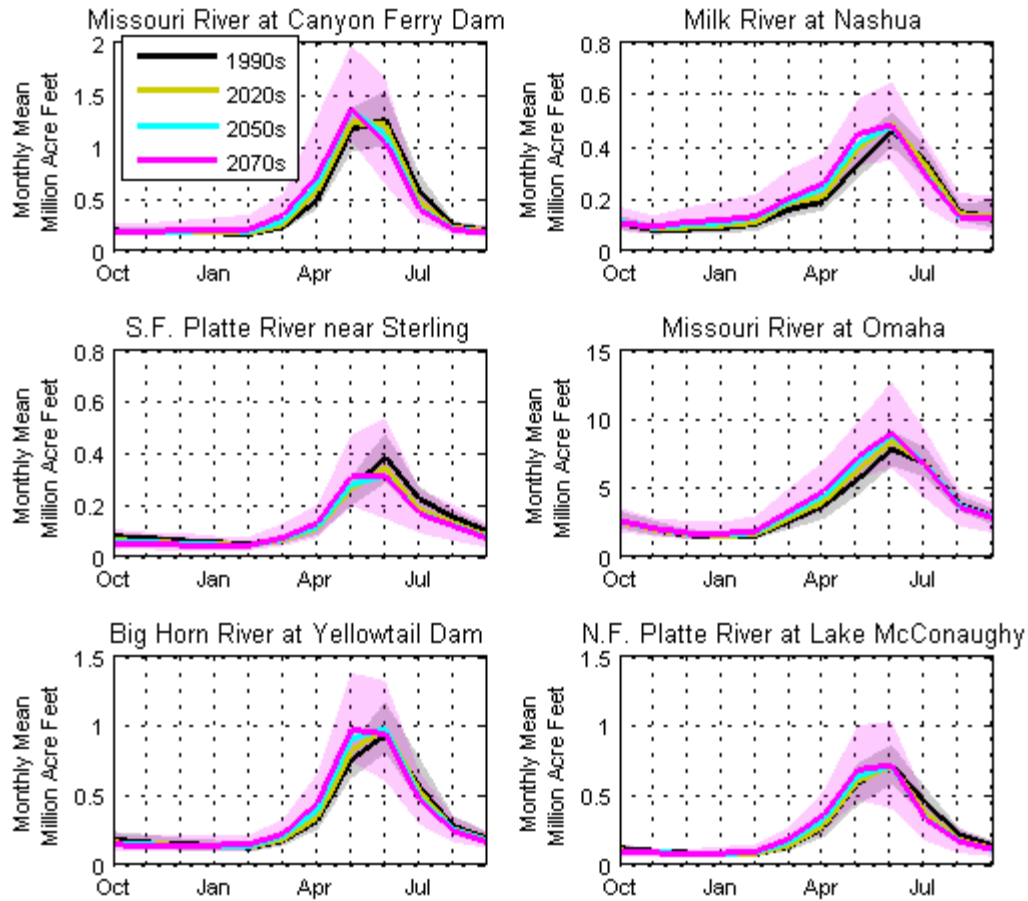


Figure 44. Missouri Basin – Simulated Mean-Monthly Runoff for Various Subbasins.

Figure 45 shows ensemble-distribution (boxplot) of changes in mean-seasonal values (heavy lines) for the 2020s, 2050s, and 2070s relative to the 1990s, where the boxplots box represents the ensemble’s interquartile range and the box-midline represents ensemble-median. Results generally suggest increasing winter and spring–summer runoff for the future decades from the 1990s’ reference, except for the South Fork of the South Platte River near Sterling, Colorado. This site shows a decline in the median change value from the 1990s’ reference.

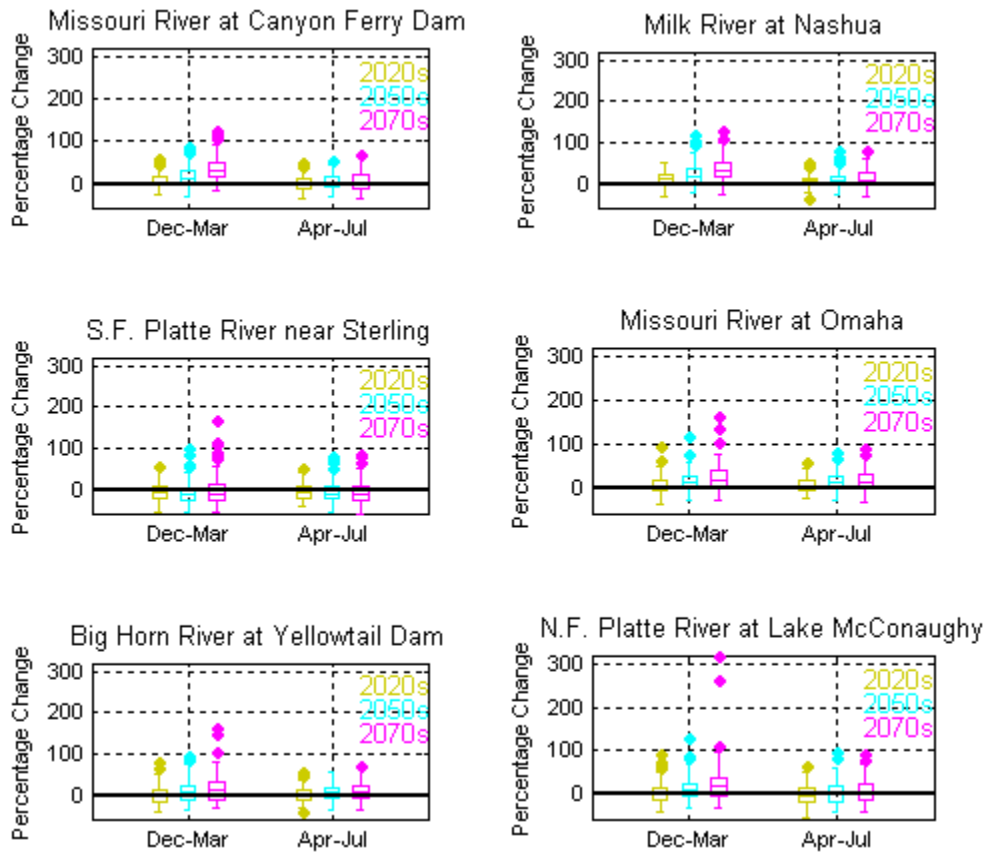


Figure 45. Missouri Basin – Simulated Mean-Seasonal Runoff for Various Subbasins.

5.6 Rio Grande Basin

5.6.1 Hydroclimate Projections

Figure 46 shows six ensembles of hydroclimate projections for the basin above the Rio Grande at Elephant Butte Dam: annual total precipitation (top left), annual mean temperature (top right), April 1st SWE (middle left), annual runoff (middle right), December–March runoff season (bottom left), and April–July runoff season (bottom right). The heavy black line is the annual time series of 50 percentile values (i.e., ensemble-median). The shaded area is the annual time series of 5th to 95th percentile.

Annual total precipitation shows a nominally decreasing trend through time. The annual mean temperature shows an increasing trend. The April 1st SWE shows a decreasing trend. Annual runoff, winter season runoff, and spring–summer runoff all show a declining trend.

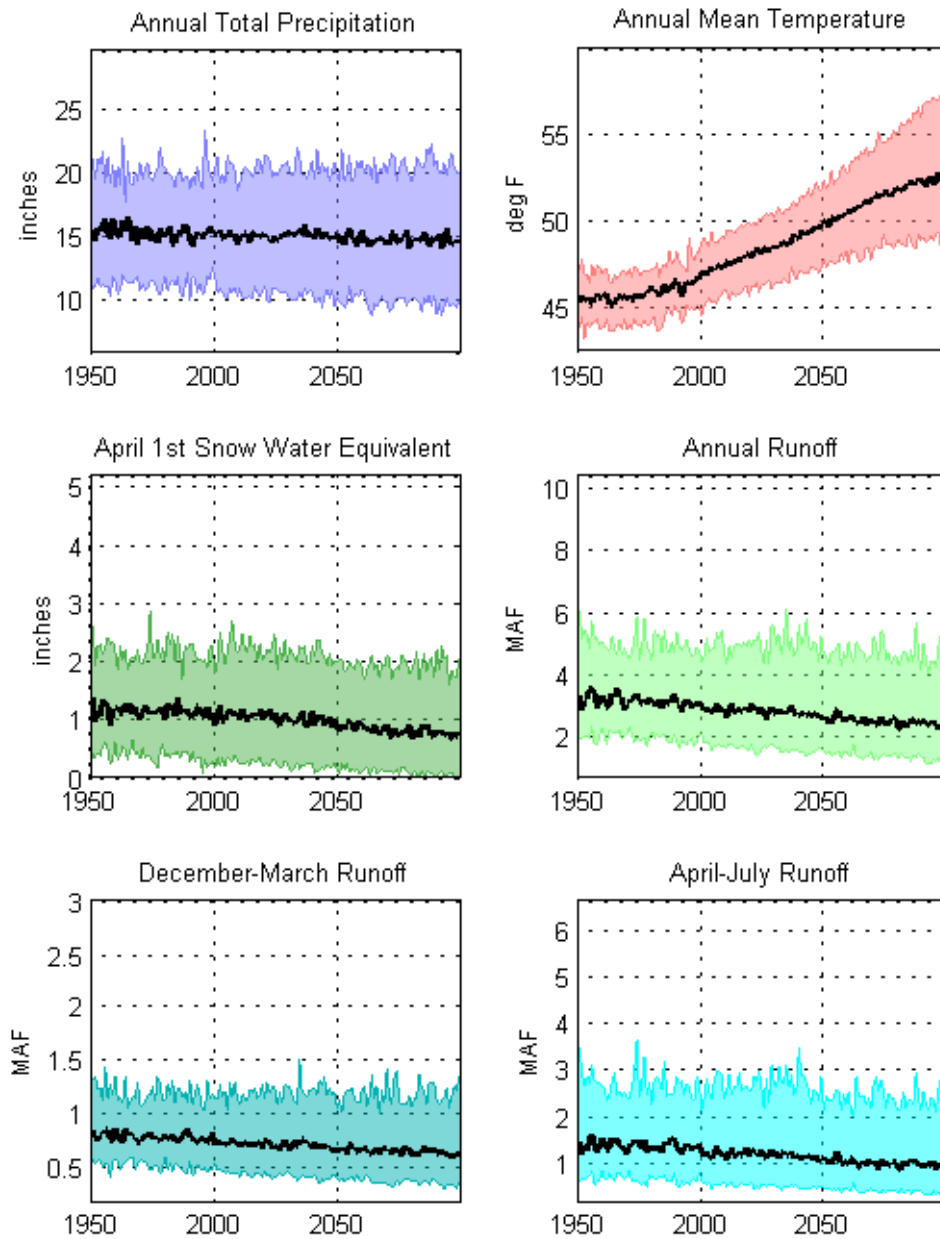


Figure 46. Rio Grande Basin – Projections Ensembles for Six Hydroclimate Indicators.

Figure 46 shows six ensembles of hydroclimate projections for the basin above the Rio Grande at Elephant Butte Dam: annual total precipitation (top left), annual mean temperature (top right), April 1st SWE (middle left), annual runoff (middle right), December–March runoff season (bottom left), and April–July runoff season (bottom right). The heavy black line is the annual time series of 50 percentile values (i.e., ensemble-median). The shaded area is the annual time series of 5th to 95th percentile.

Figure 47 shows the spatial distribution of simulated decadal precipitation in the basin above the Rio Grande at Elephant Butte Dam: simulated 1990s' distribution of ensemble-median decadal mean condition (upper middle) and changes in decadal mean condition for three look aheads (2020s, 2050s, 2070s relative to 1990s) and at three change percentiles within the ensemble (25, 50, and 75). The ensemble-median change for all the future decades shows decrease in the spatial distribution of decade-mean precipitation relative to the 1990s. The ensemble-median precipitation also shows an increase in intensity relative to the 1990s for each successive look ahead decade.

Figure 48 shows spatial distribution of simulated decadal temperature in the basin above "Rio Grande at Elephant Butte Dam": simulated 1990s' distribution of ensemble-median decadal mean condition (upper middle) and changes in decadal mean condition for three look ahead periods (2020s, 2050s, 2070s relative to 1990s) and at three change percentiles within the ensemble (25, 50 and 75).

Figure 49 shows spatial distribution of April 1st snow water equivalent (SWE) in the basin above "Rio Grande at Elephant Butte Dam": simulated 1990s' distribution of ensemble-median decadal mean condition (upper middle) and ensemble-median change in decadal mean condition for the three look ahead periods (2020s, 2050s, 2070s relative to 1990s). The April 1st SWE shows persistent decline through the future decades from the 1990s' distribution.

5.6.2 Impacts on Runoff Annual and Seasonal Cycles

Figure 50 shows ensemble-median mean-monthly values (heavy lines) for the 1990s, 2020s, 2050s, and 2070s and the decadal-spread of mean-monthly runoff for the 1990s (black shaded area) and 2070s (magenta shaded area) where spread is bound by the ensemble's 5th to 95th percentile values for each month. For most locations in this basin, the runoff peaks appear to be occurring earlier in the later decade (2070) than the earlier decade (2020).

Figure 51 shows ensemble-distribution (boxplot) of changes in mean-seasonal values (heavy lines) for the 2020s, 2050s, and 2070s relative to the 1990s, where the boxplots box represents the ensemble's interquartile range and the box-midline represents ensemble-median. For all the locations, there is a general decline in the seasonal runoff in all the future decades from the 1990s' reference.

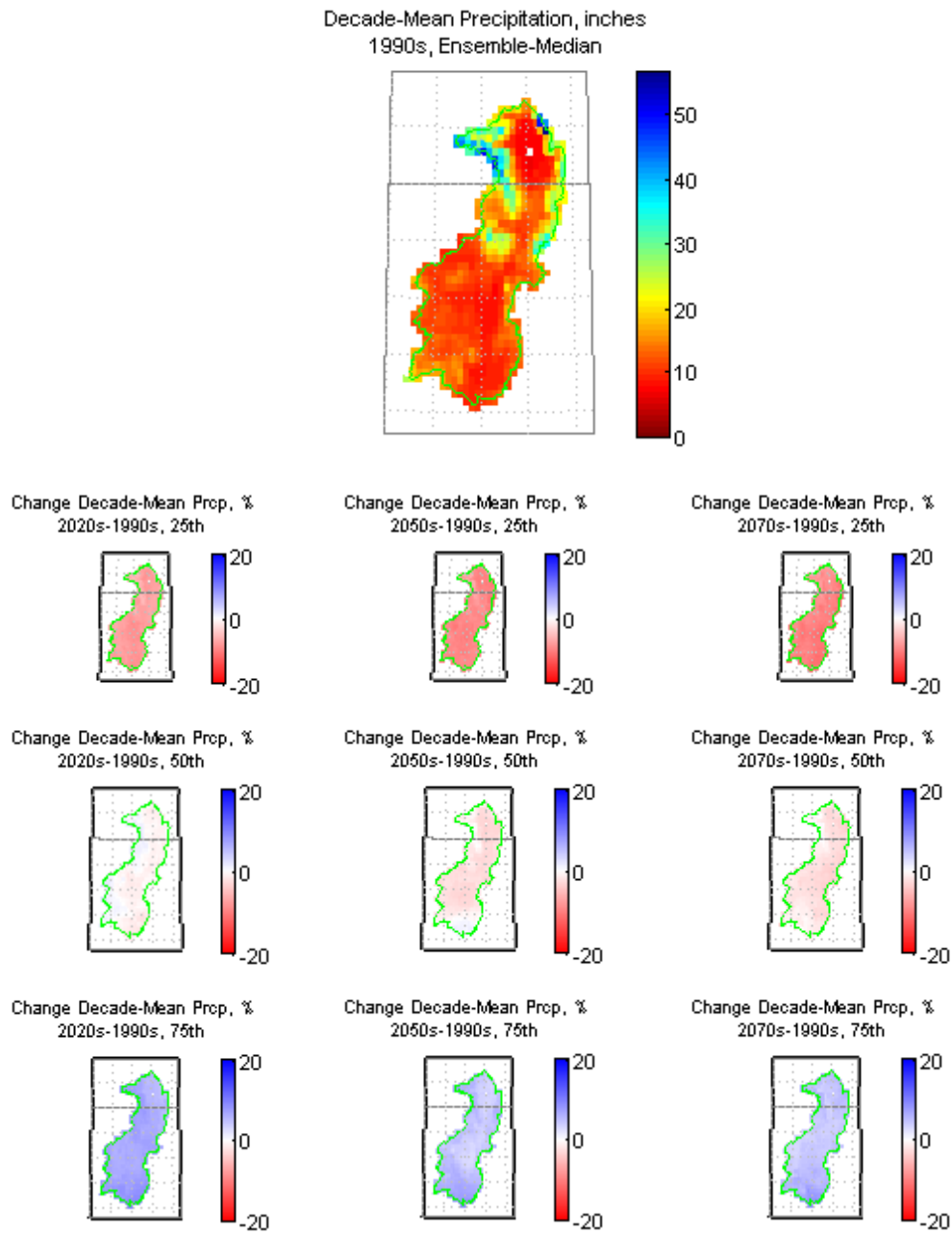


Figure 47. Rio Grande Basin – Spatial Distribution of Simulated Decadal Precipitation.

West-Wide Climate Risk Assessments:
BCSD Surface Water Projections

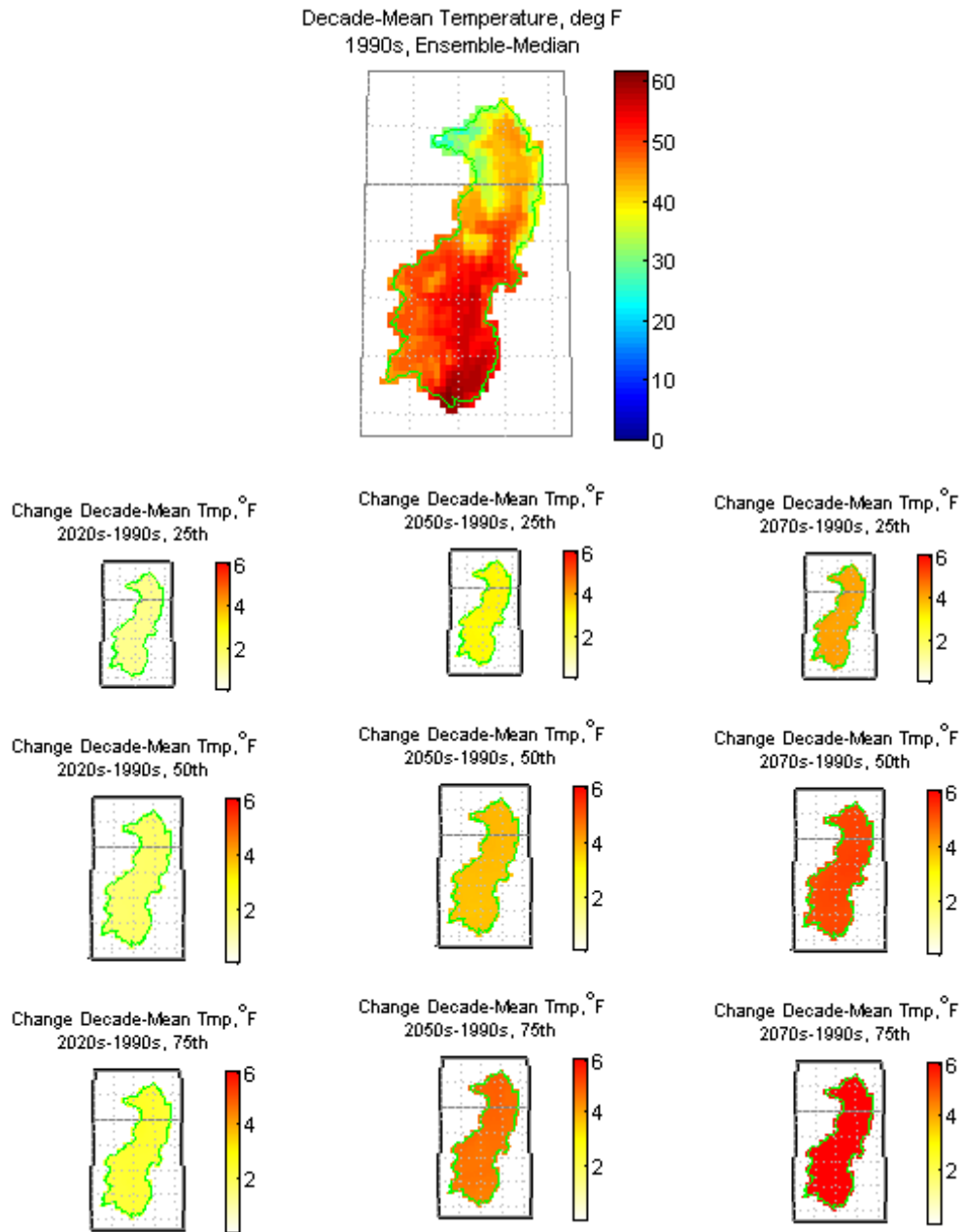


Figure 48. Rio Grande Basin – Spatial Distribution of Simulated Decadal Temperature.

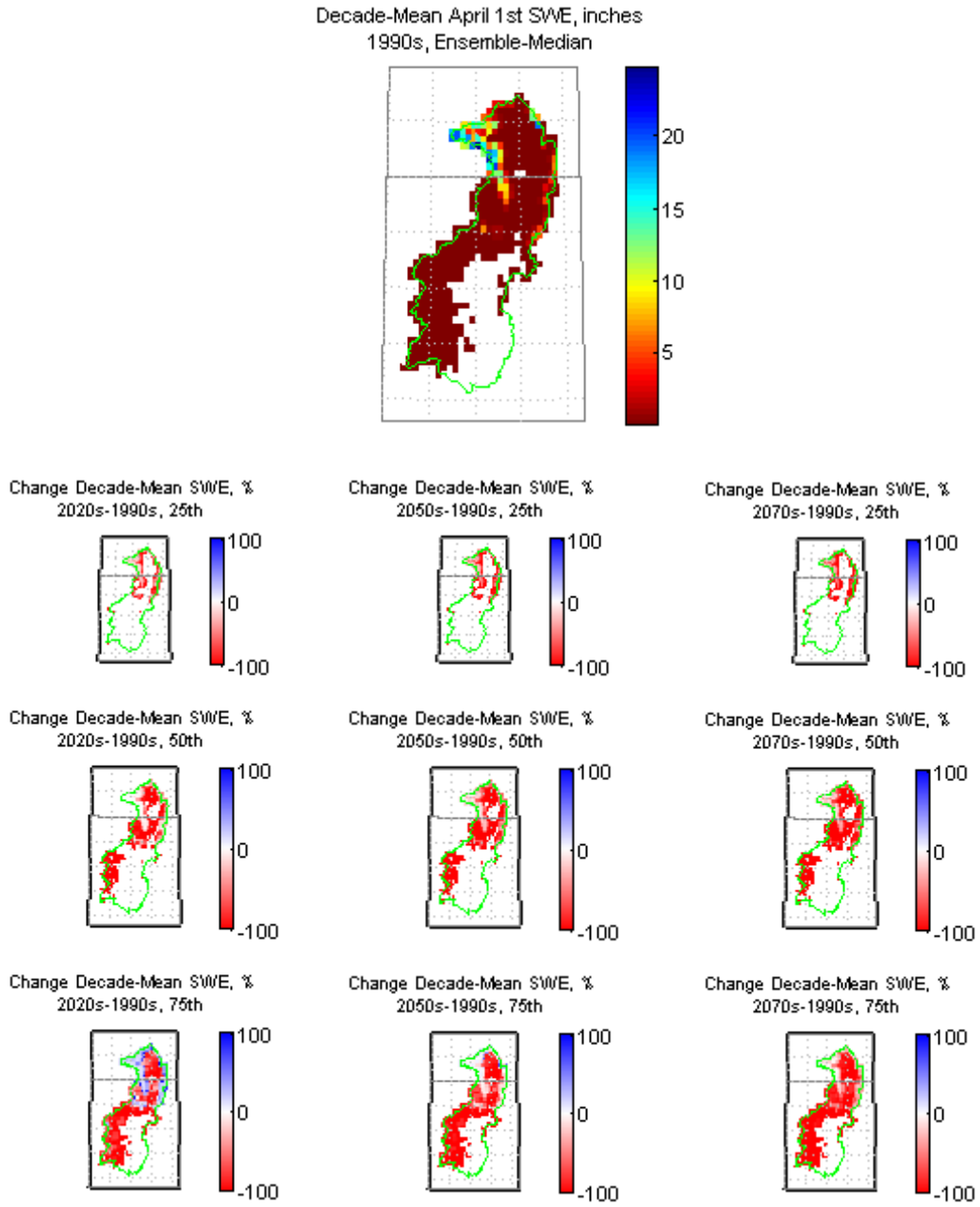


Figure 49. Rio Grande Basin – Spatial Distribution of Simulated Decadal April 1st SWE.

West-Wide Climate Risk Assessments:
BCSD Surface Water Projections

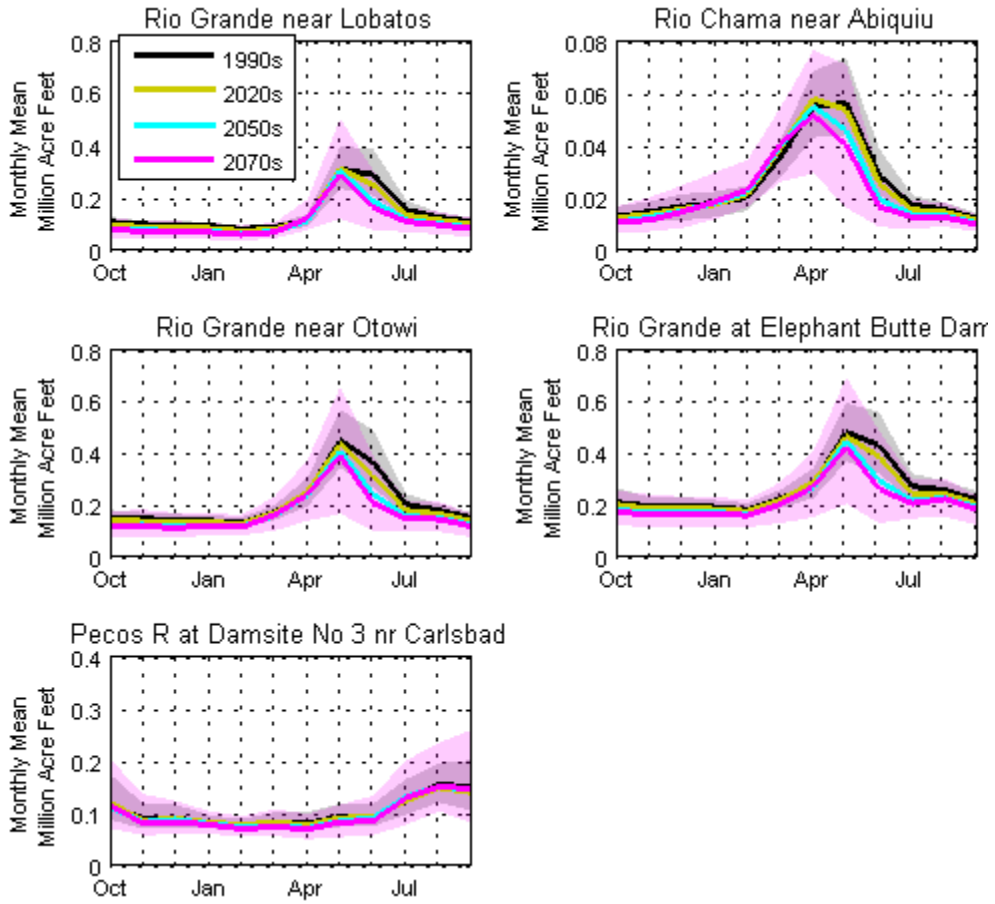


Figure 50. Rio Grande Basin – Simulated Mean-Monthly Runoff for Various Subbasins.

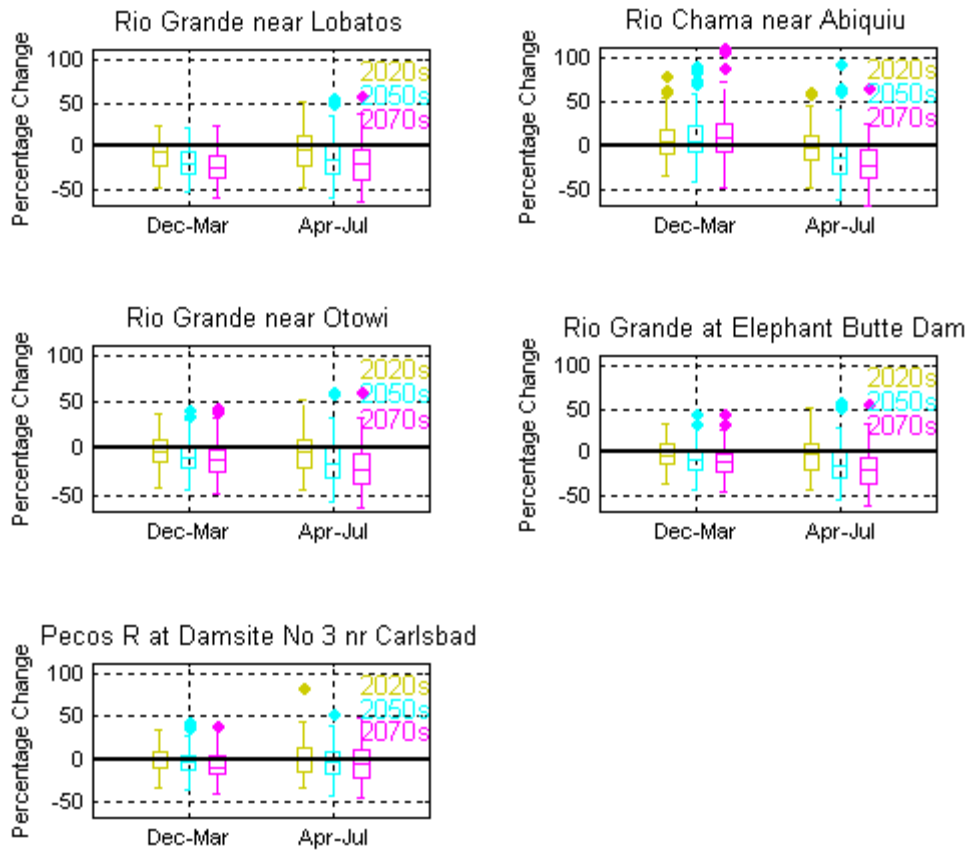


Figure 51. Rio Grande Basin – Simulated Mean-Seasonal Runoff for Various Subbasins.

5.7 Sacramento and San Joaquin River Basins

5.7.1 Hydroclimate Projections

Figure 52 shows six ensembles of hydroclimate projections for the basin above the Sacramento and San Joaquin Rivers at the Delta: annual total precipitation (top left), annual mean temperature (top right), April 1st SWE (middle left), annual runoff (middle right), December–March runoff season (bottom left), and April–July runoff season (bottom right). The heavy black line is the annual time series of 50 percentile values (i.e., ensemble-median). The shaded area is the annual time series of 5th to 95th percentile.

Annual total precipitation shows a decreasing trend. Annual mean temperature shows an increasing trend. April 1st SWE shows a decreasing trend. Annual runoff shows only a nominally decreasing trend. Winter season runoff shows a nominal increasing trend, and the April–July runoff shows decreasing trend.

West-Wide Climate Risk Assessments:
BCSD Surface Water Projections

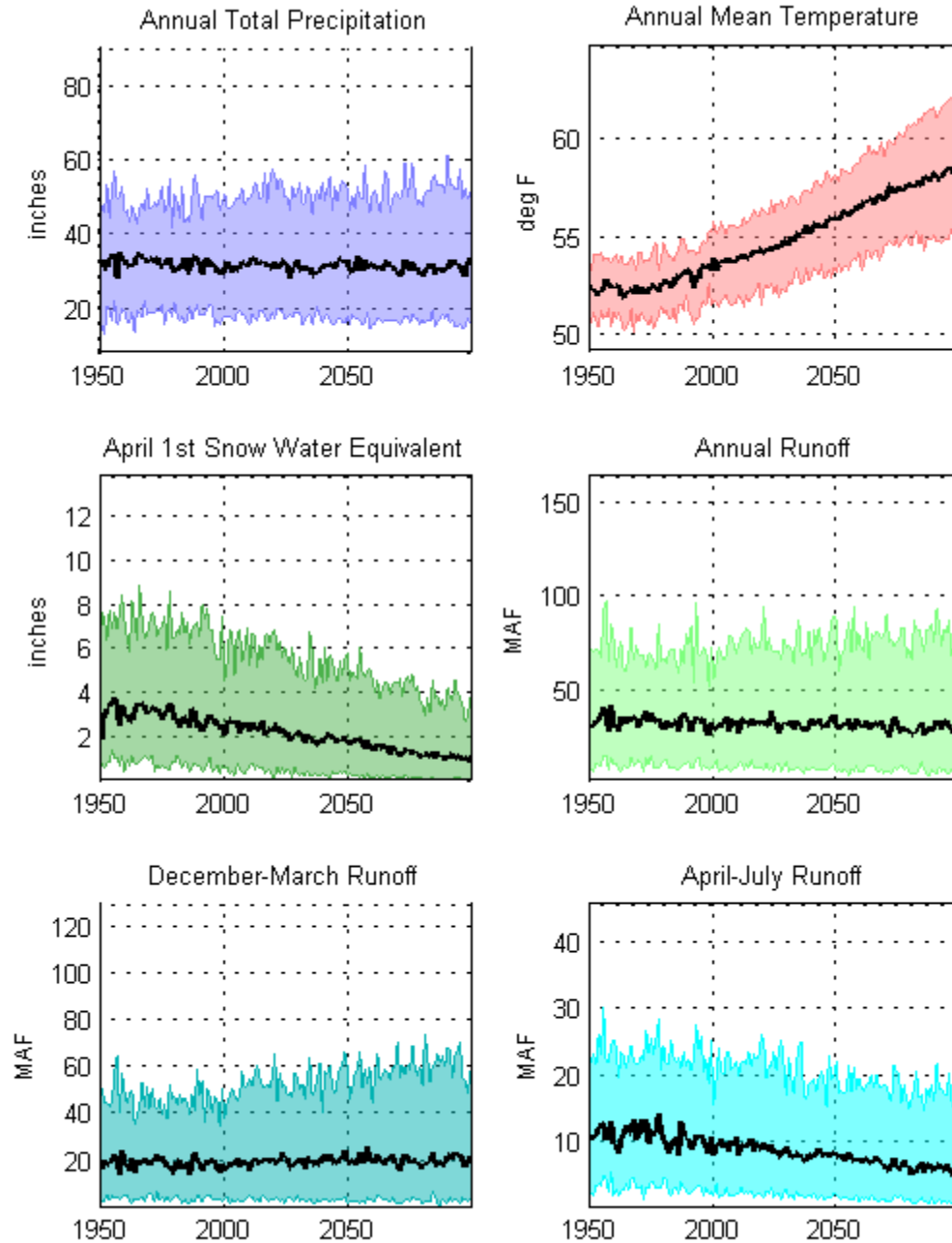


Figure 52. Sacramento and San Joaquin Basins – Hydroclimate Projections.

Figure 53 shows the spatial distribution of simulated decadal precipitation in the basin above the Sacramento and San Joaquin Rivers at the Delta: simulated 1990s' distribution of ensemble-median decadal mean condition (upper middle) and changes in decadal mean condition for three look aheads (2020s, 2050s, 2070s relative to 1990s) and at three change percentiles within the ensemble (25,

50, and 75). The ensemble-median change shows some increase in precipitation over the basin during the 2020s' decade from the 1990s' reference. By the 2050s, the northern part of the basin still continues to show precipitation increases from the 1990s' reference, but the southern parts of the basin show a decline in precipitation from the 1990s' reference decade. By the 2070s, precipitation across the entire basin shows a decline from the 1990s' reference.

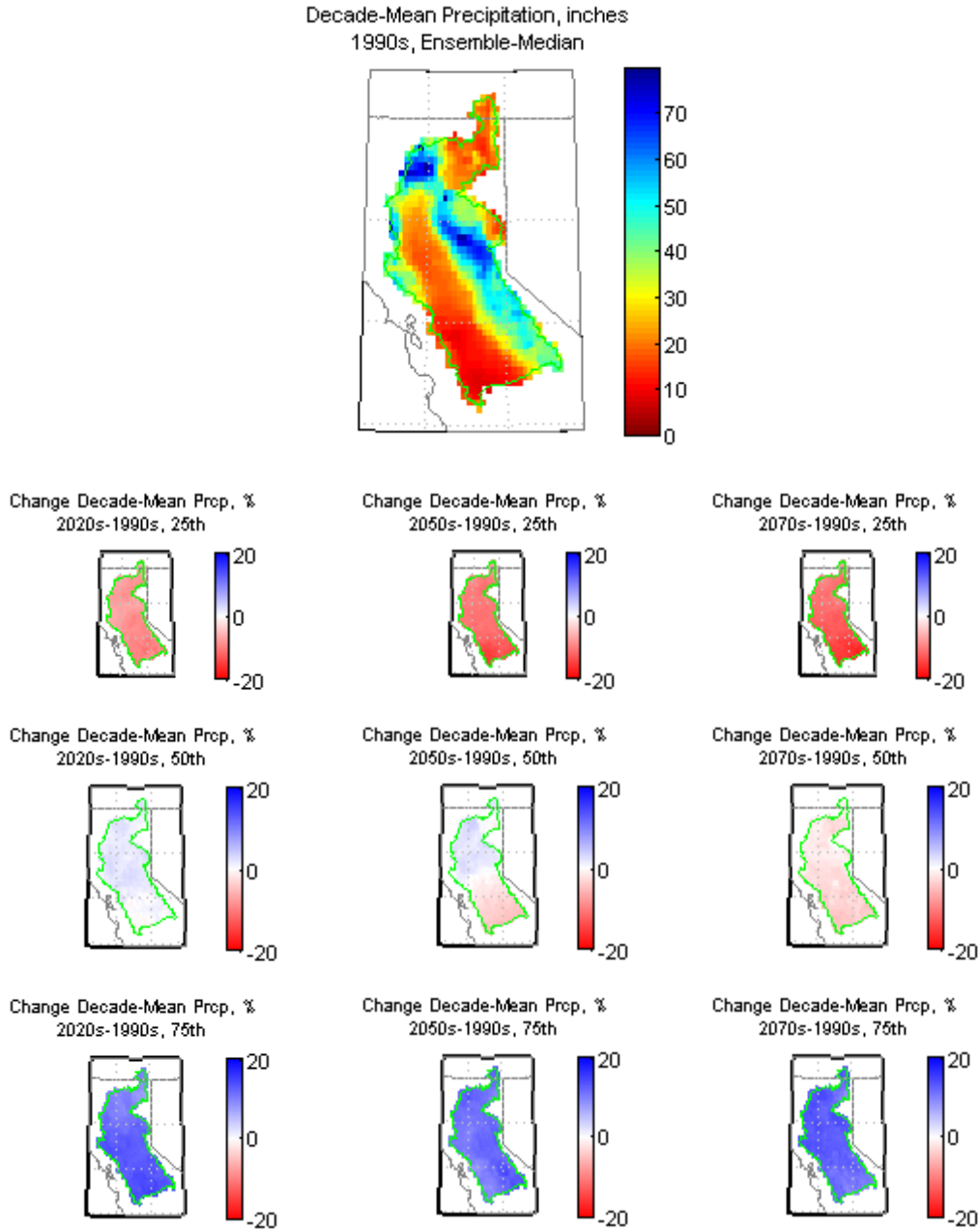


Figure 53. Sacramento and San Joaquin Basins – Spatial Distribution of Simulated Decadal Precipitation.

Figure 54 shows the spatial distribution of simulated decade mean temperature in the basin above the Sacramento and San Joaquin Rivers at the Delta: simulated 1990s' distribution of ensemble-median decadal mean condition (upper middle) and changes in decadal mean condition for three look aheads (2020s, 2050s, 2070s relative to 1990s) and at three change percentiles within the ensemble (25, 50, and 75). The median change for the 2020s', 2050s', and 2070s' decades relative to the 1990s shows an increasing temperature value throughout the basin.

Figure 55 shows the spatial distribution of April 1st SWE in the basin above the Sacramento and San Joaquin Rivers at the Delta: simulated 1990s' distribution of ensemble-median decadal mean condition (upper middle) and ensemble-median change in decadal mean condition for three look aheads (2020s, 2050s, 2070s relative to 1990s). The April 1st SWE shows persistent decline through the future decades from the 1990s' distribution.

5.7.2 Impacts on Runoff Annual and Seasonal Cycles

Figure 56 shows ensemble-median mean-monthly values (heavy lines) for the 1990s, 2020s, 2050s, and 2070s and the decadal-spread of mean-monthly runoff for the 1990s (black shaded area) and 2070s (magenta shaded area) where spread is bound by the ensemble's 5th to 95th percentile values for each month. For all the locations, there appears to be an earlier shift in the peak runoff timing; and for some locations, for example the Stanislaus River at New Melones Dam and the San Joaquin River near Vernalis, there is significant earlier shift to the peak runoff timing.

Figure 57 shows an ensemble-distribution (boxplot) of changes in mean-seasonal values (heavy lines) for the 2020s, 2050s, and 2070s relative to the 1990s, where the boxplots box represents the ensemble's interquartile range and the box-midline represents ensemble-median. All locations show increases in median flow (horizontal line in the boxplot) for the December–March winter runoff season, and decrease in median flow for the April–July spring–summer runoff season.

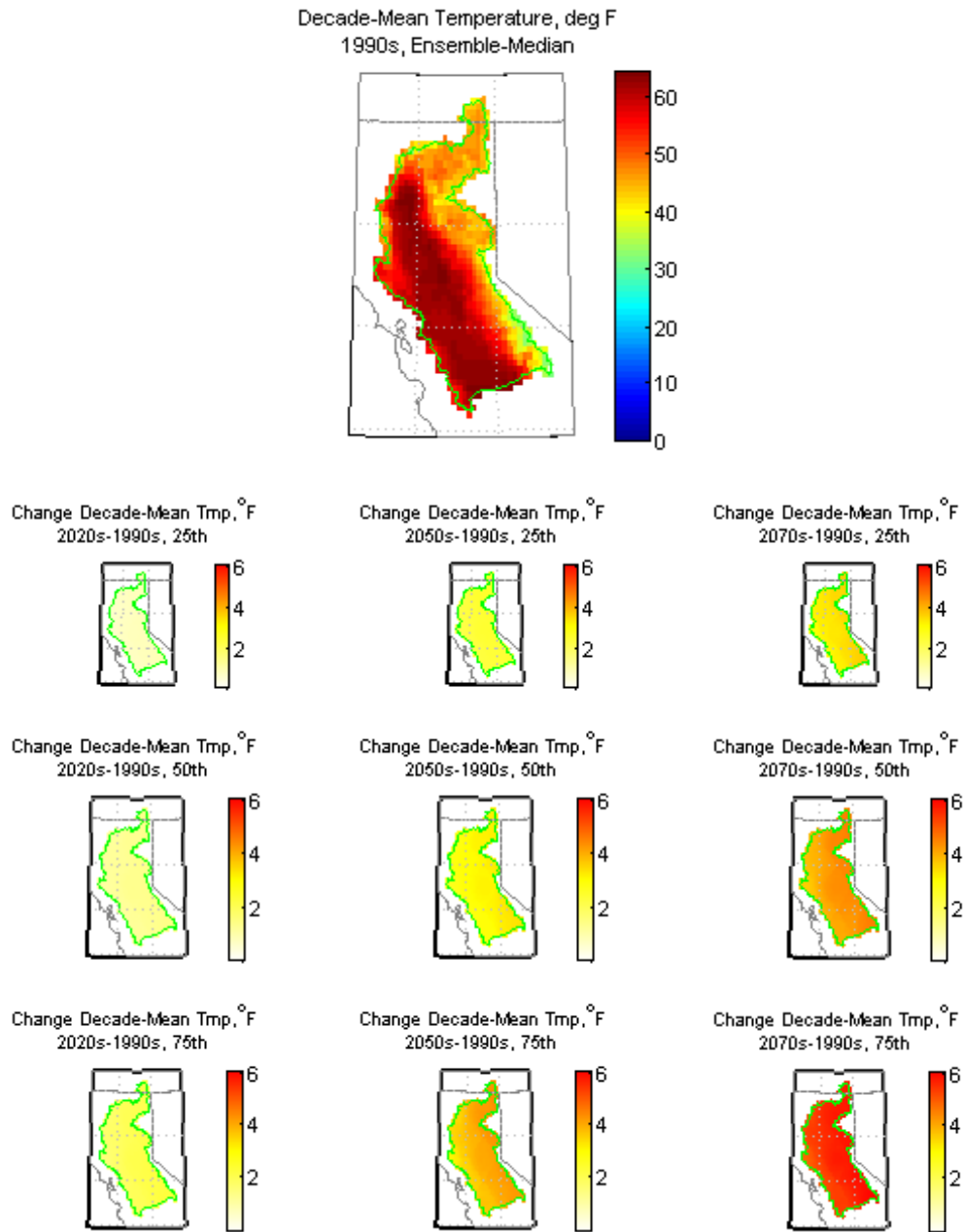


Figure 54. Sacramento and San Joaquin Basins – Spatial Distribution of Simulated Decadal Temperature.

West-Wide Climate Risk Assessments:
BCSD Surface Water Projections

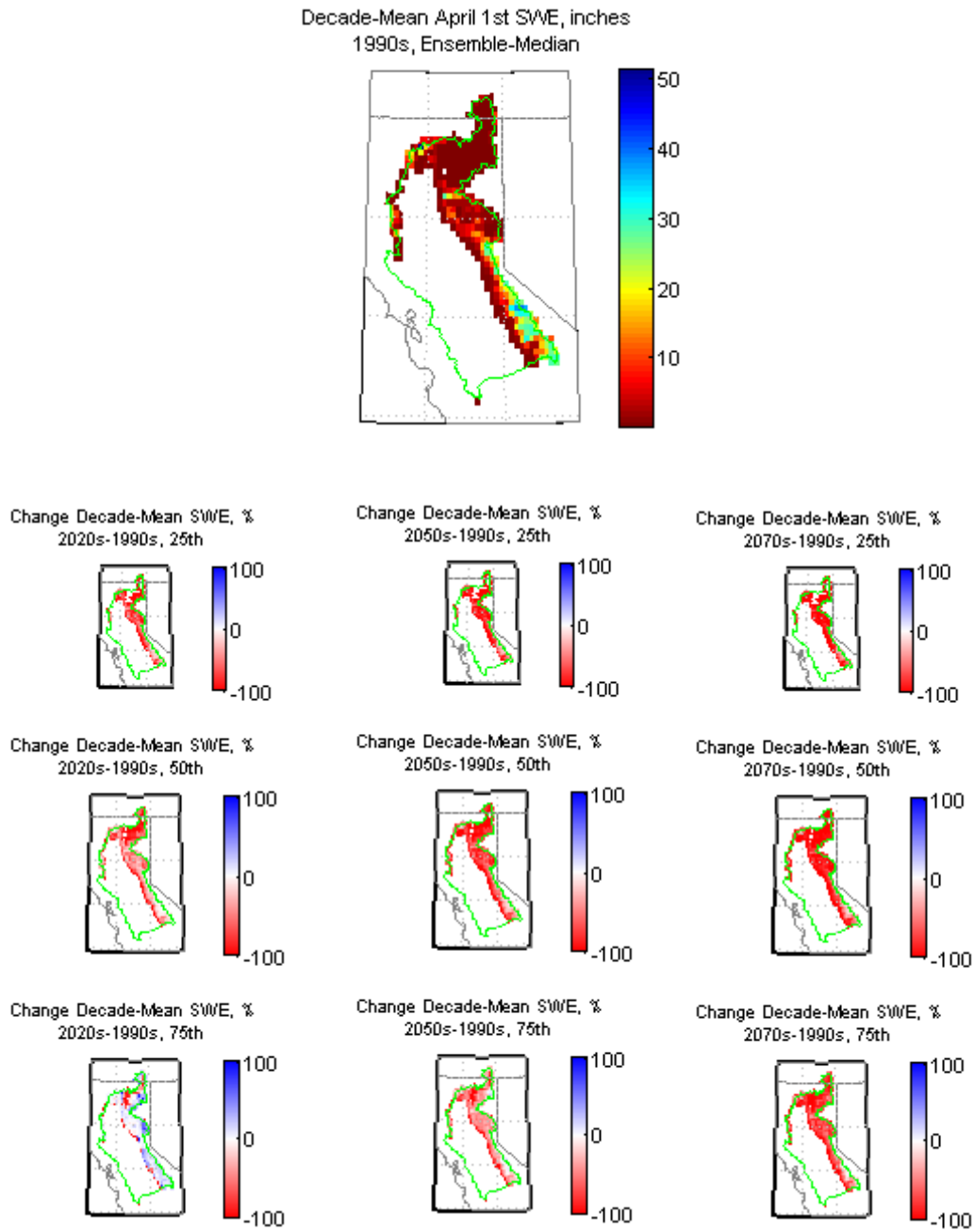


Figure 55. Sacramento and San Joaquin Basins – Spatial Distribution of Simulated Decadal April 1st SWE.

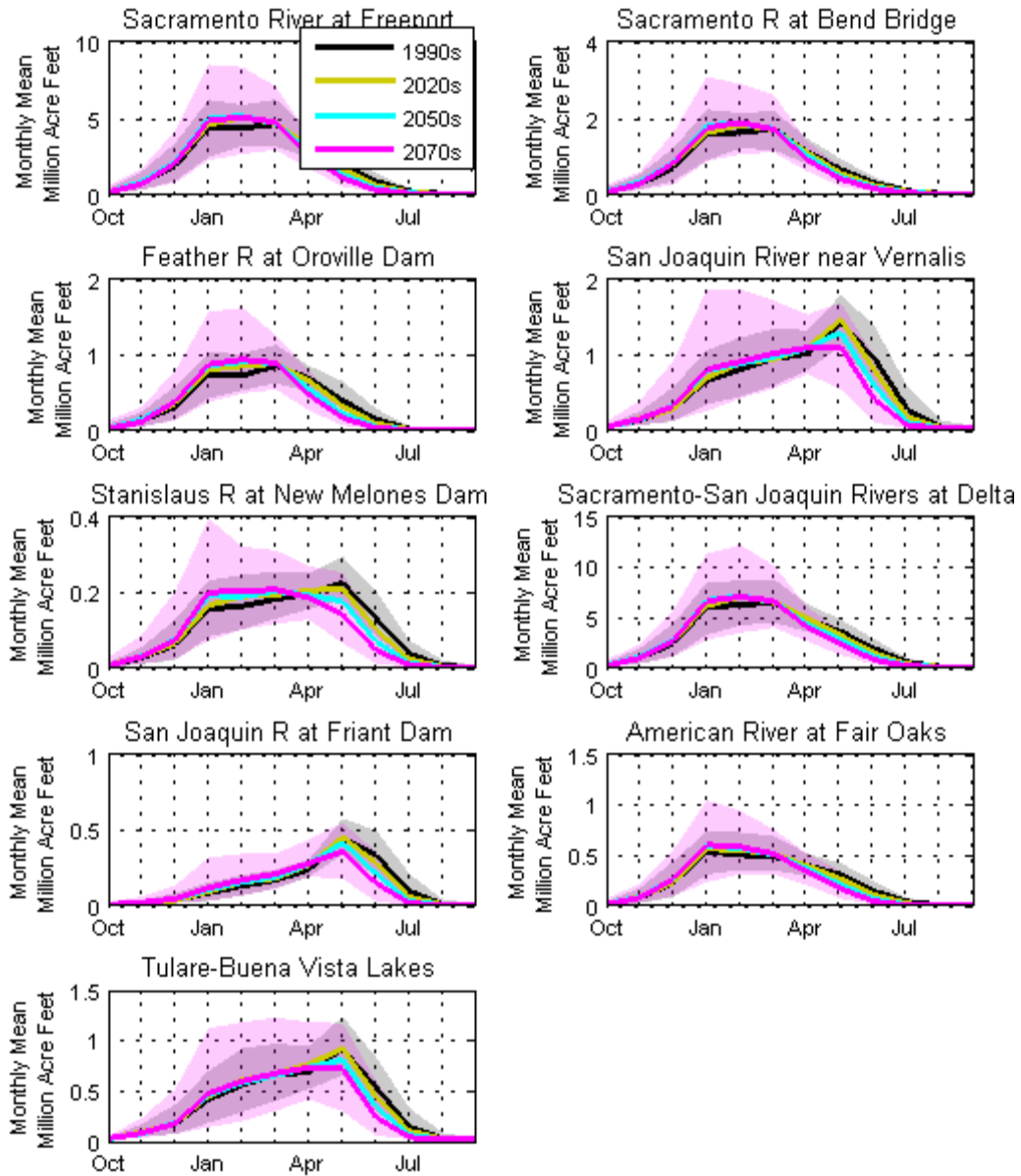


Figure 56. Sacramento and San Joaquin Basins – Simulated Mean-Monthly Runoff for Various Subbasins.

West-Wide Climate Risk Assessments:
BCSD Surface Water Projections

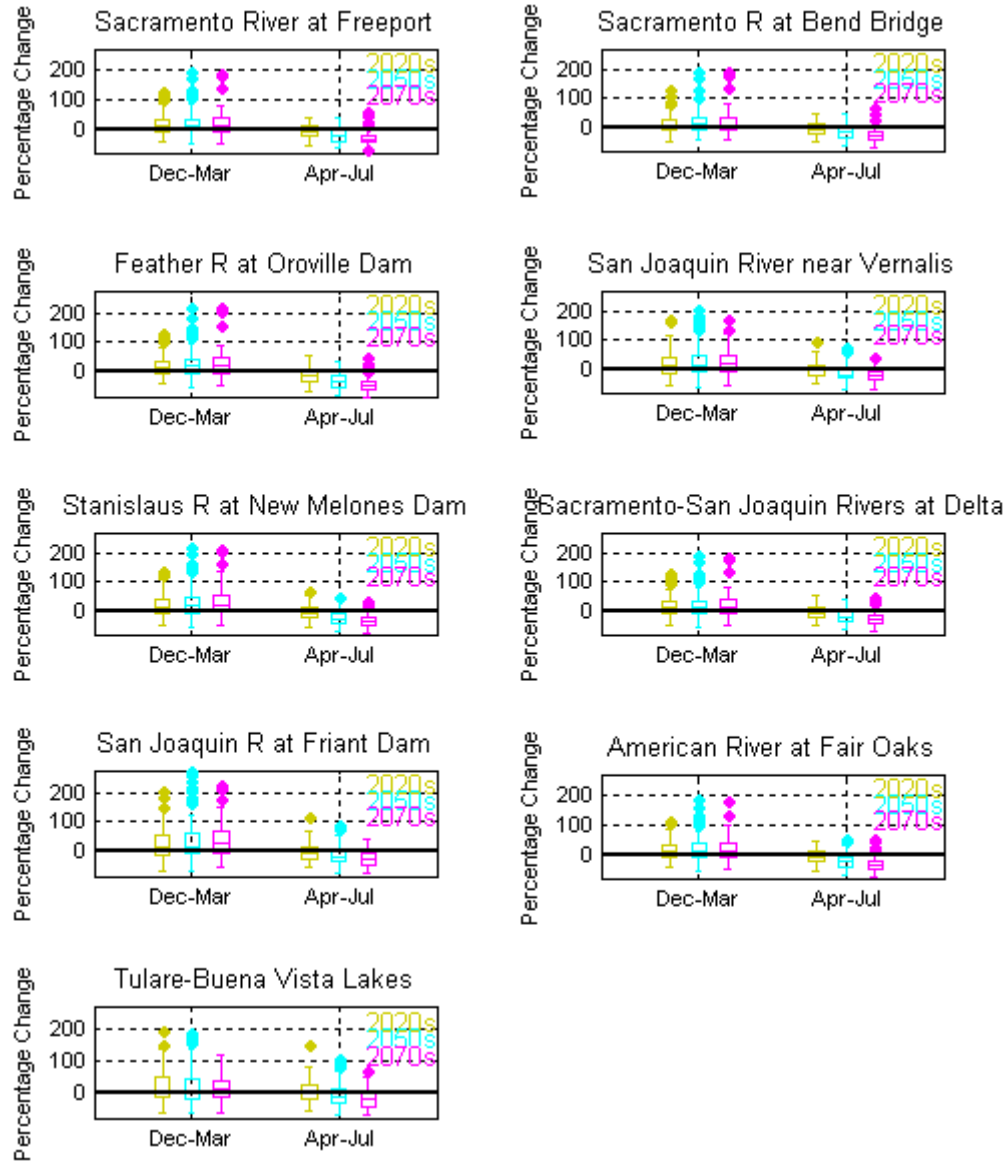


Figure 57. Sacramento and San Joaquin Basins – Simulated Mean-Seasonal Runoff for Various Subbasins.

5.8 Truckee and Carson River Basins

5.8.1 Hydroclimate Projections

Figure 58 shows six ensembles of hydroclimate projections for the basin above the Truckee River at Nixon gauge: annual total precipitation (top left), annual mean temperature (top right), April 1st SWE (middle left), annual runoff (middle right), December–March runoff season (bottom left), and April–July runoff season (bottom right). The heavy black line is the annual time series of 50 percentile values (i.e., ensemble-median). The shaded area is the annual time series of 5th to 95th percentile.

There is practically no trend in total annual precipitation across the basin through time. The uncertainty envelope for precipitation is also somewhat diverging. Mean annual temperature shows an increasing trend with an expanding uncertainty envelope through time. The April 1st SWE has a decreasing trend. The total annual runoff has a nominally decreasing trend. The December–March runoff has a nominally increasing trend, and the April–July runoff shows a decreasing trend.

Figure 59 shows the spatial distribution of simulated decadal precipitation in the basin above the Truckee River at Nixon gauge: simulated 1990s' distribution of ensemble-median decadal mean condition (upper middle) and changes in decadal mean condition for three look ahead periods (2020s, 2050s, 2070s relative to 1990s) and at three change percentiles within the ensemble (25, 50, and 75). For the 2020s' decade, there appears to be an increase in the median decade-mean precipitation from the 1990s' reference. The 2050s' decade shows the same level of median precipitation as the 1990s' decade. The 2070s' decade shows decrease in median-precipitation from the 1990s.

Figure 60 shows the spatial distribution of simulated decade-mean temperature in the basin above the Truckee River at Nixon gauge: simulated 1990s' distribution of ensemble-median decadal mean condition (upper middle) and changes in decadal mean condition for three look ahead periods (2020s, 2050s, 2070s relative to 1990s) and at three change percentiles within the ensemble (25, 50, and 75). The median change for the 2020s', 2050s', and 2070s' decades relative to the 1990s shows an increasing temperature value throughout the basin.

Figure 61 shows spatial distribution of April 1st SWE in the basin above the Truckee River at Nixon gauge: simulated 1990s' distribution of ensemble-median decadal mean condition (upper middle), and ensemble-median change in

West-Wide Climate Risk Assessments:
BCSD Surface Water Projections

decadal mean condition for three look aheads (2020s, 2050s, 2070s relative to 1990s). The April 1st SWE shows persistent decline through the future decades from the 1990s' distribution.

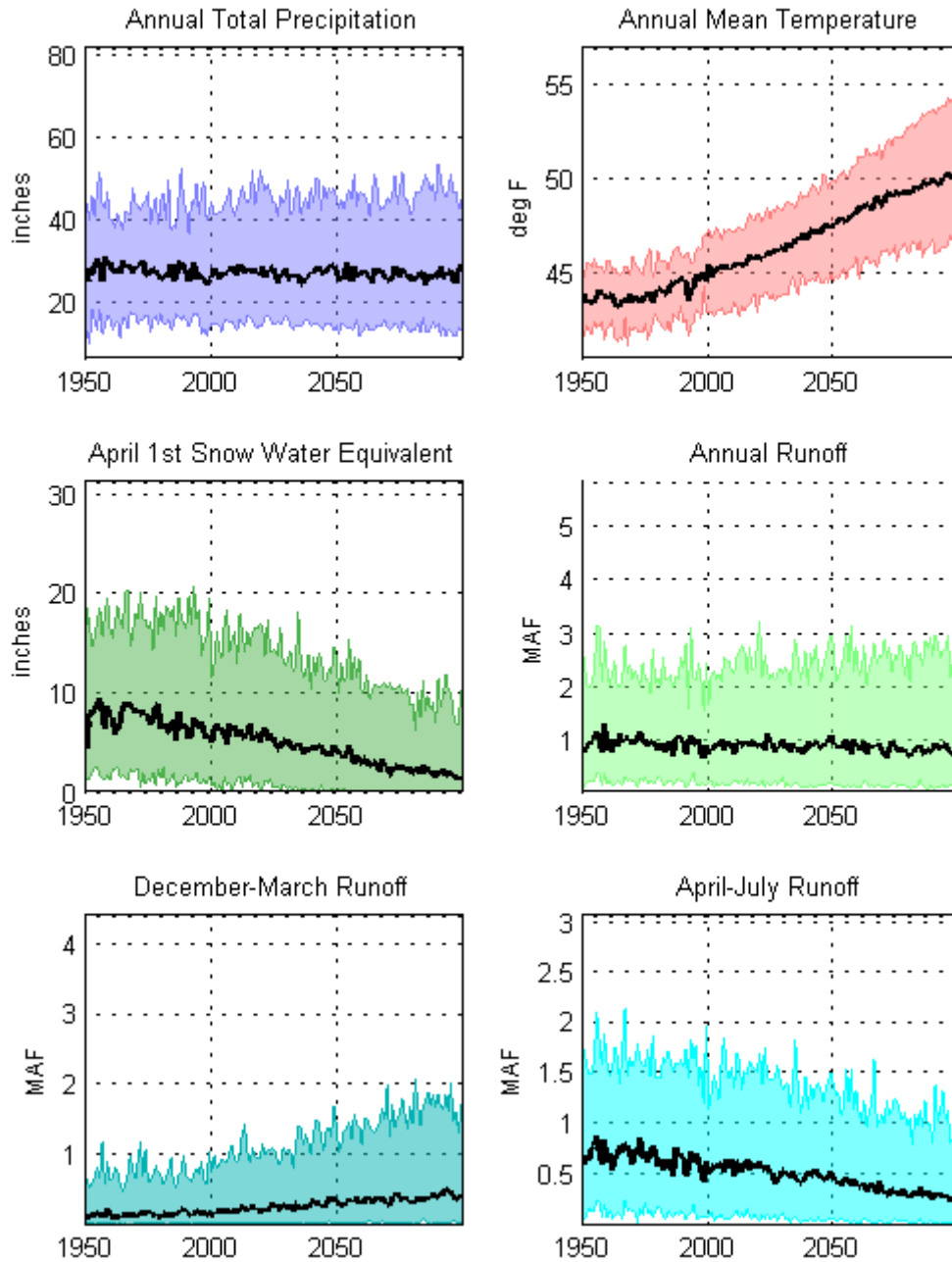


Figure 58. Truckee Basin – Hydroclimate Projections.

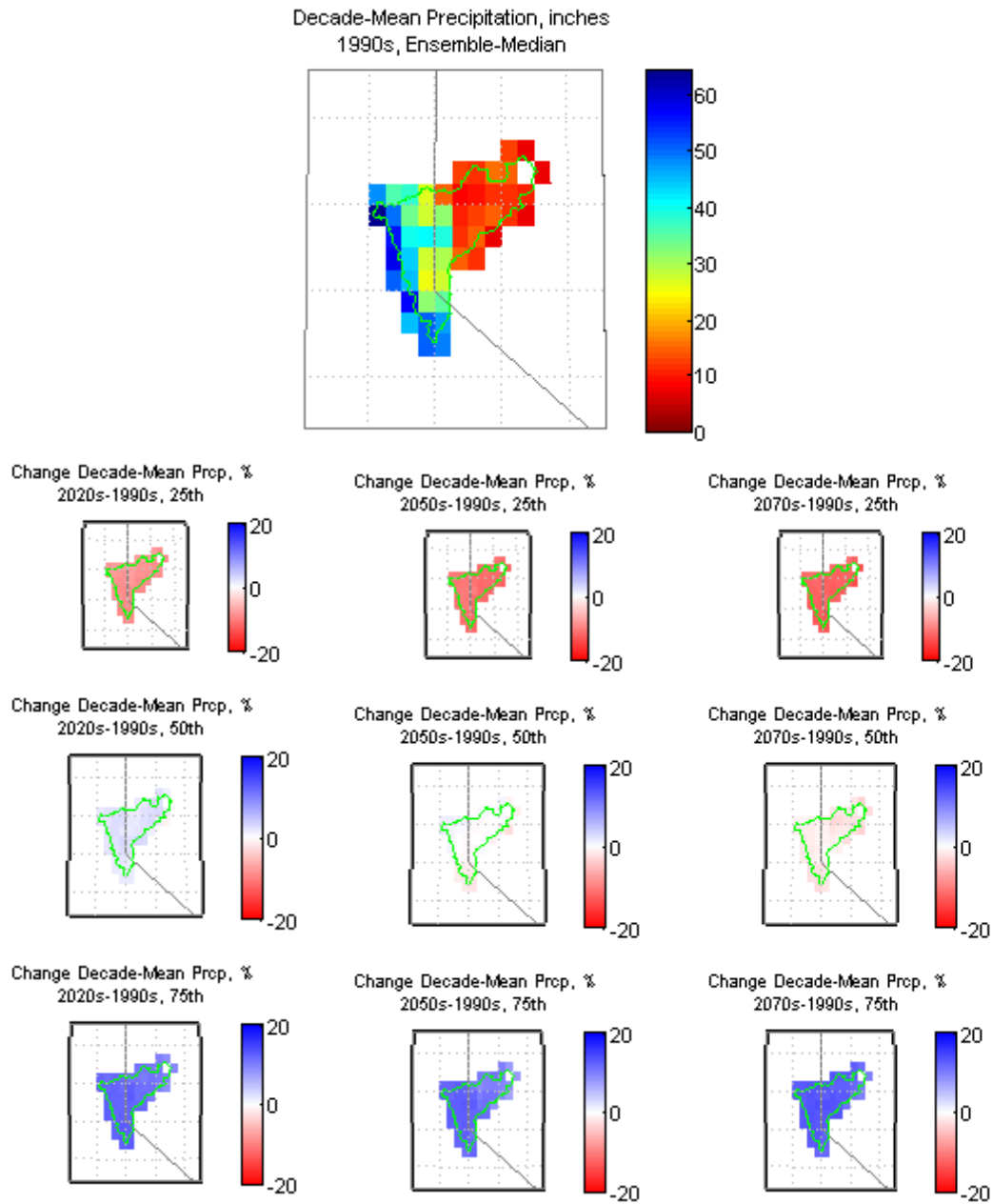


Figure 59. Truckee Basin – Spatial Distribution of Simulated Decadal Precipitation.

West-Wide Climate Risk Assessments:
BCSD Surface Water Projections

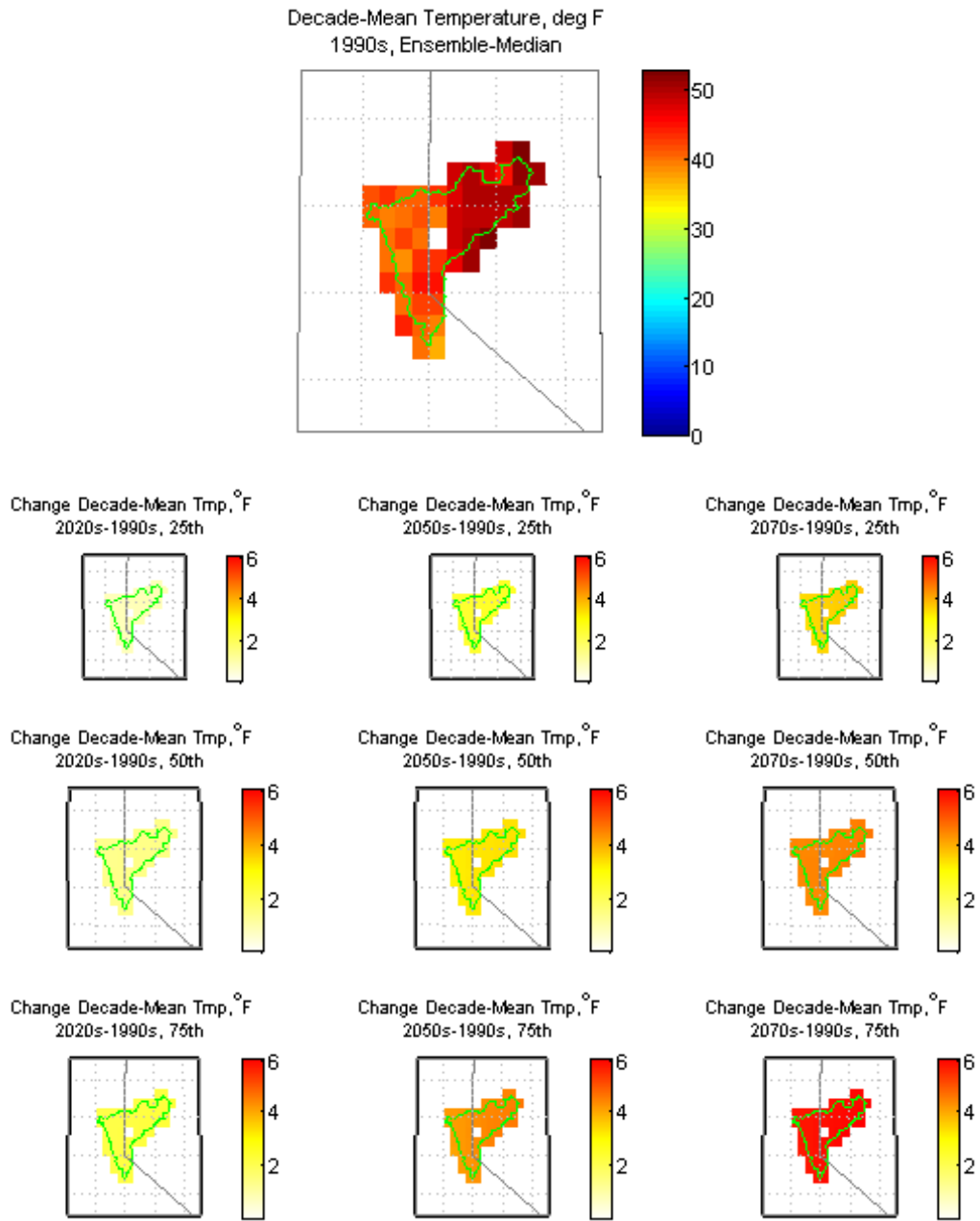


Figure 60. Truckee Basin – Spatial Distribution of Simulated Decadal Temperature.

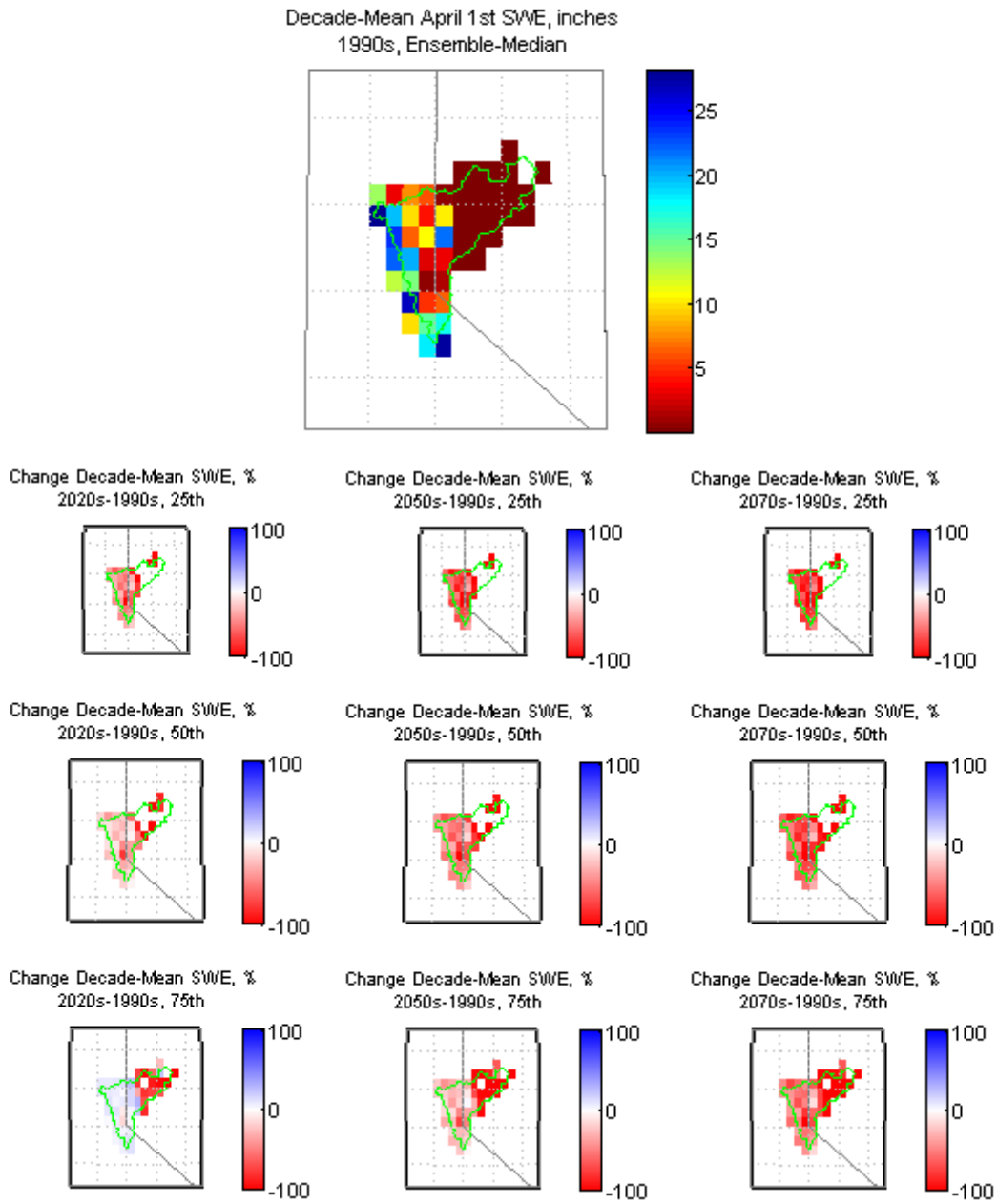


Figure 61. Truckee Basin – Spatial Distribution of Simulated Decadal April 1st SWE.

5.8.2 Impacts on Runoff Annual and Seasonal Cycles

Figure 62 shows the ensemble-median mean-monthly values (heavy lines) for the 1990s, 2020s, 2050s, and 2070s, and the decadal-spread of mean-monthly runoff for the 1990s (black shaded area) and 2070s (magenta shaded area), where spread is bound by the ensemble's 5th to 95th percentile values for each month. For the 2070s' decade, there appears to be a large uncertainty in runoff shifts, and there does not appear to be large shifts in the peak runoff timing.

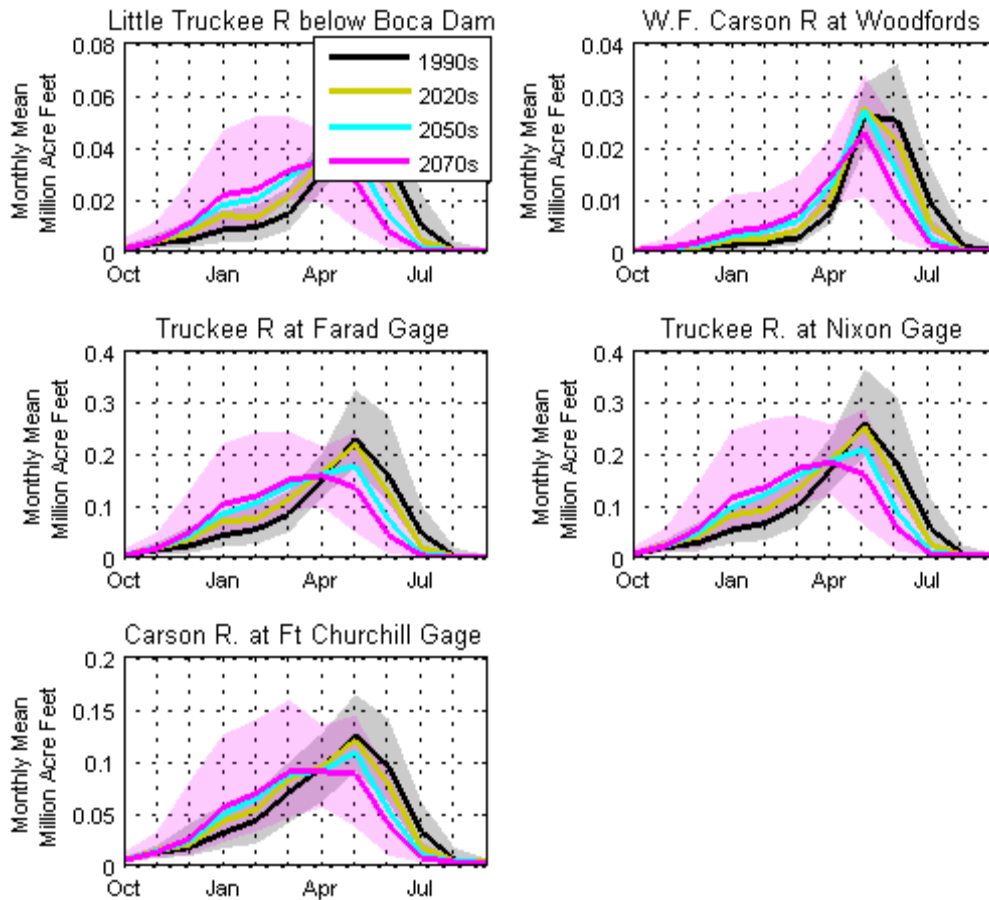


Figure 62. Truckee and Carson Basins – Simulated Mean-Monthly Runoff for Various Subbasins.

Figure 63 shows an ensemble-distribution (boxplot) of changes in mean-seasonal values (heavy lines) for the 2020s, 2050s, and 2070s relative to the 1990s, where the boxplots box represents the ensemble's interquartile range and the box-midline represents ensemble-median. For all the locations in the basin, there is significant increase in the median seasonal flow volume in the winter, and

decrease in spring–summer time runoff. The runoff changes during winter also appear to be quite high because of the relatively small monthly flow magnitudes.

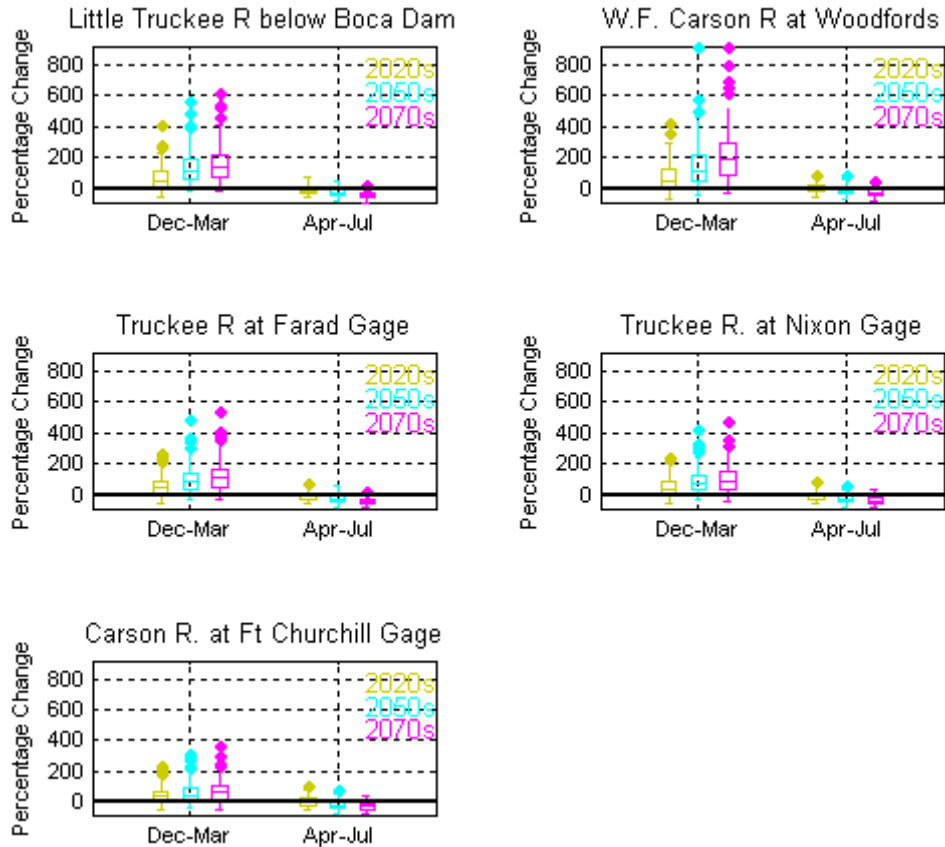


Figure 63. Truckee and Carson Basins – Simulated Mean-Seasonal Runoff for Various Subbasins.

5.9 West-Wide Summary of Results

This section summarizes the findings on hydroclimate and runoff impacts from section 5.2 through section 5.8. The summaries are provided in a series of tables—table 3, table 4, and table 5—corresponding to the three future decades, 2020s, 2050s, and 2070s, respectively, from the 1990s’ reference decade. Each table provides summaries of impacts (change statistics for each future decade from the 1990s’ reference decade) in subbasins that are *tributary* to the 43 WWCRA runoff reporting locations. Change statistics are reported for the following variables.

West-Wide Climate Risk Assessments:
BCSD Surface Water Projections

- Decade mean total annual precipitation – median of the median (50th percentile) change in spatially distributed precipitation (e.g., see figure 23 for spatially distributed ensemble median change).
- Decade mean average annual temperature – median of the median (50th percentile) change in spatially distributed temperature (e.g., see figure 24 for spatially distributed ensemble median change).
- Decade mean April 1st SWE – median of the median (50th percentile) change in spatially distributed April 1st SWE (e.g., see figure 25 for spatially distributed ensemble median change).
- Decade mean annual runoff – median of the ensemble specific change in decade average annual runoff.
- Decade mean winter season (December–March) runoff – median of the ensemble specific change in decade average December–March runoff.
- Decade mean spring–summer season (April–July) runoff – median of the ensemble specific change in decade average April–July runoff.

Note that median of median change applies to the spatially distributed variables, precipitation, mean temperature, and April 1st SWE. First, ensemble-median change at each grid cell for a given subbasin is calculated. Then, median of grid cell level ensemble-median change is calculated to summarize the change for a given subbasin. Since runoffs are a point estimate, the ensemble-median change is reported.

The impacts across the 43 subbasins vary, but there appears to be emerging patterns that, in summary, are the following.

- Precipitation is expected to increase from the 1990s' level during the 2020s and 2050s but to decline nominally during the 2070s (though the early to middle 21st century, increases could be artifacts of the BCSD climate projections development leading to slightly wetter projections, as discussed in section 3.4).
- Temperature shows a persistent increasing trend from the 1990s' level.
- April 1st SWE shows a persistent decreasing trend from the 1990s' level.
- Annual runoff shows some increase for the 2020s' decade from the 1990s' level but shows decline moving forward to the 2050s' and 2070s' decade from the 1990s' reference, suggesting that, although precipitation changes are projected to remain positive through the 2050s, temperature changes

West-Wide Climate Risk Assessments:
BCSD Surface Water Projections

begin to offset these precipitation increases leading to net loss in the water balance through increased evapotranspiration losses.

- Winter season (December–March) runoff shows an increasing trend.
- Spring–summer season (April–July) runoff shows a decreasing trend.

Table 3. Median of median change for precipitation, mean temperature, April 1st SWE from the 1990s for the 43 WWCRA reporting watersheds in 2020s; for runoff, it is the median change

Count	Location	Precipitation (%)	Mean Temperature (deg F)	April 1st SWE (%)	Annual Runoff (%)	December–March Runoff (%)	April–July Runoff (%)
1	Williamson R. below the Sprague River	2.26	1.34	-62.01	7.15	22.26	-2.03
2	Sacramento River at Freeport	1.83	1.29	-52.01	3.48	9.02	-11.10
3	Klamath River below Iron Gate Dam	2.20	1.29	-55.96	5.36	29.08	-5.59
4	Sacramento R at Bend Bridge near Red Bluff	1.47	1.28	-61.20	3.28	7.01	-8.76
5	Feather R at Oroville	1.79	1.33	-40.70	4.42	13.84	-14.42
6	San Joaquin River near Vernalis	0.38	1.32	-12.82	0.77	10.10	-4.78
7	Stanislaus R at New Melones Dam	1.36	1.36	-21.76	1.30	11.02	-7.63
8	Klamath River near Seiad Valley	2.02	1.25	-50.50	3.68	16.85	-6.54
9	Sacramento-Sanjoaquin Rivers at Delta	1.50	1.29	-46.17	2.72	10.53	-6.40
10	San Joaquin R at Friant Dam	0.70	1.41	-12.56	0.66	13.90	-6.09
11	Klamath River at Orleans	1.93	1.24	-42.95	3.03	12.77	-5.90
12	American River at Fair Oaks	2.00	1.34	-31.48	2.76	10.79	-9.94
13	Tulare-Buena Vista Lakes	-0.27	1.23	-21.47	1.07	5.63	-3.10
14	Klamath River near Klamath	1.74	1.18	-42.12	2.64	8.68	-7.49
15	Colorado River at Lees Ferry	1.10	1.78	-27.19	-3.08	0.15	-1.00
16	Colorado River above Imperial Dam	1.87	1.69	-42.85	-1.72	3.51	0.31
17	Green R near Greendale	0.87	1.78	-78.40	-2.34	-4.94	0.27
18	Colorado R near Cameo	1.04	1.84	-5.40	-3.22	-3.70	-0.71
19	Gunnison R near Grand Junction	0.74	1.83	-4.43	-2.18	-0.24	-2.64
20	San Juan R near Bluff	1.28	1.67	-88.89	-3.18	-0.37	-1.66
21	Little Truckee R below Boca Dam	2.28	1.36	-20.12	4.72	54.04	-11.06
22	W.F. Carson R at Woodfords	2.02	1.40	-18.50	1.07	49.75	-3.45
23	Truckee R at Farad Gage	2.00	1.38	-20.04	3.76	46.67	-9.97
24	Truckee R. at Nixon Gage	1.99	1.40	-24.60	4.34	38.85	-8.49
25	Carson R. at Ft Churchill Gage	2.18	1.43	-39.57	4.10	30.08	-7.92
26	Missouri River at Canyon Ferry Dam	1.32	1.47	-13.71	0.83	4.24	0.45
27	Milk River at Nashua	4.89	1.28	-87.66	8.25	11.85	7.62
28	S.F. Platte River near Sterling	-1.90	1.88	-76.00	-8.47	-7.83	-7.20
29	Missouri River at Omaha	2.90	1.47	-99.73	3.69	5.16	5.47
30	Big Horn River at Yellowtail Dam	0.02	1.60	-36.47	0.65	1.63	2.88
31	N.F. Platte River at Lake McConaughy	-0.74	1.77	-82.67	-3.25	-0.89	-2.45
32	Deschutes River near Madras	1.87	1.34	-63.64	2.79	9.76	-0.97
33	Snake River near Heise	2.63	1.67	-0.17	-0.63	1.42	0.12
34	Flathead R at Columbia Falls	3.56	1.31	-6.11	2.50	12.07	1.00
35	Snake River at Brownlee Dam	2.29	1.55	-26.08	-0.11	5.62	-1.34
36	Columbia River at Grand Coulee	3.00	1.30	-8.83	3.20	9.71	3.59
37	Columbia River at the Dalles	2.60	1.36	-15.31	2.30	9.78	2.15
38	Yakima River at Parker	3.80	1.21	-15.04	3.80	19.65	-1.99
39	Rio Grande near Lobatos	-0.47	1.84	-25.63	-4.98	-7.12	-2.87
40	Rio Chama near Abiquiu	0.91	1.79	-87.13	-0.24	4.76	-1.27
41	Rio Grande near Otowi	-0.54	1.82	-42.20	-4.45	-3.07	-2.48
42	Rio Grande at Elephant Butte Dam	-0.53	1.79	-93.16	-4.05	-3.59	-1.64
43	Pecos R at Damsite No 3 nr Carlsbad	-1.48	1.79	-100.00	-2.45	-0.63	-1.39

West-Wide Climate Risk Assessments:
BCSD Surface Water Projections

Table 4. Median of median change for precipitation, mean temperature, April 1st SWE from the 1990s for the 43 WWCRA reporting watersheds in 2050s; for runoff, it is the median change

Count	Location	Precipitation (%)	Mean Temperature (deg F)	April 1st SWE (%)	Annual Runoff (%)	December-March Runoff (%)	April-July Runoff (%)
1	Williamson R. below the Sprague River	3.41	3.07	-84.58	9.55	29.68	-8.35
2	Sacramento River at Freeport	1.67	3.07	-80.58	2.51	13.62	-23.01
3	Klamath River below Iron Gate Dam	3.22	3.00	-79.47	4.84	52.89	-18.17
4	Sacramento R at Bend Bridge near Red Bluff	1.85	3.09	-85.22	4.11	11.63	-17.70
5	Feather R at Oroville	1.84	3.10	-73.64	1.88	20.59	-32.38
6	San Joaquin River near Vernalis	-3.83	3.14	-36.64	-5.85	10.73	-20.55
7	Stanislaus R at New Melones Dam	-2.50	3.22	-50.66	-5.46	16.12	-27.90
8	Klamath River near Seiad Valley	2.54	2.92	-76.79	2.92	31.24	-17.62
9	Sacramento-Sanjoaquin Rivers at Delta	0.37	3.05	-77.80	0.78	11.20	-20.58
10	San Joaquin R at Friant Dam	-4.55	3.30	-31.45	-8.74	15.76	-20.17
11	Klamath River at Orleans	2.11	2.89	-73.02	3.57	24.38	-19.93
12	American River at Fair Oaks	-0.82	3.12	-64.69	-2.31	11.10	-26.44
13	Tulare-Buena Vista Lakes	-5.55	3.09	-52.06	-10.98	3.24	-18.26
14	Klamath River near Klamath	1.82	3.09	-75.50	3.95	15.50	-19.53
15	Colorado River at Lees Ferry	-0.46	2.81	-57.91	-8.53	-1.12	-7.36
16	Colorado River above Imperial Dam	-1.25	3.90	-78.45	-7.43	-2.95	-6.59
17	Green R near Greendale	1.38	3.81	-90.40	-3.48	-3.98	0.75
18	Colorado R near Cameo	1.17	3.85	-14.61	-5.42	-0.98	-4.92
19	Gunnison R near Grand Junction	-0.37	3.90	-21.94	-10.39	-1.71	-9.26
20	San Juan R near Bluff	-1.49	3.97	-99.57	-11.59	-6.53	-9.71
21	Little Truckee R below Boca Dam	1.13	3.82	-48.49	0.46	111.10	-28.83
22	W.F. Carson R at Woodfords	-1.90	3.20	-37.65	-9.05	113.62	-16.31
23	Truckee R at Farad Gage	-0.19	3.30	-46.29	-2.81	82.42	-27.16
24	Truckee R. at Nixon Gage	-0.11	3.23	-52.18	-2.49	72.90	-25.94
25	Carson R. at Ft Churchill Gage	-1.66	3.28	-69.69	-4.54	41.65	-23.95
26	Missouri River at Canyon Ferry Dam	4.12	3.35	-32.11	2.09	13.60	1.81
27	Milk River at Nashua	6.90	3.55	-92.19	8.48	20.05	8.23
28	S.F. Platte River near Sterling	-1.01	3.40	-92.56	-13.89	-12.23	-10.84
29	Missouri River at Omaha	6.77	3.74	-100.00	9.70	13.01	12.30
30	Big Horn River at Yellowtail Dam	3.49	3.44	-60.35	4.21	7.52	7.83
31	N.F. Platte River at Lake McConaughy	1.55	3.59	-92.48	-1.68	9.55	0.61
32	Deschutes River near Madras	2.52	3.60	-93.10	3.68	17.34	-4.41
33	Snake River near Heise	4.97	3.09	-7.79	-1.68	10.74	-1.80
34	Flathead R at Columbia Falls	6.06	3.73	-14.10	3.21	25.31	1.39
35	Snake River at Brownlee Dam	4.21	3.32	-52.11	1.16	13.72	-1.96
36	Columbia River at Grand Coulee	5.67	3.67	-24.00	4.96	19.25	5.30
37	Columbia River at the Dalles	5.02	3.18	-36.54	3.69	18.47	4.11
38	Yakima River at Parker	5.55	3.30	-35.16	3.71	39.89	-9.52
39	Rio Grande near Lobatos	-2.29	2.98	-49.46	-18.89	-20.55	-15.37
40	Rio Chama near Abiquiu	-1.07	3.83	-96.37	-7.28	5.53	-13.85
41	Rio Grande near Otowi	-2.42	3.82	-63.92	-14.40	-10.41	-15.91
42	Rio Grande at Elephant Butte Dam	-2.31	3.82	-98.37	-13.48	-8.95	-15.42
43	Pecos R at Damsite No 3 nr Carlsbad	-0.72	3.76	-100.00	-2.75	-3.76	-3.63

West-Wide Climate Risk Assessments:
BCSD Surface Water Projections

Table 5. Median of median change for precipitation, mean temperature, April 1st SWE from the 1990s for the 43 WWCRA reporting watersheds in 2070s; for runoff, it is the median change

Count	Location	Precipitation (%)	Mean Temperature (deg F)	April 1st SWE (%)	Annual Runoff (%)	December-March Runoff (%)	April-July Runoff (%)
1	Williamson R. below the Sprague River	0.48	4.32	-99.20	4.36	36.66	-20.47
2	Sacramento River at Freeport	-1.80	4.24	-96.39	-3.59	11.02	-36.14
3	Klamath River below Iron Gate Dam	-0.03	4.20	-98.91	2.13	62.18	-32.03
4	Sacramento R at Bend Bridge near Red Bluff	-1.69	4.28	-98.16	-3.77	8.56	-30.87
5	Feather R at Oroville	-1.17	4.38	-92.57	-2.62	20.84	-46.62
6	San Joaquin River near Vernalis	-3.78	4.22	-53.78	-8.42	17.23	-25.81
7	Stanislaus R at New Melones Dam	-3.45	4.31	-71.12	-8.30	20.82	-35.34
8	Klamath River near Seiad Valley	-0.55	4.07	-96.80	3.48	35.10	-32.56
9	Sacramento-Sanjoaquin Rivers at Delta	-2.47	4.21	-94.26	-4.32	10.63	-32.79
10	San Joaquin R at Friant Dam	-4.05	4.47	-44.55	-10.68	31.05	-25.03
11	Klamath River at Orleans	-0.56	4.01	-94.56	1.19	28.63	-34.46
12	American River at Fair Oaks	-2.58	4.34	-84.25	-5.35	11.29	-38.56
13	Tulare-Buena Vista Lakes	-5.35	4.17	-71.04	-7.58	8.72	-23.53
14	Klamath River near Klamath	-0.88	3.90	-94.79	-0.97	17.80	-34.17
15	Colorado River at Lees Ferry	1.11	5.16	-78.49	-6.94	4.92	-6.52
16	Colorado River above Imperial Dam	0.13	5.10	-93.90	-7.71	1.27	-6.08
17	Green R near Greendale	2.73	5.11	-95.46	-2.39	-0.06	2.45
18	Colorado R near Cameo	2.27	5.16	-24.62	-8.71	3.45	-5.76
19	Gunnison R near Grand Junction	0.92	5.17	-35.99	-10.18	4.54	-11.18
20	San Juan R near Bluff	-0.54	5.13	-99.89	-15.21	-4.37	-14.86
21	Little Truckee R below Boca Dam	-1.12	4.41	-68.65	-2.19	138.51	-43.06
22	W.F. Carson R at Woodfords	-1.98	4.38	-55.51	-10.90	191.32	-27.06
23	Truckee R at Farad Gage	-1.44	4.41	-64.29	-3.07	106.41	-40.46
24	Truckee R. at Nixon Gage	-1.69	4.42	-71.69	-2.55	90.84	-37.57
25	Carson R. at Ft Churchill Gage	-2.01	4.50	-88.79	-6.12	57.52	-32.44
26	Missouri River at Canyon Ferry Dam	5.79	4.79	-45.08	6.22	28.45	3.65
27	Milk River at Nashua	7.23	4.37	-99.59	12.88	32.52	10.60
28	S.F. Platte River near Sterling	0.17	5.03	-95.79	-17.45	-11.45	-9.89
29	Missouri River at Omaha	7.65	4.64	-100.00	12.59	19.55	15.10
30	Big Horn River at Yellowtail Dam	4.70	4.83	-71.79	7.21	13.83	8.77
31	N.F. Platte River at Lake McConaughy	3.66	4.87	-94.56	-3.18	18.02	0.50
32	Deschutes River near Madras	2.57	4.26	-99.67	3.39	27.65	-12.58
33	Snake River near Heise	7.91	5.01	-13.96	1.52	24.70	0.68
34	Flathead R at Columbia Falls	9.84	4.49	-17.75	7.11	47.13	2.86
35	Snake River at Brownlee Dam	6.13	4.96	-70.79	3.35	20.98	-0.95
36	Columbia River at Grand Coulee	8.60	4.47	-32.79	8.01	29.32	6.62
37	Columbia River at the Dalles	7.73	4.52	-50.55	7.49	27.28	2.45
38	Yakima River at Parker	7.09	4.16	-51.74	5.60	56.92	-17.00
39	Rio Grande near Lobatos	-2.23	5.18	-68.97	-22.41	-23.69	-20.13
40	Rio Chama near Abiquiu	-1.12	5.19	-98.50	-10.96	8.61	-21.68
41	Rio Grande near Otowi	-2.40	5.19	-84.56	-19.90	-12.00	-21.83
42	Rio Grande at Elephant Butte Dam	-2.25	5.17	-99.72	-16.41	-10.86	-20.01
43	Pecos R at Damsite No 3 nr Carlsbad	-1.91	4.97	-100.00	-4.36	-9.42	-5.06

To provide additional insights on the spatial distribution of runoff changes and to get a full west-wide coverage, the ensemble-median change in annual runoff at the 152 HCDN locations is shown in figures 64–66 for the three future decades, 2020s, 2050s, and 2070s, respectively. During the 2020s, the changes in annual runoff are modest (< 20% from the 1990s’ level), and show clusters of runoff increases and decreases. But by the middle of the 21st century (2050s’ decade), there appears to be a dipole in the ensemble-median streamflow change, where the basins in the South are showing increasing decline and in the North are showing nominal to modest increases. During the 2070s’ decade, the 2050s’

distribution of change pattern continues to hold; but on the west coast, more locations are starting to show streamflow decline from the 1990s' level.

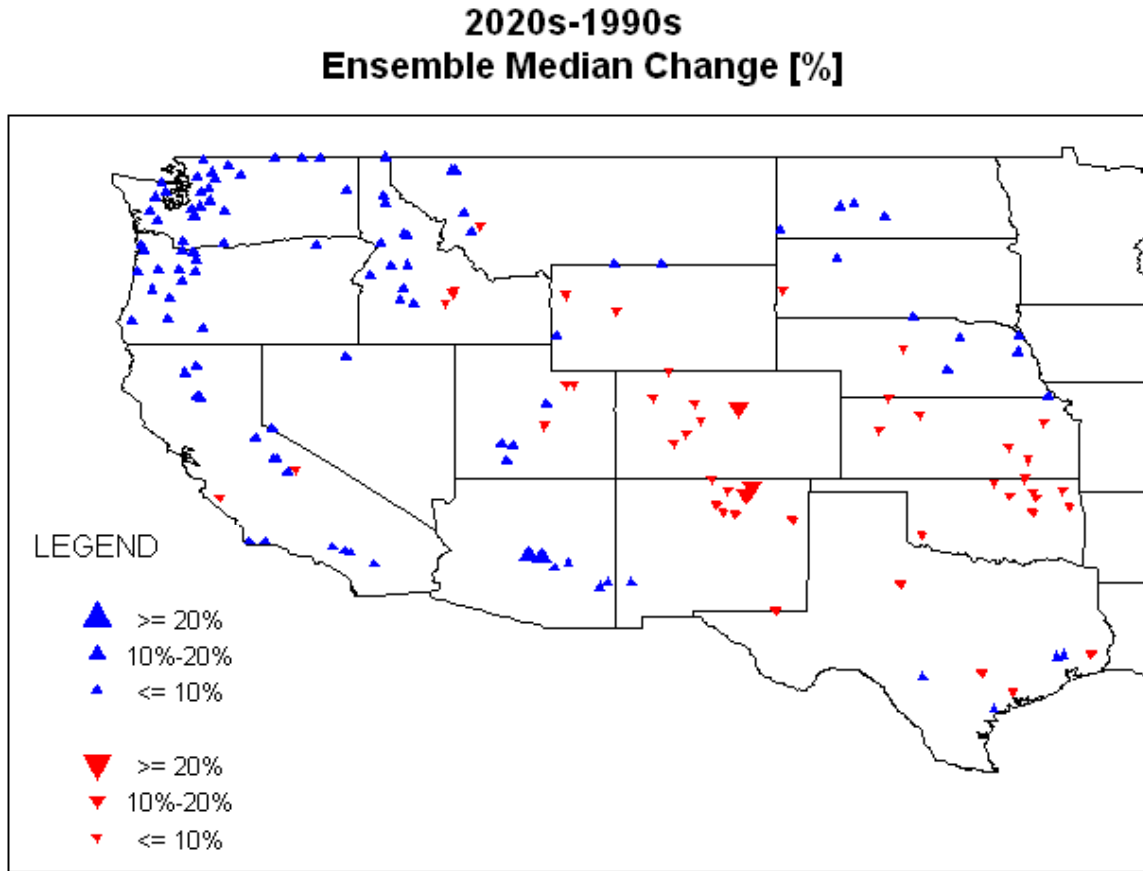


Figure 64. Ensemble Median Percentage Change in Annual Runoff for 2020s from the 1990s Across HCDN Sites.

2050s-1990s
Ensemble Median Change [%]

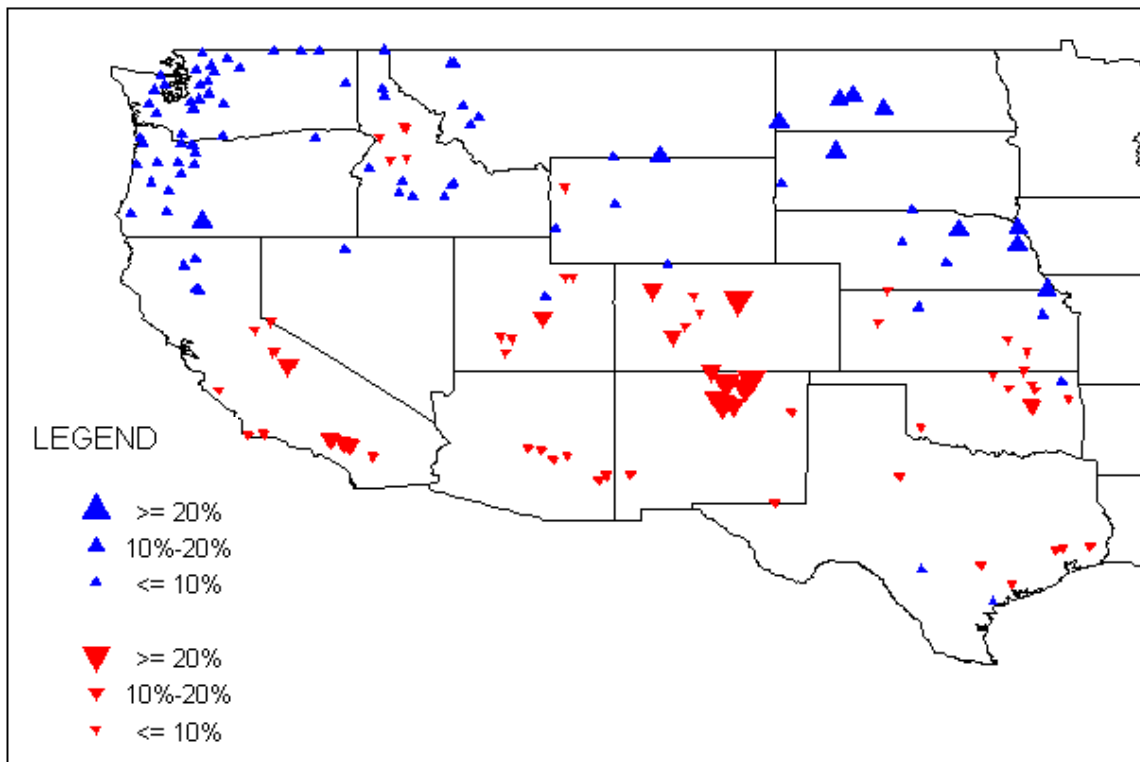


Figure 65. Ensemble Median Percentage Change in Annual Runoff for 2050s from the 1990s Across HCDN Sites.

2070s-1990s Ensemble Median Change [%]

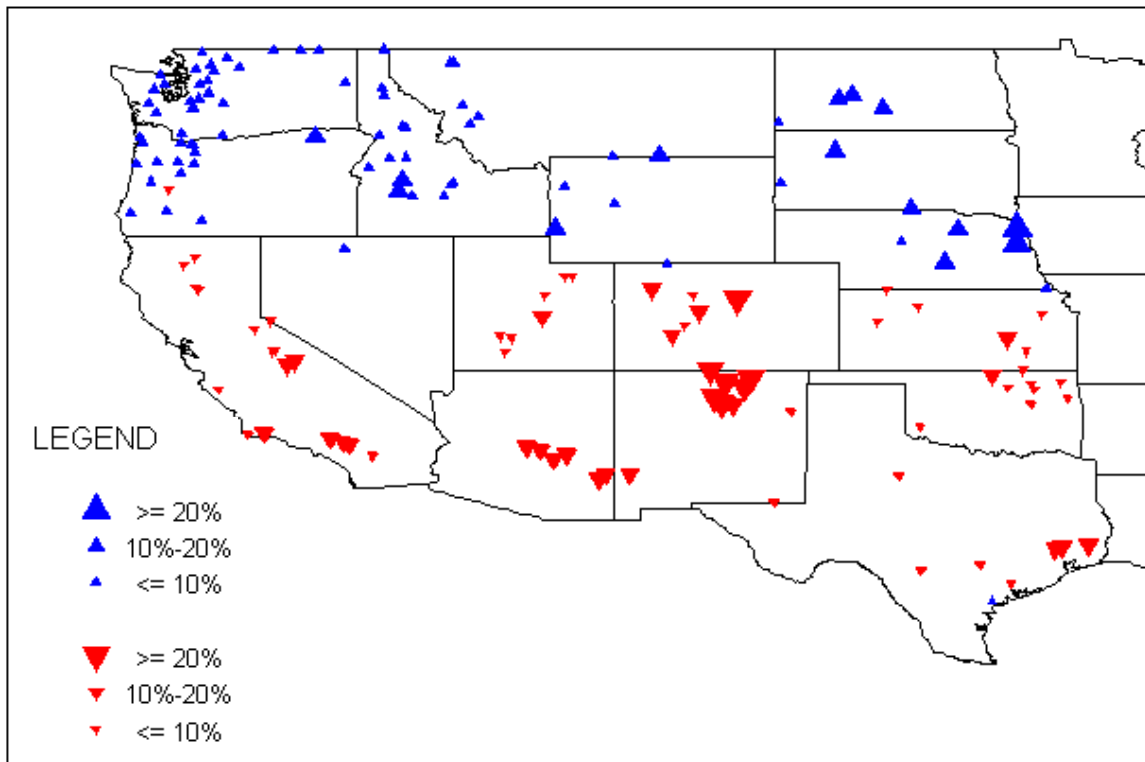


Figure 66. Ensemble Median Percentage Change in Annual Runoff for 2070s from the 1990s Across HCDN Sites.

CHAPTER 6

Uncertainties

This analysis is designed to provide quantitative representation of how runoff in the major Reclamation river basins may respond to a range of future climate projections. The activity was designed to take advantage of best available datasets and modeling tools and to follow methodologies documented in peer-reviewed literature. However, there are a number of analytical uncertainties that are not reflected in study results, including uncertainties associated with the following analytical areas that can be grouped under two categories—climate projection information and assessing hydrologic impacts.

6.1 Climate Projection Information

6.1.1 Global Climate Forcing

Although this surface water hydrologic projection activity considers future climate projections representing a range of future greenhouse emission paths, the uncertainties associated with these pathways are not explored. Such uncertainties include those introduced by assumptions about technological and economic developments, globally and regionally; how those assumptions translate into global energy use involving greenhouse gas emissions; and biogeochemical analysis to determine the fate of GHG emissions in the oceans, land, and atmosphere. Also, not all of the uncertainties associated with climate forcing are associated with GHG assumptions. Considerable uncertainty remains associated with natural forcings, with the cooling influence of aerosols being regarded as the most uncertain on a global scale (e.g., figure SPM-2 in IPCC 2007).

6.1.2 Global Climate Simulation

While the activity presented in this report considers climate projections produced by state-of-the-art coupled ocean-atmosphere climate models and even though these models have shown an ability to simulate the influence of increasing GHG emissions on global climate (IPCC 2007), there are still uncertainties about the scientific understanding of physical processes that affect climate; how to represent such processes in climate models (e.g., atmospheric circulation, clouds, ocean circulation, deep ocean heat update, ice sheet dynamics, sea level, land cover effects from water cycle, vegetative other biological changes); and how to do so in a mathematically efficiently manner given computational limitations.

6.1.3 Climate Projection Bias Correction

This surface water hydrologic projection activity is designed on the philosophy that GCM biases toward being too wet, too dry, too warm, or too cool should be identified and accounted for as bias-corrected climate projections data prior to use in implications studies. Bias correction of climate projections data affects results on incremental runoff and water supply response.

6.1.4 Climate Projection Spatial Downscaling

This activity uses projections that have been empirically downscaled, using spatial disaggregation on a monthly time step (following GCM bias correction on a monthly time step). Although this technique has been used to support numerous water resources impacts studies (e.g., Van Rheen et al. 2004; Maurer 2007; Anderson et al. 2008; Reclamation 2008; Reclamation 2010; McGuire et al. 2010), uncertainties remain about the limitations of empirical downscaling methodologies. One potential limitation relates to how empirical methodologies require historical reference information use on spatial climatic patterns at the downscaled spatial resolution. These finer-grid patterns are implicitly related to historical large-scale atmospheric circulation patterns, which presumably would change somewhat with global climate change. Application of the historical finer-grid spatial patterns to guide downscaling of future climate projections implies an assumption that the historical relationship between finer-grid surface climate patterns and large-scale atmospheric circulation is still valid under the future climate. In other words, the relationship is assumed to have statistical stationarity. In actuality, it is possible that such stationarity will not hold at various space and time scales, over various locations, and for various climate variables. However, the significance of potential nonstationarity in empirical downscaling methods and the need to utilize alternative downscaling methodologies remains to be established.

6.2 Assessing Hydrologic Impacts

6.2.1 Generating Weather Sequences Consistent with Climate Projections

This temporal disaggregation method from Wood et al. (2002) translated monthly BCSD climate projections into daily VIC weather forcings. However, other techniques might have been considered. Choice of weather generation technique depends on aspects of climate change that are being targeted in a given study. Preference among available techniques remains to be established. Various characteristics, such as that the resampling approach does not allow daily temperature ranges to vary from those selected with the sample, make the disaggregation approach unsuitable for studies focusing on potential changes in

daily extremes. In contrast, it may be sufficient for monthly time step hydrological assessments if the disaggregation is performed with thoughtful sampling constraints.

6.2.2 Natural Runoff Response

This activity analyzes natural runoff response to changes in precipitation, temperature, and change in natural vegetation PET while holding other watershed features constant. Other watershed features might be expected to change as climate changes and affects runoff (e.g., vegetation affecting ET and infiltration, etc.). On the matter of land cover response to climate change, the runoff models' calibrations would have to change if land cover changed, because the models were calibrated to represent the historical relationship between weather and runoff as mediated by historical land cover. Adjustment to watershed land cover and model parameterizations are difficult to consider due to lack of available information to guide such an adjustment. Ecohydrological frameworks, perhaps involving dynamic vegetation response, may be suitable to represent such land surface changes for studies in which such sensitivities are important.

6.2.3 Hydrologic Modeling

The hydrology model used excludes ground water interaction with surface water systems. The fate of precipitation is modeled as loss only to runoff and evapotranspiration; and loss of precipitation to deep percolation and return flows to stream channel networks is not considered in the VIC hydrology model.

6.2.4 Bias and Calibration

Where the VIC applications have been calibrated, they do a good job reproducing the past with little bias (e.g., Colorado River at Imperial Dam, or Feather River at Oroville). Where the VIC applications have not been calibrated, they can exhibit significant bias. The location-specific implications of calibration or lack thereof on the conclusions of the study have not been quantified, but it is clear from the streamflow bias correction analysis that calibration can make a large (first order) difference in the simulated flows and have some significant effects on the simulated changes in some flow metrics as well (Maurer et al. 2010). This study recommends that greater emphasis be placed on model calibration in future west-wide studies. For perspective, note that such a step likely would be required in any locality specific analysis.

6.2.5 Spatial Resolution of the Applications

In addition to these issues, and related to the calibration issue, there's also probably a threshold spatial scale below which the simulated runoff results should be interpreted cautiously, except it is not altogether clear how to determine this

scale. For example, it seems to be the general case that for larger basins (e.g., Feather River above Oroville and larger), the VIC applications are capable of doing a sufficient job simulating monthly to annual runoff aspects. However, for smaller basins (e.g., Little Truckee River above Boca), it's questionable whether the VIC applications do a sufficient job given their 12-km by 12-km gridded nature. Users are invited to keep this issue in mind as they extract information from this data resource.

6.2.6 Time Resolution of the Applications

Similar considerations might be given toward temporal aspects of these data. Although simulations were conducted at daily time steps, the applications were calibrated to reproduce monthly and annual runoff characteristics at a subset of locations in the basin. For this reason, users should cautiously interpret the daily hydrologic information coming from these simulations. The daily runoff information is physically consistent with assumed weather forcings and hydrologic model structure; however, there could be significant simulation biases at the submonthly level, just as there are spatial biases for small watersheds (as discussed in the section above).

CHAPTER 7

References

- Anderson, E.A. 1973. *National Weather Service River Forecast System-Snow Accumulation and Ablation Model*, Technical Memorandum NWS HYDRO-17, NOAA, November 1973.
- _____. 2006. *Snow Accumulation and Ablation Model – SNOW-17*, NWS Technical Memorandum, NOAA, Silver Spring, Maryland, 61 pp.
- Anderson, J., F. Chung, M. Anderson, L. Brekke, D. Easton, M. Ejeta, R. Peterson, and R. Snyder. 2008. “Progress on Incorporating Climate Change into Management of California’s Water Resources,” *Climatic Change*, Springer, Netherlands, 89, Supplement 1, 91–108.
- Andreadis K., P. Storck, and D.P. Lettenmaier. 2009. “Modeling snow accumulation and ablation processes in forested environments,” *Water Resources Research*, 45, W05429, doi:10.1029/2008WR007042.
- Barnett, T., D.W. Pierce, H. Hidalgo, C. Bonfils, B.D. Santer, T. Das, G. Bala, A.W. Wood, T. Nazawa, A. Mirin, D. Cayan, and M. Dettinger. 2008. “Human-induced changes in the hydrology of the Western United States,” *Science/Science Express Reports*, 10.1126/science.1152538.
- Brekke, L.D., E.P. Maurer, J.D. Anderson, M.D. Dettinger, E.S. Townsley, A. Harrison, and T. Pruitt. 2009b. “Assessing Reservoir Operations Risk under Climate Change,” *Water Resources Research*, doi:10.1029/2008WR006941.
- Brekke, L.D., J.E. Kiang, J.R. Olsen, R.S. Pulwarty, D.A. Raff, D.P. Turnipseed, R.S. Webb, and K.D. White. 2009a. *Climate change and water resources management—A federal perspective*, U.S. Geological Survey Circular 1331, 65 pp. Also available online at <http://pubs.usgs.gov/circ/1331/>.
- Brekke, L.D., M.D. Dettinger, E.P. Maurer, and M. Anderson. 2008. “Significance of model credibility in estimating climate projection distributions for regional hydroclimatological risk assessments,” *Climatic Change*, 89(3–4), 371–394.

- Burnash, R.J.C., R.L. Ferral, and R.A. McGuire. 1973. *A generalized streamflow simulation system - Conceptual modeling for digital computers*, Technical Report, Joint Federal and State River Forecast Centers of the U.S. National Weather Service and California Department of Water Resources, Sacramento, California, 204 pp.
- Burnash, R., and L. Ferral. 1996. "Conceptualization of the Sacramento Soil Moisture Accounting Model," *NWSRFS Users Manual, Part II.3*, National Weather Service, NOAA, DOC, Silver Spring, Maryland.
- Cherkauer, K.A., and D.P. Lettenmaier. 2003. "Simulation of spatial variability in snow and frozen soil field," *J. Geophys. Res.* Vol. 108, No. D22, doi:10.1029/2003JD003575.
- Christensen, N.S., A.W. Wood, D.P. Lettenmaier, and R.N. Palmer. 2004. "Effects of Climate Change on the Hydrology and Water Resources of the Colorado River Basin," *Climatic Change* Vol. 62, Issue 1–3, 337–363.
- Christensen, N.S., and D.P. Lettenmaier. 2007. "A multimodel ensemble approach to assessment of climate change impacts on the hydrology and water resources of the Colorado River basin," *Hydrology and Earth System Sciences*, 11, 1417–1434.
- Climate Change and Water Working. 2010. "Assessing a Portfolio of Approaches for Producing Climate Change Information to Support Adaptation Decisions," Climate Change and Water Working Group Workshop. Boulder, Colorado, November 2010.
- Covey, C., K.M. AchutaRao, U. Cubasch, P.D. Jones, S.J. Lambert, M.E. Mann, T.J. Phillips, and K.E. Taylor. 2003. "An Overview of Results from the Coupled Model Intercomparison Project," *Global and Planetary Change*, 769, 1–31.
- Dettinger, M.D. 2005. "From Climate Change Spaghetti to Climate Change Distributions for 21st Century," *San Francisco Estuary and Watershed Science* 3(1).
- Ficklin, D.L., Y. Luo, E. Lunedeling, and M. Zhang, 2009. "Climate change sensitivity assessment of a highly agricultural watershed using SWAT," *Journal of Hydrology* 374(1–2): 16–29.

- Fowler, H.J., S. Blenkinsop, and C. Tebaldi. 2007. "Linking climate change modelling to impacts studies: recent advances in downscaling techniques for hydrological modeling," *International Journal of Climatology*, 27: 1547–1578, doi: 10.1002/joc.1556.
- Gleckler, P.J., K.E. Taylor, and C. Doutriaux. 2008. "Performance metrics for climate models," *Journal of Geophysical Research* 113(D06104).
- Hamlet, A.F., and D.P. Lettenmaier. 1999. "Effects of climate change on hydrology and water resources in the Columbia River Basin," *Journal of the American Water Resources Association* 35(6):1597–1623.
- Hamlet A.F., S.Y. Lee, K.E.B. Mickelson, and M.M. Elsner. 2010. "Effects of projected climate change on energy supply and demand in the Pacific Northwest and Washington State," *Climatic Change*, DOI: 10.1007/s10584-010-9857-y.
- Hawkins, E., and R.T. Sutton. 2009. "The potential to narrow uncertainty in regional climate predictions," *Bulletin of the American Meteorological Society*, 90 (8). pp. 1095–1107.
- _____. 2010. "The potential to narrow uncertainty in projections of regional precipitation change," *Climate Dynamics*, DOI: 10.1007/s00382-010-0810-6.
- Intergovernmental Panel on Climate Change. 2000. *Special Report on Emissions Scenarios*. Nakicenovic, N. and R. Swart (eds.). Cambridge University Press, Cambridge, United Kingdom, 599 pp. Available at <http://www.grida.no/climate/ipcc/emission/>.
- _____. 2007. *Climate Change 2007: The Physical Science Basis*. Contribution of Working Group I to the Fourth Assessment Report of the Intergovernmental Panel on Climate Change. Solomon, S., D. Qin, M. Manning, Z. Chen, M. Marquis, K.B. Averyt, M. Tignor, and H.L. Miller (eds.). Cambridge University Press, Cambridge, United Kingdom and New York, New York, United States, 996 pp. Available at <http://www.ipcc.ch/ipccreports/ar4-wg1.htm>.
- Leavesley, G.H., R.W. Lichty, B.M. Troutman, and L.G. Saindon. 1983. *Precipitation-runoff modeling system—User's manual*, U.S. Geological Survey Water-Resources Investigation Report 83-4238, 207 pp.

- Lettenmaier, D.P., and T.Y. Gan. 1990. "Hydrologic sensitivities of the Sacramento-San Joaquin River basin, California, to global warming," *Water Resour Res* 26:69–86.
- Lettenmaier, D.P., A.W. Wood, R.N. Palmer, E.F. Wood, and E.Z. Stakhiv. 1999. "Water Resources Implications of Global Warming: A U.S. Regional Perspective," *Climatic Change* Vol. 43, No.3, November, 537–79.
- Liang, X., D.P. Lettenmaier, E.F. Wood, and S.J. Burges. 1994. "A simple hydrologically based model of land surface water and energy fluxes for general circulation models," *Journal of Geophysical Research*, 99(D7), 14415–14428.
- Liang X., E.F. Wood, and D.P. Lettenmaier. 1996. "Surface soil moisture parameterization of the VIC-2L model: Evaluation and modifications," *Glob Planet Chang* 13: 195–206.
- Lohmann, D., R. Nolte-Holube, and E. Raschke. 1996. "A large-scale horizontal routing model to be coupled to land surface parameterization schemes," *Tellus* 48 A, pp. 708–72.
- Maidment, D.R. (ed.). 1993. *Handbook of Hydrology*, McGraw-Hill, New York, New York, 1424 pp.
- Mastin, M.C. 2008. "Effects of potential future warming on runoff in the Yakima River Basin," *U.S. Geological Survey Scientific Investigations Report 2008-5124*, 12 pp.
- Maurer, E.P. 2007. "Uncertainty in hydrologic impacts of climate change in the Sierra Nevada, California under two emissions scenarios," *Climatic Change*, 82, 309–325.
- Maurer, E.P., A.W. Wood, J.C. Adam, D.P. Lettenmaier, and B. Nijssen. 2002. "A Long-Term Hydrologically-Based Data Set of Land Surface Fluxes and States for the Conterminous United States," *Journal of Climate* 15(22), 3237–3251.
- Maurer, E.P., H.G. Hidalgo, T. Das, M.D. Dettinger, and D.R. Cayan. 2010. "The utility of daily large-scale climate data in the assessment of climate change impacts on daily streamflow in California," *Hydrology and Earth System Sciences* 14, 1125–1138, doi:10.5194/hess-14-1125-2010.

- Maurer, E.P., L. Brekke, T. Pruitt, and P.B. Duffy. 2007. "Fine-resolution climate projections enhance regional climate change impact studies," *Eos Trans. AGU*, 88(47), 504.
- Maurer, E.P., L.D. Brekke, and T. Pruitt. 2010. "Contrasting lumped and distributed hydrology models for estimating climate change impacts on California watersheds," *Journal of the American Water Resources Association (JAWRA)* 46(5):1024–1035. DOI: 10.1111/j.1752-1688.2010.00473.x.
- McGuire, E.M., and A. Hamlet. 2010. "Hydrologic Climate Change Scenarios for the Pacific Northwest Columbia River Basin and Coastal Drainages – Chapter 5," *Macro-scale Hydrologic Model Implementation*, 34 pp, available at <http://www.hydro.washington.edu/2860/report/>.
- McGuire, E.M., L. Cuo, N. Voisin, J.S. Deems, A.F. Hamlet, J.A. Vano, K.E.B. Mickelson, S.Y. Lee, and D.P. Lettenmaier. 2010. "Implications of 21st century climate change for the hydrology of Washington State," *Climatic Change*, DOI:10.1007/s10584-010-9855-0.
- Meehl, G.A., C. Covey, T. Delworth, M. Latif, B. Mcavaney, J.F.B. Mitchell, R.J. Stouffer, and K.E. Taylor. 2007. "THE WCRP CMIP3 MULTIMODEL DATASET – A New Era in Climate Change Research," *Bulletin of the American Meteorological Society*, 88(9), 1383–1394.
- Meehl, G.A., G.J. Boer, C. Covey, M. Latif, and R.J. Stouffer. 2000. "The Coupled Model Intercomparison Project (CMIP)," *Bulletin of the American Meteorological Society*, 81(2), 313–318.
- Miller, N.L., K. Bashford, and E. Strem. 2003. "Potential Climate Change Impacts on California Hydrology," *Journal of the American Water Resources Association*, 39, 771–784.
- Mote, P.W., and E.P. Salathé. 2010. "Future climate in the Pacific Northwest," *Climatic Change*, DOI: 10.1007/s10584-010-9848.
- Nijssen, B., D.P. Lettenmaier, X. Liang, S.W. Wetzel, and E F. Wood. 1997. "Streamflow simulation for continental-scale river basins," *Water Resour. Res.*, 33, 711–724.
- Payne, J.T., A.W. Wood, A.F. Hamlet, R.N. Palmer, and D.P. Lettenmaier. 2004. "Mitigating the effects of climate change on the water resources of the Columbia River basin," *Climatic Change*, 62(1–3):233–256.

- Pierce, D.W., T.P. Barnett, B.D. Santer, and P.J. Gleckler. 2009. "Selecting global climate models for regional climate change studies," *Proc National Academy Sciences*, v106 (21), 8441–8446.
- Purkey D.R., A. Huber-Lee, D.N. Yates, M. Hanemann, S. Herrod-Jones. 2007. "Integrating a climate change assessment tool into stakeholder-driven water management decision-making processes in California," *Water Resources Management*, 21, 315–329.
- Reclamation. 2008. "Sensitivity of Future CVP/SWP Operations to Potential Climate Change and Associated Sea Level Rise," Appendix R in *Biological Assessment on the Continued Long-term Operations of the Central Valley Project and the State Water Project*. Prepared by the U.S. Department of the Interior, Bureau of Reclamation, Mid-Pacific Region, Central Valley Operations Office, Sacramento, California. August 2008. 134 pp.
- _____. 2010. *Climate Change and Hydrology Scenarios for Oklahoma Yield Studies*, prepared by the U.S. Department of the Interior, Bureau of Reclamation, Technical Services Center, Denver Colorado. April 2010. 71 pp.
- Reichler, T., and J. Kim. 2008. "How Well Do Coupled Models Simulate Today's Climate?" *Bulletin of the American Meteorological Society*, 89(3) pp. 303–311.
- Rosenberg, N.J., D.J. Epstein, D. Wang, L. Vail, R. Srinivasan, and J.G. Arnold. 1999. "Possible Impacts of Global Warming on the Hydrology of the Ogallala Aquifer Region," *Climatic Change* 42:677–692.
- Salathé, E.P., P.W. Mote, and M.W. Wiley. 2007. "Review of scenario selection and downscaling methods for the assessment of climate change impacts on hydrology in the United States Pacific Northwest," *International Journal of Climatology*, 27: 1611–1621.
- Santer, B.D., K.E. Taylor, P.J. Gleckler, C. Bonfils, T.P. Barnett, D.W. Pierce, T.M.L. Wigley, C. Mears, F.J. Wentz, W. Bruggemann, N.P. Gillett, S.A. Klein, S. Solomon, P.A. Stott, and M.F. Wehner. 2009. "Incorporating model quality information in climate change detection and attribution studies," *Proc National Academy Sciences*, v 106 (35), 14778–14783.

- Shi, X., A.W. Wood, and D.P. Lettenmaier. 2008. "How Essential is Hydrologic Model Calibration to Seasonal Streamflow Forecasting?" *J. Hydrometeorol*, 9, 1350–1363.
- Slack, J.R., A.M. Lumb, and J.M. Landwehr. 1993. "Hydroclimatic data network (HCDN): A U.S. Geological Survey streamflow data set for the United States for the study of climate variation, 1874–1988," *USGS Water Resour. Invest. Rep.*, 93-4076.
- Smith, J.A., G.N. Day, and M.D. Kane. 1992. "Nonparametric framework for long-range streamflow forecasting," *J. Water Resour. Planning and Management*, 118, 82–92.
- Snover A.K., A.F. Hamlet, and D.P. Lettenmaier. 2003. "Climate change scenarios for water planning studies: Pilot applications in the Pacific Northwest," *Bull Am Meteorol Soc* 84(11):1513–1518.
- Stone, M.C., R.H. Hotchkiss, C.M. Hubbard, T.A. Fontaine, L.O. Mearns, and J.G. Arnold. 2001. "Impacts Of Climate Change On Missouri River Basin Water Yield," *JAWRA* 37:1119–1129.
- Tebaldi, C., R.L. Smith, D. Nychka, and L.O. Mearns. 2005. "Quantifying Uncertainty in Projections of Regional Climate Change: A Bayesian Approach to the Analysis of Multi-model Ensembles," *Journal of Climate*, 18 pp. 1524–1540.
- Tootle, G.A., T.C. Piechota, and A.K. Singh. 2005. "Coupled Interdecadal and Interannual Oceanic/Atmospheric Variability and United States Streamflow," *Water Resources Research*, 41(W12408).
- U.S. Global Change Research Program. 2009. *Global Climate Change Impacts in the United States*, T.R. Karl, J.M. Melillo, and T.C. Peterson, (eds.). Cambridge University Press, 196 pp.
- Vano, J.A., N. Voisin, L. Cuo, A.F. Hamlet, M.M. Elsner, R.N. Palmer, A. Polebitski, and D.P. Lettenmaier. 2010. "Climate change impacts on water management in the Puget Sound region, Washington, USA." *Climatic Change* 102(1-2): 261–286, doi: 10.1007/s10584-010-9846-1.
- Van Rheezen, N.T., A.W. Wood, R.N. Palmer, D.P. Lettenmaier. 2004. "Potential implications of PCM climate change scenarios for Sacramento-San Joaquin River Basin hydrology and water resources," *Climatic Change*, 62, 257–281.

- Vicuna, S. and J.A. Dracup. 2007. "The evolution of climate change impact studies on hydrology and water resources in California," *Climatic Change*, 82, 327–350.
- Wigley, T.M.L. 2004. "Input Needs for Downscaling of Climate Data." Discussion paper prepared for California Energy Commission Public Interest Energy Research Program, Rep 500-04-027.
- Wigmosta, M.S., L.W. Vail, and D.P. Lettenmaier. 1994. "A distributed hydrology vegetation model for complex terrain," *Water Resour. Res.*, 30:1665–1679.
- Wiley, M.W. 2004. "Analysis techniques to incorporate climate change information into Seattle's long range water supply planning," Masters thesis, University of Washington, Seattle, Washington.
- Wood, A.W., A. Kumar, and D.P. Lettenmaier. 2005. "A retrospective assessment of climate model-based ensemble hydrologic forecasting in the western U.S.," *J. Geophys. Res.* 110, D04105, doi:10.1029/2004JD004508.
- Wood, A.W., and D.P. Lettenmaier. 2006. "A Test Bed for New Seasonal Hydrologic Forecasting Approaches in the Western United States," *Bull. Amer. Meteor. Soc.*, 87, 1699–1712.
- Wood, A.W., E.P. Maurer, A. Kumar, and D.P. Lettenmaier. 2002. "Long-range experimental hydrologic forecasting for the Eastern United States," *J. Geophysical Research-Atmospheres*, 107(D20), 4429, doi:10.1029/2001JD000659.
- Wood, A.W., L.R. Leung, V. Sridhar, and D.P. Lettenmaier. 2004. "Hydrologic implications of dynamical and statistical approaches to downscaling climate model outputs," *Climatic Change*, 15, 189–216.
- Yates, D., J. Sieber, D. Purkey, and A. Huber-Lee. 2005. "WEAP21 – A Demand-, Priority-, and Preference-Driven Water Planning Model. Part 1: Model Characteristics," *Water International*, 30(4):487–500.